NACA TN 2979

NATIONAL ADVISORY COMMITTEE FOR AERONAUTICS

TECHNICAL NOTE 2979

EFFECTS OF SYMMETRIC AND ASYMMETRIC THRUST REVERSAL ON THE AERODYNAMIC CHARACTERISTICS OF A MODEL OF A TWIN-ENGINE AIRPLANE

By Kenneth W. Goodson and John W. Draper

Langley Aeronautical Laboratory
Langley Field, Va.

Washington
September 1953

1F

NATIONAL ADVISORY COMMITTEE FOR AERONAUTICS

TECHNICAL NOTE 2979

EFFECTS OF SYMMETRIC AND ASYMMETRIC THRUST REVERSAL ON THE AERODYNAMIC CHARACTERISTICS OF A MODEL OF A TWIN-ENGINE AIRPLANE

By Kenneth W. Goodson and John W. Draper

SUMMARY

An investigation has been conducted with a twin-engine airplane model in the Langley 300 MPH 7- by 10-foot tunnel to determine the magnitude of the changes in aerodynamic forces and moments resulting from propeller pitch reversal. The effects of both positive and negative thrust coefficients were investigated at a Reynolds number of 550,000. The investigation indicated that the lift, longitudinal-force, and pitching-moment coefficients varied almost linearly with total thrust coefficient through the negative and positive thrust range. The lateral-force, yawing-moment, and rolling-moment coefficients were found to vary as approximately linear functions of asymmetric thrust coefficient. From analyzing the basic data of the investigation, a method is suggested which will give a reasonable estimate of the effects of thrust reversal on the aerodynamic characteristics of an airplane by using existing wind-tunnel data. The investigation showed that, for extreme asymmetric-thrust conditions, the rolling and yawing moments are of such magnitudes that marginal or inadequate lateral and directional control may possibly be encountered on twin-engine airplanes.

INTRODUCTION

Numerous twin-engine and multiengine airplanes have experienced difficulty in maintaining flight because of the large untrimmed forces and moments obtained when one or more of the propellers inadvertently move to reverse pitch. An investigation of the forces experienced on a twin-engine airplane (tractor propellers) with symmetric or asymmetric thrust reversal has been made in the Langley 300 MPH 7- by 10-foot tunnel. The investigation was made with a model representative of a typical twin-engine airplane.

Static-force tests were made through the lift-coefficient range up through the stall to determine the effects of various amounts of positive and negative thrust on the longitudinal and lateral aerodynamic forces and moments of the model. The tests included both symmetric- and asymmetric-thrust conditions through a negative and positive thrust range. Rudder and aileron effectiveness tests were made to determine whether the controls were capable of trimming out the moments resulting from maximum-asymmetric-thrust conditions. Some results of the sideslip characteristics of the model with asymmetric thrust through an angle-of-sideslip range are also presented.

A method of estimating the aerodynamic forces and moments caused by asymmetric-thrust conditions has been developed through analysis of the test data.

An example of performance calculations to cover asymmetric-thrust conditions and an estimate of the untrimmed moments and forces caused by asymmetric thrust as compared to the available control power are presented.

SYMBOLS

All forces and moments are presented with respect to the stability axes and are referred to a center-of-gravity location of 25 percent mean aerodynamic chord of the model. A sketch showing the positive directions of the forces, moments, and angles is given in figure 1.

W	weight, lb
S	wing area, sq ft
$\bar{c}$	mean aerodynamic chord, ft
b	wing span, ft
y	lateral distance from fuselage center line to center line of thrust, ft
q	dynamic pressure, $\frac{1}{2}\rho V^2$, lb/sq ft
ρ	mass density of air, slugs/cu ft
V	free-stream velocity, ft/sec
V_i	indicated velocity, mph

W/S wing loading, lb/sq ft

α angle of attack of fuselage center line, deg

β angle of sideslip, deg

C_L lift coefficient, $\frac{\text{Lift}}{qS}$

C_D drag coefficient, $\frac{\text{Drag}}{qS}$

C_X longitudinal-force coefficient, $\frac{\text{Longitudinal force}}{qS}$

C_m pitching-moment coefficient, $\frac{\text{Pitching moment}}{qS\bar{c}}$

C_n yawing-moment coefficient, $\frac{\text{Yawing moment}}{qSb}$

C_l rolling-moment coefficient, $\frac{\text{Rolling moment}}{qSb}$

C_Y lateral-force coefficient, $\frac{\text{Lateral force}}{qS}$

ΔC_L incremental change in lift coefficient caused by change in total thrust coefficient

ΔC_m incremental change in pitching-moment coefficient caused by change in total thrust coefficient

ΔC_l incremental change in rolling-moment coefficient caused by asymmetric thrust coefficient

ΔC_n incremental change in yawing-moment coefficient caused by asymmetric thrust coefficient

ΔC_Y incremental change in lateral-force coefficient caused by asymmetric thrust coefficient

i_t tail incidence with respect to fuselage center line, deg

δ_f wing flap deflection, deg

δ_a aileron deflection, deg

δ_r rudder deflection, deg

T thrust, lb

T_c' effective thrust coefficient, $\frac{\text{Thrust}}{qS}$

$\Delta T_c'$ thrust-coefficient differential caused by asymmetric thrust; positive when a positive yawing moment is produced, $T_{c'_L} - T_{c'_R}$

Subscripts:

R right

L left

a aileron

r rudder

APPARATUS AND METHODS

Description of Model

The investigation was made in the Langley 300 MPH 7- by 10-foot tunnel with a model of a typical twin-engine airplane. A sketch of the model is presented in figure 2 and a photograph of the model mounted in the tunnel is shown in figure 3, whereas table I presents the physical characteristics of the model. The airfoil section used on the wing was 19 percent thick at the root and 15 percent thick at the tip. The model wing had an aspect ratio of 10.07 and a taper ratio of 0.388. In general, the model was constructed of wood with steel reinforcing members.

The geometric characteristics of the cast-aluminum model propeller as compared to a representative full-scale propeller are given in figure 4. The thickness ratio of the model propeller was shown to be more than twice that of the representative full-scale propeller. As the thickness primarily influences the torque coefficient and since the torque of the model propeller was too small to be measured by the tunnel balance system, thickness effects were neglected in this investigation. The blade angles used in the tests (18° at 0.75R for positive thrust conditions and 0° at 0.75R for negative thrust conditions) were selected

to simulate the thrust that might be encountered in both the normal and negative thrust ranges of a twin-engine airplane.

The model propellers were driven by two independently operated, water-cooled, variable-speed 16-horsepower electric motors. The rotational speed of the propellers was independently determined by observation of stroboscopic-type indicators which indicated the output frequency of each of two small alternators connected to the motor shafts. The accuracy of the frequency indicators was within ±0.05 percent.

The model was equipped with one plain flap-type aileron located on the left wing, double slotted lift flaps, an adjustable horizontal tail, and an adjustable rudder.

Tests

Tests were made at a dynamic pressure of 12.25 pounds per square foot, which corresponds to a Reynolds number of 550,000 based on the mean aerodynamic chord of the wing.

A propeller calibration was made with the propeller mounted in front of a streamlined fairing which housed the driving motor. Each propeller was calibrated by measuring the resultant longitudinal force with the propeller thrust axis at 0° angle of attack for a range of propeller speeds and blade-angle settings. The effective thrust coefficients were computed from the following relationship:

$$T = X_{on} - X_{off}$$

$$T_c' = \frac{T}{\frac{1}{2}\rho V^2 S}$$

where X_{on} is the longitudinal force obtained with the propeller operating and X_{off} is the longitudinal force of the fairing with the propeller removed. The propeller calibration was checked on the model and no appreciable interference effects were noted.

For the constant-thrust-coefficient tests, the propeller speed was held constant while the angle of attack of the model was varied. The thrust coefficients investigated for an individual propeller ranged from 0.167 to -0.150.

Corrections

The angle-of-attack, longitudinal-force, and pitching-moment results have been corrected for jet boundary effects computed by the methods of reference 1. All coefficients have been corrected for tunnel blockage by the method of reference 2.

Corrections for tare forces and moments produced by the interference of the support strut have not been applied. The strut tare correction would affect the absolute levels of the drag and pitching-moment curves; however, past experience has shown that this would not appreciably affect incremental results and therefore should not alter any conclusions made in the present paper. For the tests in sideslip, the strut tare would produce small corrections to the pitching-moment, longitudinal-force, lateral-force, and yawing-moment coefficients. The tares caused by the restraint of the power cables and cooling-water tubing were erratic, especially when the model was moved through 0° sideslip. Care was exercised, in making the investigation, to reduce these tares to a minimum; however, it is felt that for the sideslip tests only the values of forces and moments beyond values of sideslip of $\pm 2^{\circ}$ should be used in the analysis of the data.

Vertical bouyancy on the support strut, tunnel air-flow misalinement, and longitudinal-pressure gradient have been accounted for in computation of the test data.

RESULTS AND DISCUSSION

Presentation of Data

The figures of the basic data, cross plots, and performance calculations are presented as follows: All data are presented for the complete model unless otherwise noted.

Basic Data

Characteristic in pitch attitude.- The characteristics of the model were quite similar when the right propeller instead of the left propeller produced the negative thrust as shown in figure 5. The effect of extending the landing gear is shown in figure 6. As no appreciable effects of propeller mode of rotation or of extending the landing gear were evident, the remaining tests were made with the landing gear retracted and with asymmetric-thrust conditions being produced only by the left propeller.

The basic data presented in figures 7 to 12 indicate that the lift coefficient increased as expected with increased thrust while the lateral moments varied as a function of asymmetric thrust. These data show that a large thrust differential and large negative symmetric-thrust conditions caused an abrupt roll-off above the stall ($\alpha \approx 17^\circ$). It should be noted, however, that the stall progression might very well be affected by the low Reynolds number (550,000) of these tests.

Characteristics in sideslip.- The effects of asymmetric thrust on the characteristics of the model in sideslip are shown in figures 17 to 20 with the flaps neutral and deflected. The rudder characteristics for asymmetric-thrust conditions in sideslip are shown in figure 17. The results of the tests in sideslip should in most cases be used only beyond $\pm 2^\circ$ sideslip where the erratic restraining forces of the power cable are assumed to be small.

Analysis of Effects of Symmetric and Asymmetric Thrust on the Aerodynamic Characteristics

In an attempt to analyze the data obtained in this investigation, cross plots of figures 7 to 11 were made to determine the effects of thrust coefficient on the aerodynamic characteristics. (See figs. 21 to 24.)

The scatter of the test points in the cross plots could be caused in part by the absence of the propeller normal force for the test conditions of zero thrust when both propellers were removed and for some of the asymmetric-thrust conditions when one propeller was removed. Estimates of normal force of these propellers (ref. 3) indicate that the normal-force corrections to lift coefficient are small but their effect on pitching moment are of significant magnitude and would tend to decrease the scatter in the data. Conditions where one or both of the propellers are removed are indicated by the flagged symbols.

The cross plots of lift ((a) parts of figs. 21 to 24) show that the lift coefficient appears to be proportional to the total thrust coefficient and that the linearity holds true through both the negative and

positive thrust-coefficient ranges tested. In cases where there is a large variation in the sizes of each incremental wing area immersed in the propeller slipstream (for example, a four-engine airplane with tapered wings), the curves might depart from linearity. In this case, if lift were plotted against $\sum \left(\text{Effective thrust coefficient} \times \text{Area in slipstream}\right)$, a linear variation would probably result.

If the effects of thrust on lift coefficient are not available by experimental methods, an estimate of the C_L against $T_c{}'_{Total}$ curve (tail off) can be made by adding the slipstream components predicted by reference 4 and the thrust component ($T_c{}' \sin \alpha$). (See fig. 25.) The curves obtained in this manner underestimate the experimental values at the higher thrust coefficients (see, for example, fig. 25); however, reasonable agreement can be obtained if a linear fairing is made through the low-thrust-coefficient range and extended into the directions of both positive and negative thrust. An examination of the cross-plotted data showed that the pitching-moment coefficients also varied linearly with total thrust coefficient. Comparison of tail-on and tail-off data (figs. 21 to 24) shows that the tail contributes to the lift and pitching moment, but does not appreciably alter their linearity with total thrust coefficient.

These data show that, on multiengine airplanes, differences in thrust between propellers produce asymmetric lift loadings over the wing which result in rolling moments about the center of gravity of the airplane; also, that such a thrust differential would produce yawing moments as a result of the individual thrust loads. Simple analysis based on figures 21 to 24 shows that rolling moments for this model can be predicted if the changes in lift caused by the propeller slipstreams are multiplied by the moment arm of each propeller $\Delta C_L \frac{y}{b}$. The rolling-moment coefficients obtained from such lift increments generally slightly overestimate the measured rolling-moment coefficients (figs. 21 to 24). The rolling moments calculated by using lift values obtained by the empirical method of reference 4 would be somewhat lower than those obtained from the experimental curve of C_L against $T_c{}'_{Total}$. In a similar manner, yawing moments can be estimated by multiplying the thrust differential between propellers by the moment arm. The yawing-moment coefficients obtained in this manner (parts (b) of figs. 21 to 24) generally underestimate the values obtained experimentally, possibly because this method does not include the effects of the slipstream on the wing and tail or the effect of thrust-axis inclination.

Typical Performance and Control Estimates

It should be noted that results presented herein should be interpreted as being purely illustrative inasmuch as the model tested does not simulate any specific airplane in all details and since the drag values were not corrected for strut tares. An example of the application of data obtained by the methods presented in the preceding section is shown in figures 26 to 34. The airplane used in this example is a scaled-up version of the model tested. In making performance and control estimates it is desirable to have plots showing the variation of aerodynamic force and moment coefficients with total and asymmetric thrust coefficients similar to those of figures 26 and 27. These curves in conjunction with the curve of trim lift coefficient plotted against indicated velocity (fig. 28) were used to obtain the thrust required to maintain level flight (fig. 29) and to determine the change in lateral control moments (fig. 34) caused by an asymmetric-thrust condition. In order to fully utilize these plots, the actual positive and negative thrust characteristics of the full-scale propeller must be known, especially the negative thrust values obtained when a propeller enters the negative pitch range. The thrust characteristics of the propellers could be obtained, if available, from the propeller manufacturer or could be estimated by using reference 5.

In order to make the estimates of thrust required for asymmetric-thrust level-flight conditions more complete, a breakdown of the thrust required for each propeller should be made similar to that of figure 30. Such a breakdown shows the range of conditions in which the airplane has sufficient thrust coefficient to maintain level flight with one engine inoperative, as encountered when inadvertent propeller pitch reversal occurs. Under extreme asymmetric-thrust conditions, a loss in thrust could be so great that level flight could not be maintained in which case it would be desirable to know the rate of descent. A typical rate of climb or descent curve extended into the negative thrust range is shown in figure 31.

It is desirable to know the extent of untrimmed lateral-control moments produced by asymmetric-thrust conditions. A carpet showing level-flight untrimmed rolling- and yawing-moment coefficients produced by various asymmetric-thrust conditions is shown in figure 34. Included in this figure are curves showing the control moments produced by $\pm 30^{\circ}$ deflection of the plain ailerons with which this model was equipped and by -30° deflection of the rudder. The control curves were obtained from figures 13 and 33 from an average curve by assuming the effect of thrust (for the flap-neutral configuration) on the aileron and rudder to be negligible. Figure 34 shows that, under certain asymmetric-thrust conditions, the rolling and yawing moments are of such magnitude that the aileron and rudder power would be insufficient or marginal in controlling the airplane. It should be noted that dynamic effects caused by transi-

tion from a symmetric- to an asymmetric-thrust condition might considerably alter the control power required. Note that for this model there is an abrupt roll-off at stall (see basic data, figs. 7 to 12).

CONCLUSIONS

The following conclusions are indicated from the investigation of the effects of symmetric and asymmetric thrust reversal on the aerodynamic characteristics of a twin-engine airplane:

1. The lift, longitudinal-force, and pitching-moment coefficients of a twin-engine airplane generally varied as linear functions of total thrust coefficient through the negative and positive thrust ranges investigated. The lateral-force, yawing-moment, and rolling-moment coefficients generally varied as linear functions of the asymmetric thrust coefficient.

2. The present investigation indicates that reasonable estimates of the effects of asymmetric thrust on the aerodynamic characteristics of a multiengine airplane can be made if symmetric-thrust data are available for obtaining a curve of lift coefficient plotted against total thrust coefficient. In the absence of experimental data the effects of asymmetric thrust can be estimated by a simple empirical method.

3. Estimates indicate that extreme asymmetric-thrust conditions can result in rolling and yawing moments which could be of such magnitude as to result in marginal or inadequate lateral and directional control.

Langley Aeronautical Laboratory,
National Advisory Committee for Aeronautics,
Langley Field, Va., May 22, 1953.

REFERENCES

1. Gillis, Clarence L., Polhamus, Edward C., and Gray, Joseph L., Jr.: Charts for Determining Jet-Boundary Corrections for Complete Models in 7- by 10-Foot Closed Rectangular Wind Tunnels. NACA WR L-123, 1945. (Formerly NACA ARR L5G31.)

2. Herriot, John G.: Blockage Corrections for Three-Dimensional-Flow Closed-Throat Wind Tunnels, With Consideration of the Effect of Compressibility. NACA Rep. 995, 1950. (Supersedes NACA RM A7B28.)

3. Ribner, Herbert S.: Notes on the Propeller and Slipstream in Relation to Stability. NACA WR L-25, 1944. (Formerly NACA ARR L4I12a.)

4. Smelt, R., and Davies, H.: Estimation of Increase in Lift Due to Slipstream. R. & M. No. 1788, British A.R.C., 1937.

5. Gray, W. H. and Gilman, Jean, Jr.: Characteristics of Several Single- and Dual-Rotating Propellers in Negative Thrust. NACA WR L-634, 1945. (Formerly NACA MR L5C07.)

TABLE I.- PHYSICAL CHARACTERISTICS OF MODEL

Wing:	
Airfoil section	
Root	19 percent thick
Tip	15 percent thick
Area, sq ft	6.169
Span, ft	8.1647
Chord	
Root, ft	1.120
Tip, ft	0.434
Aspect ratio	10.07
Taper ratio	0.388
Sweepback of $\bar{c}/4$, deg	0
Dihedral	
Inboard (0 to 1.75 ft station), deg	3
Outboard (1.75 ft station to tip), deg	10
Incidence, deg	3
Mean aerodynamic chord, ft	0.878
Flaps:	
Type	Double slotted
Chord, percent wing chord	25.67
Total area both sides, sq ft	1.15
Span (along hinge line), each	
Inboard, ft	0.950
Outboard, ft	1.655
Ailerons (plain):	
Span, ft	1.02
Location	
Center line to inboard, ft	2.96
Center line to outboard, ft	3.97
Chord	
Inboard, ft	0.145
Outboard, ft	0.103
Horizontal tail:	
Airfoil section	
Root	13 percent thick
Tip	10 percent thick
Span, ft	3.22
Area, sq ft	2.106
Chord	
Root, ft	0.950
Tip, ft	0.379
Mean aerodynamic chord, ft	0.705

TABLE I.- PHYSICAL CHARACTERISTICS OF MODEL - Concluded

Aspect ratio	4.88
Incidence	Variable
Dihedral, deg	8
Tail length ($\bar{c}/4$ wing to $\bar{c}/4$ tail), ft	3.29
Taper ratio	0.400
Sweepback of leading edge, deg	13.65
Vertical tail:	
Airfoil section	
Root and tip	11 percent thick
Area, sq ft	0.906
Span, ft	1.251
Chord	
Root, ft	1.005
Tip, ft	.453
Sweepback of leading edge, deg	3.45
Aspect ratio	1.727
Taper ratio	0.451
Mean aerodynamic chord, ft	0.765
Tail length ($\bar{c}/4$ wing to $\bar{c}/4$ tail), ft	3.070
Rudder:	
Chord, average, behind hinge line, ft	0.242
Span along hinge line, ft	1.260
Area, behind hinge line, sq ft	0.3045
Area of balance, sq ft	0.1255
Dorsal fin:	
Area, sq ft	0.5053
Engines and propellers:	
Engine rating, hp	16
Engine rotational speed, rpm	14,000
Propeller diameter, ft	1.125
Number of blades	4
Inclination of thrust axis	1° 37'

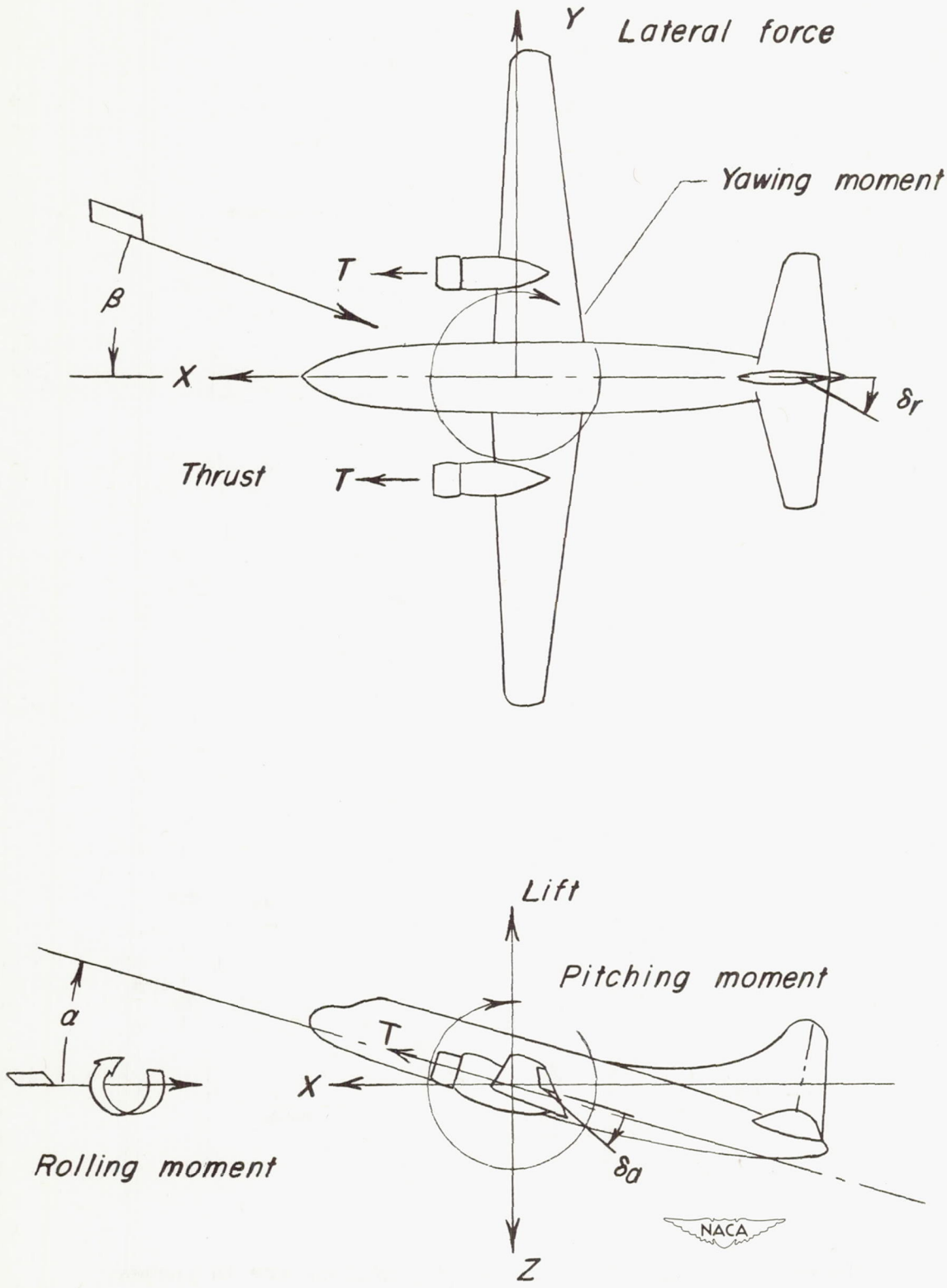

Figure 1.- System of axes showing positive directions of forces, moments, and deflections.

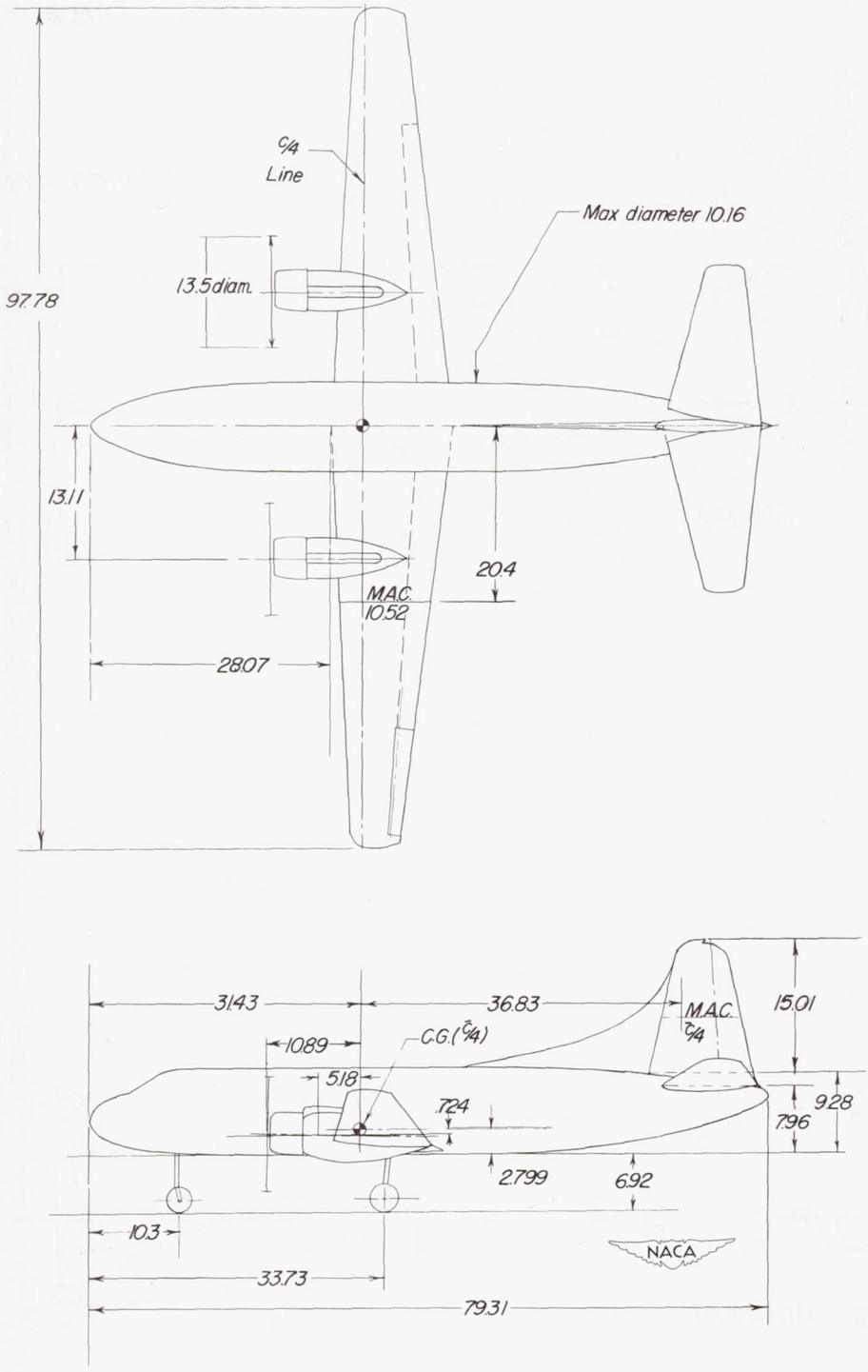

Figure 2.- Sketch of the model. Dimensions are in inches.

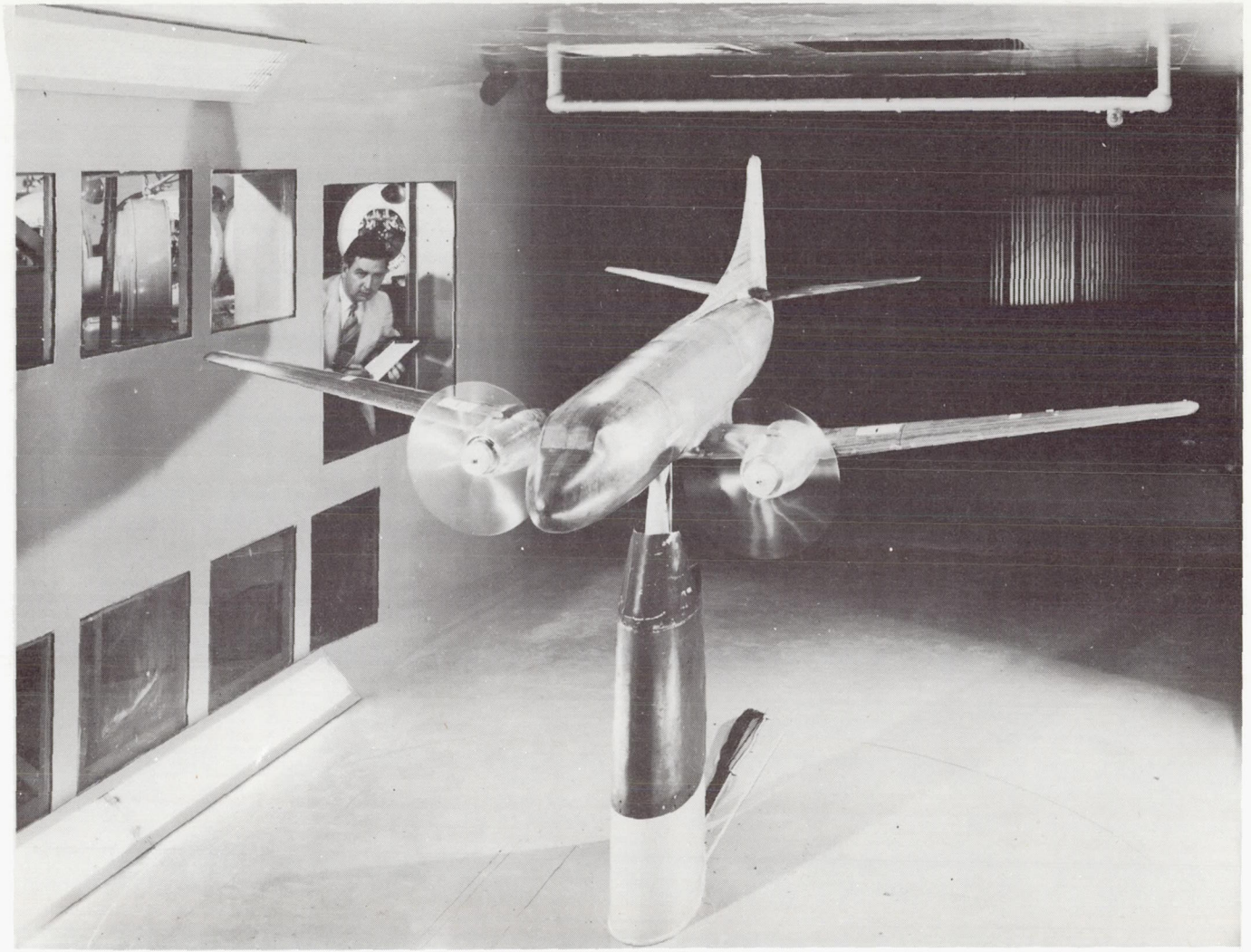

Figure 3.- Photograph of the model mounted in Langley 300 MPH 7- by 10-foot tunnel.

NACA

L-75503.1

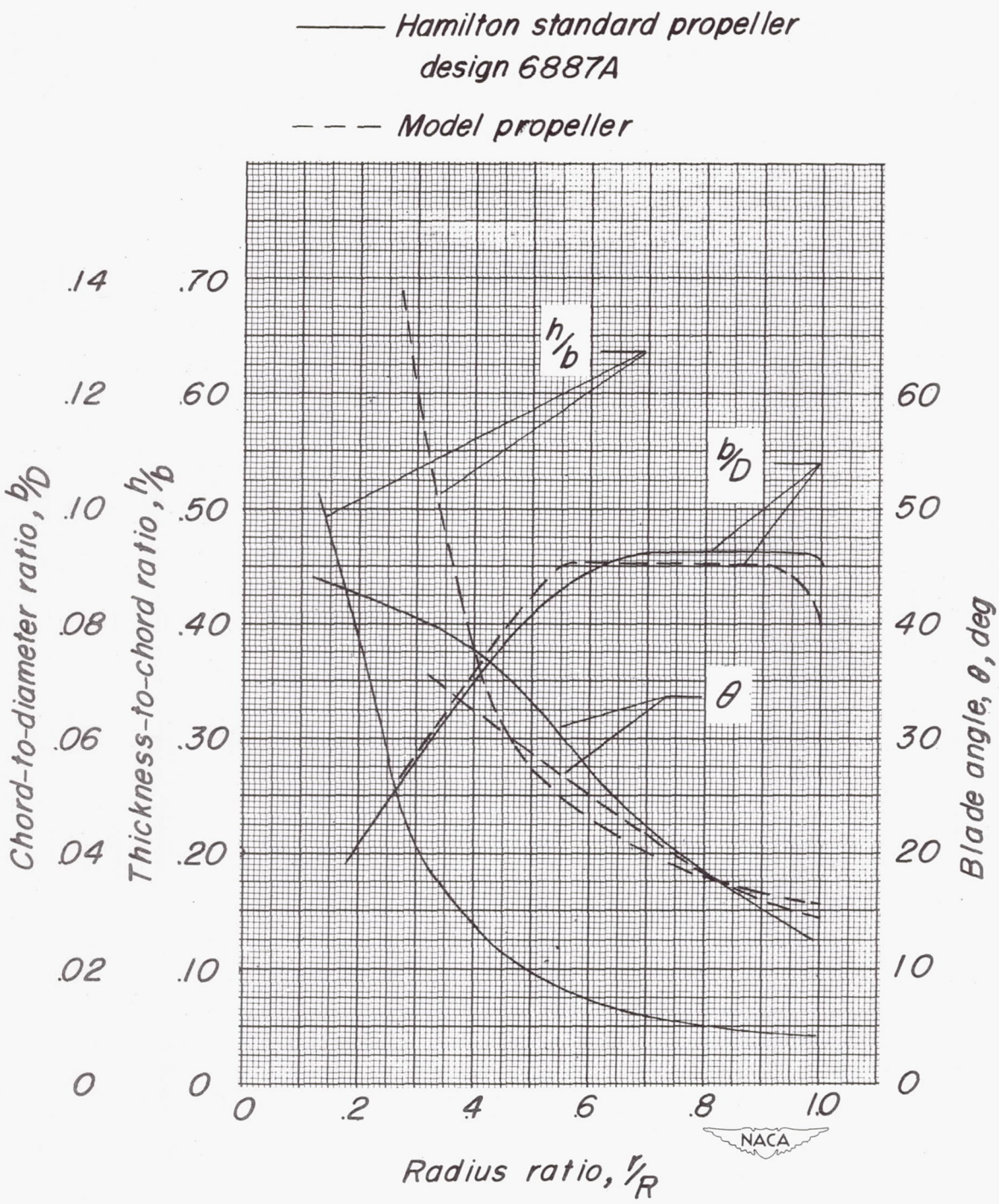

Figure 4.- A comparison of full-scale and model propeller blade characteristics.

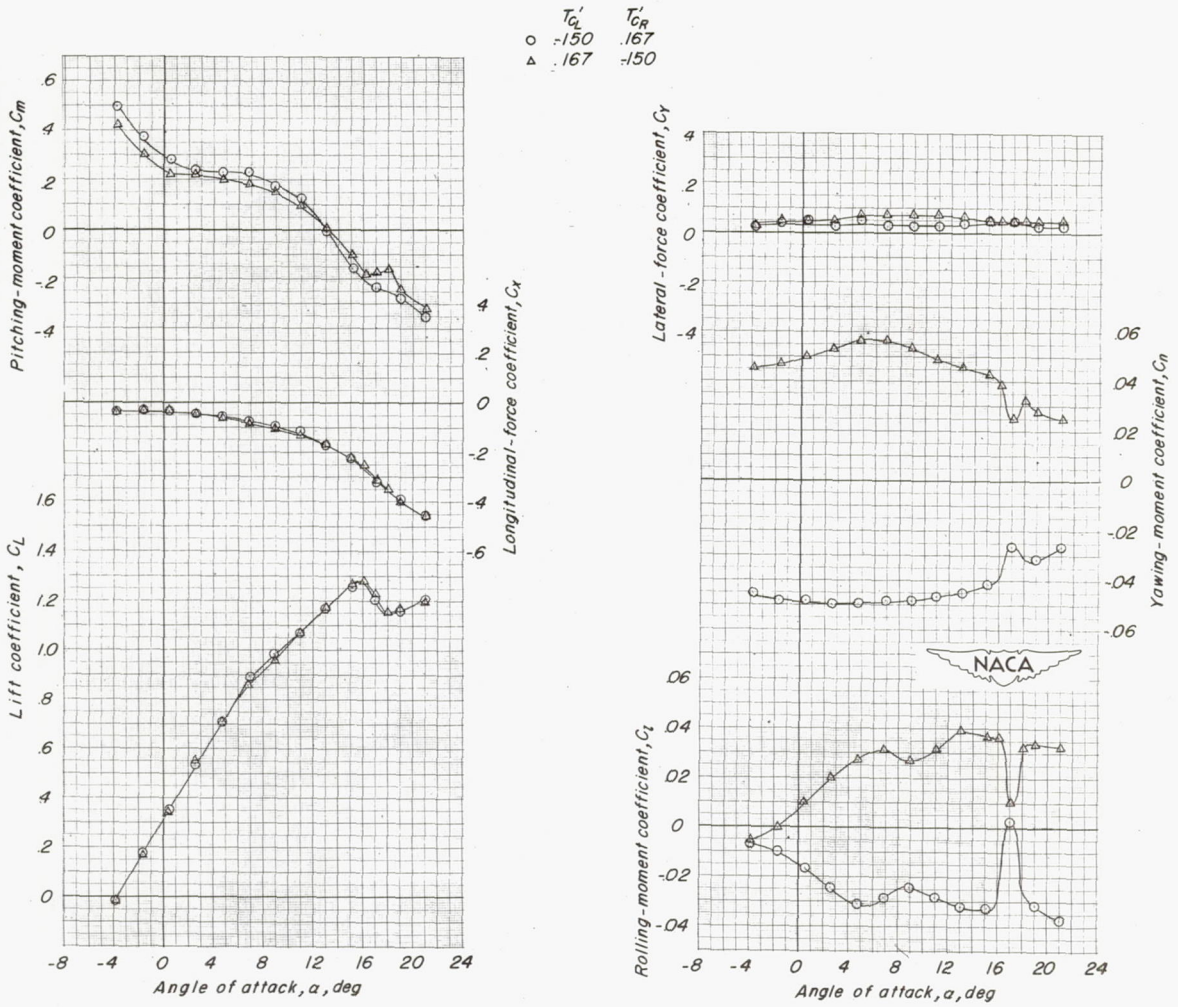

Figure 5.- A comparison of the effect of negative thrust produced by the right propeller with that of the left propeller. $\delta_f = 0^\circ$; $i_t = -4^\circ$.

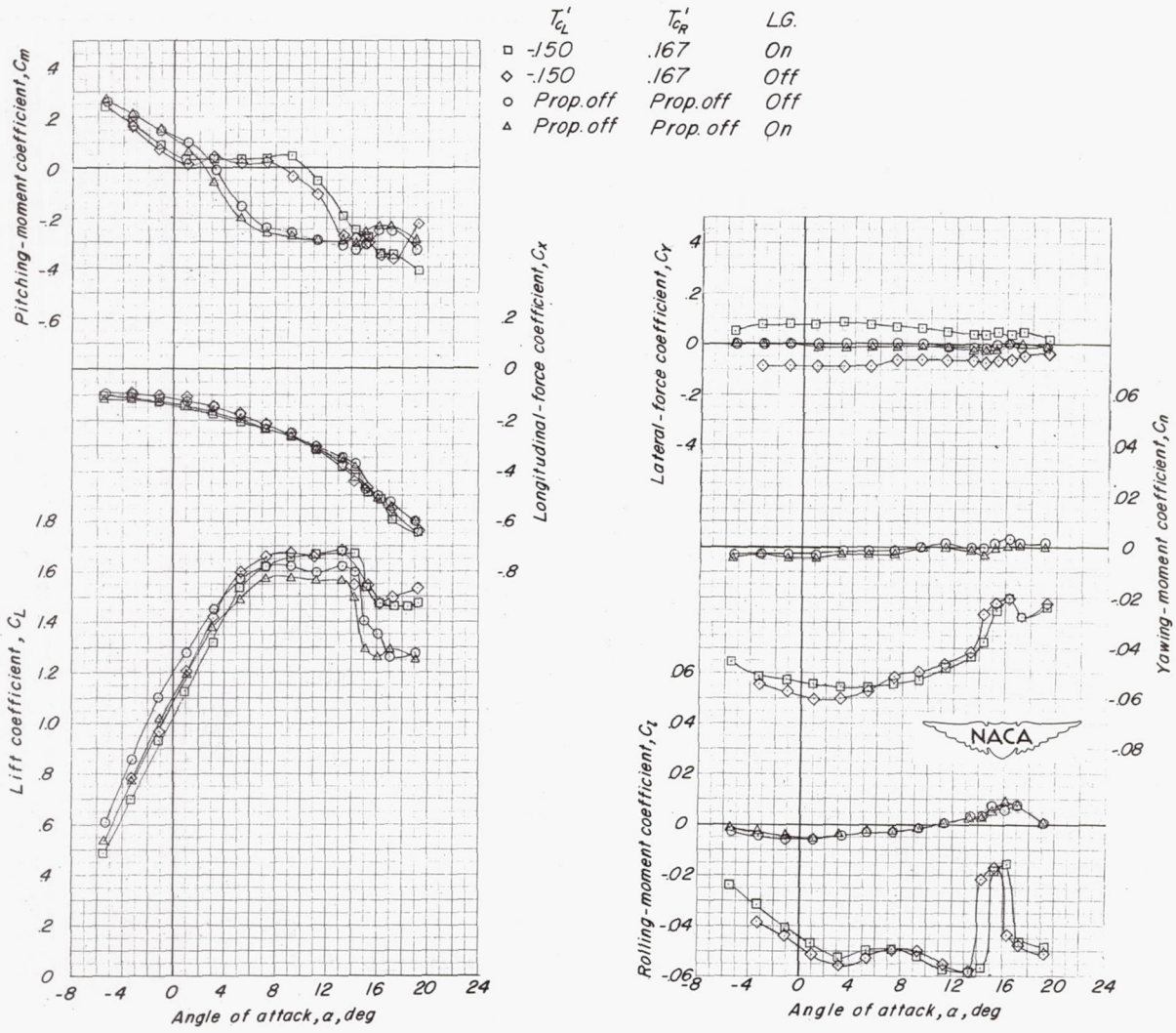

Figure 6.- The effect of lowering the landing gear with zero and asymmetric thrust. $\delta_f = 25^\circ$; $i_t = 0^\circ$.

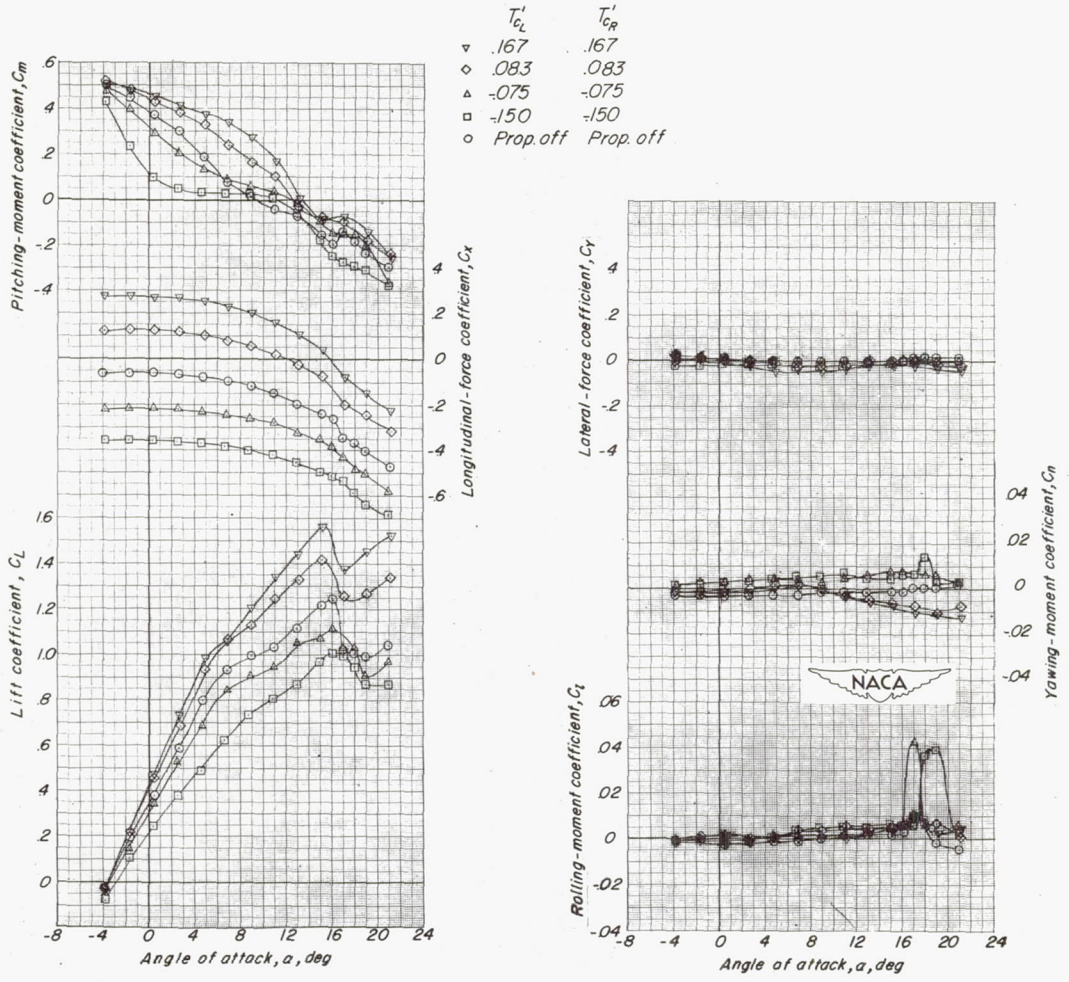

(a) Symmetric thrust.

Figure 7.- Effects of symmetric and asymmetric thrust on the aerodynamic characteristics. $\delta_f = 0^\circ$; $i_t = -4^\circ$.

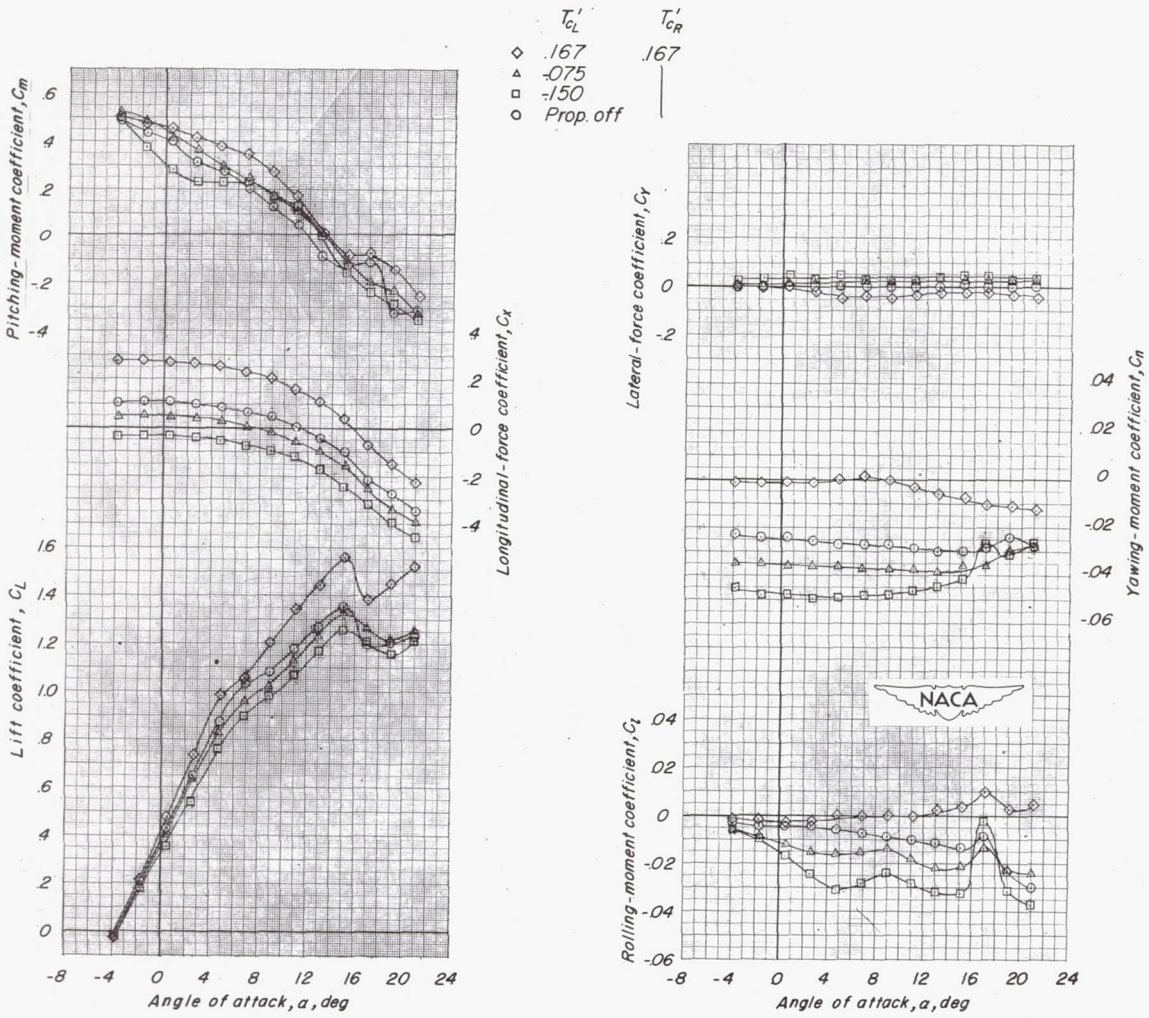

(b) Asymmetric thrust.

Figure 7.- Continued.

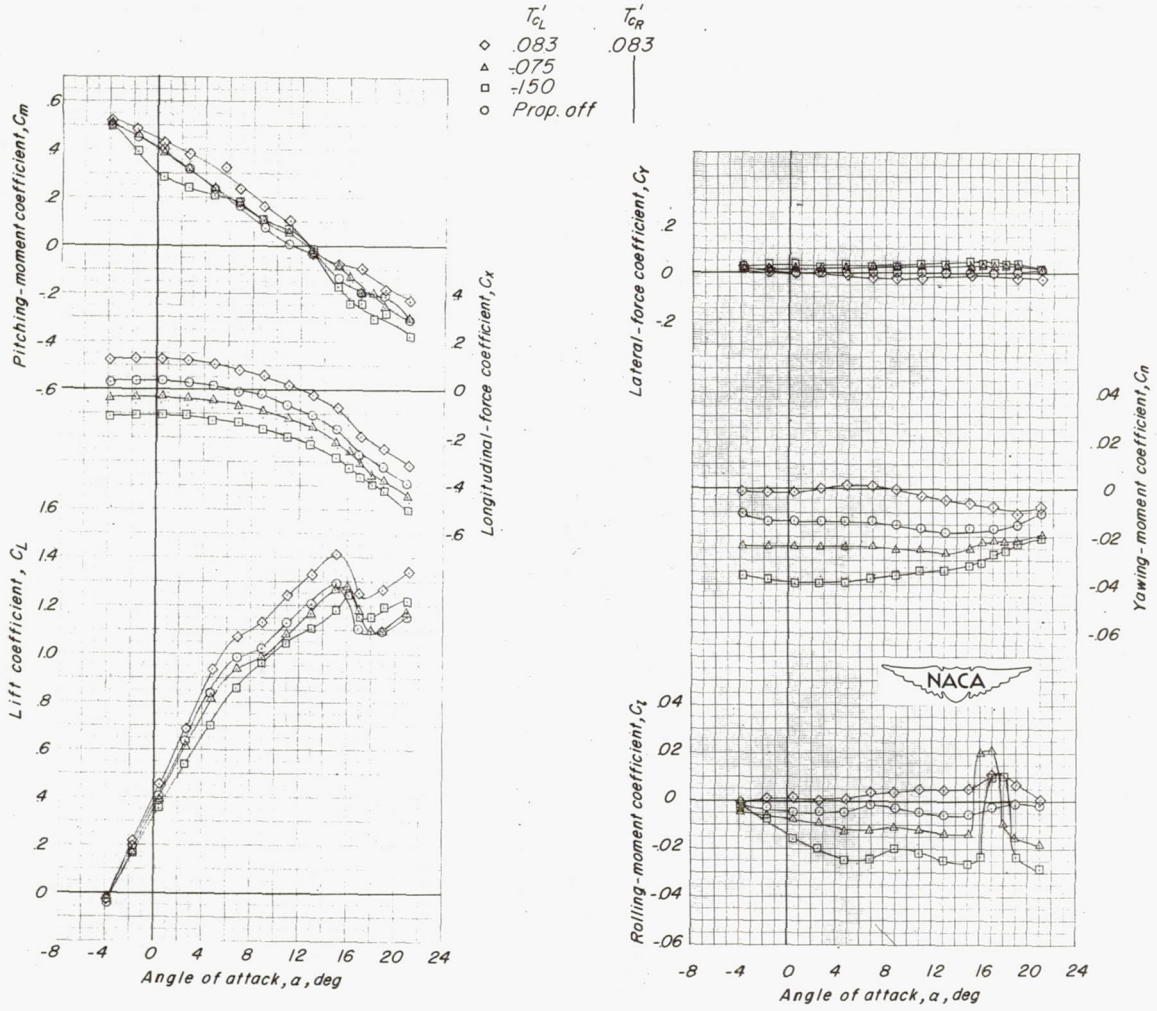

(b) Concluded.

Figure 7.- Concluded.

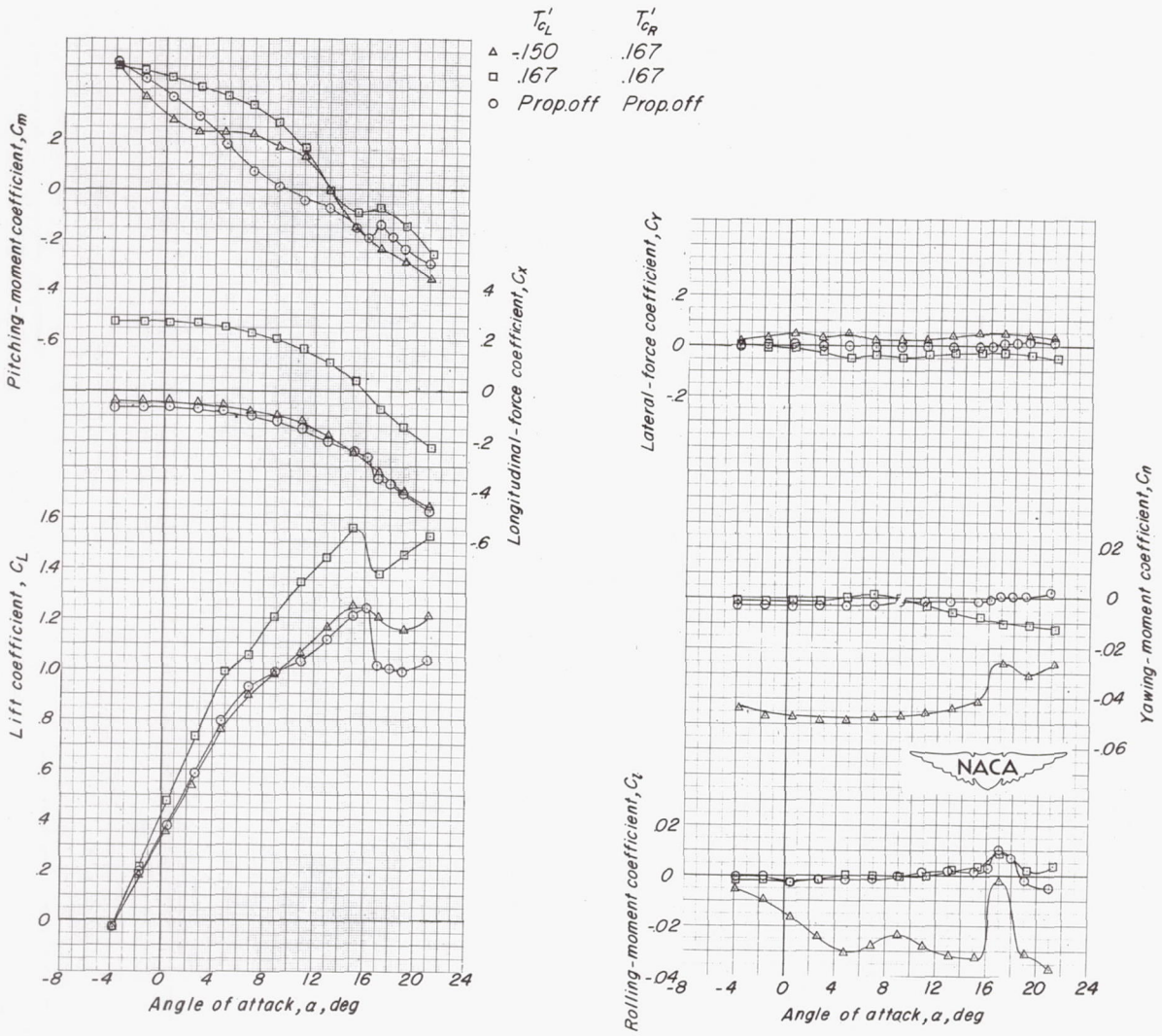

Figure 8.- Comparison of zero, full symmetric, and full asymmetric thrust. $\delta_f = 0^\circ$; $i_t = -4^\circ$.

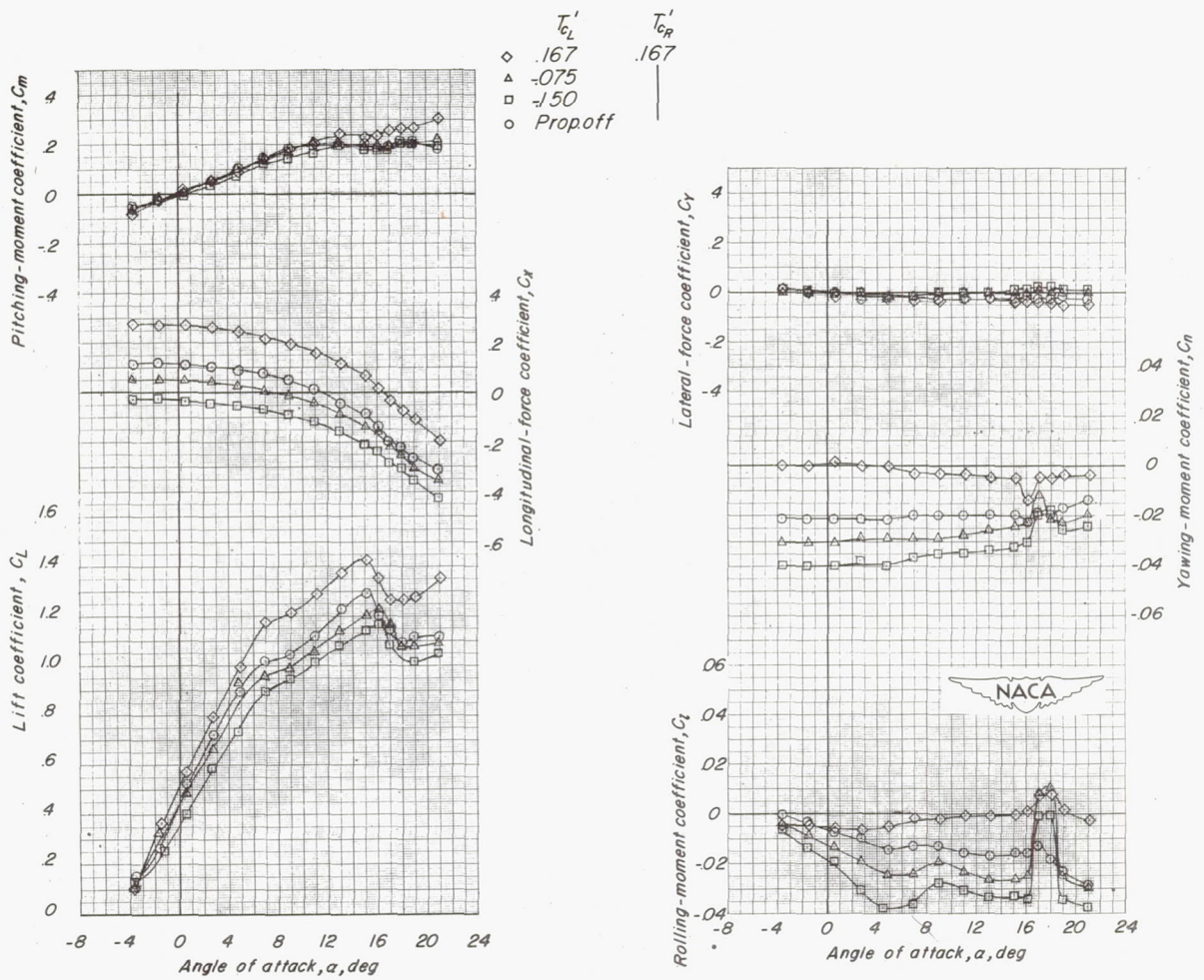

Figure 9.- Effects of asymmetric thrust on the aerodynamic characteristics. Tail off; $\delta_f = 0^\circ$.

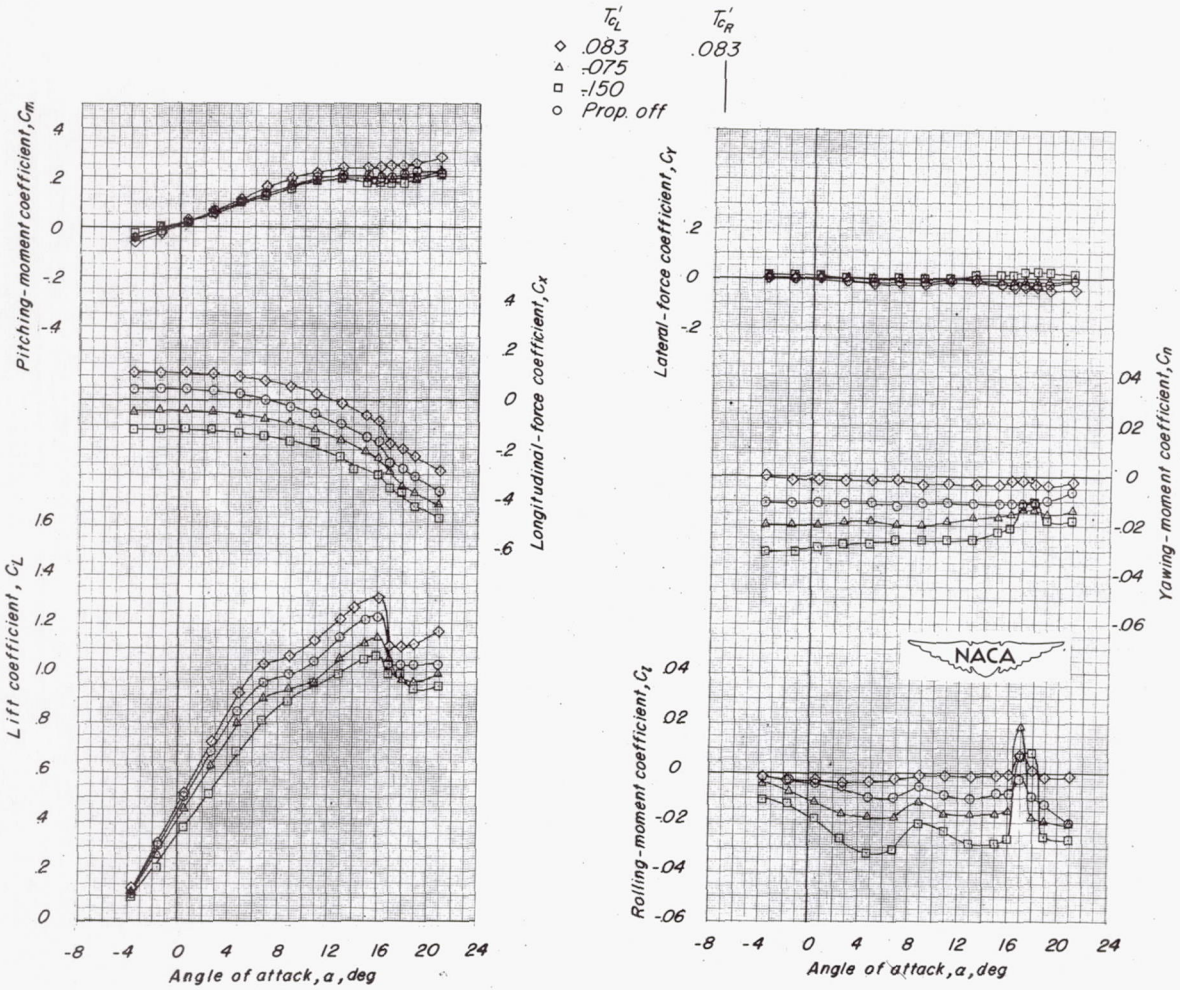

Figure 9.- Concluded.

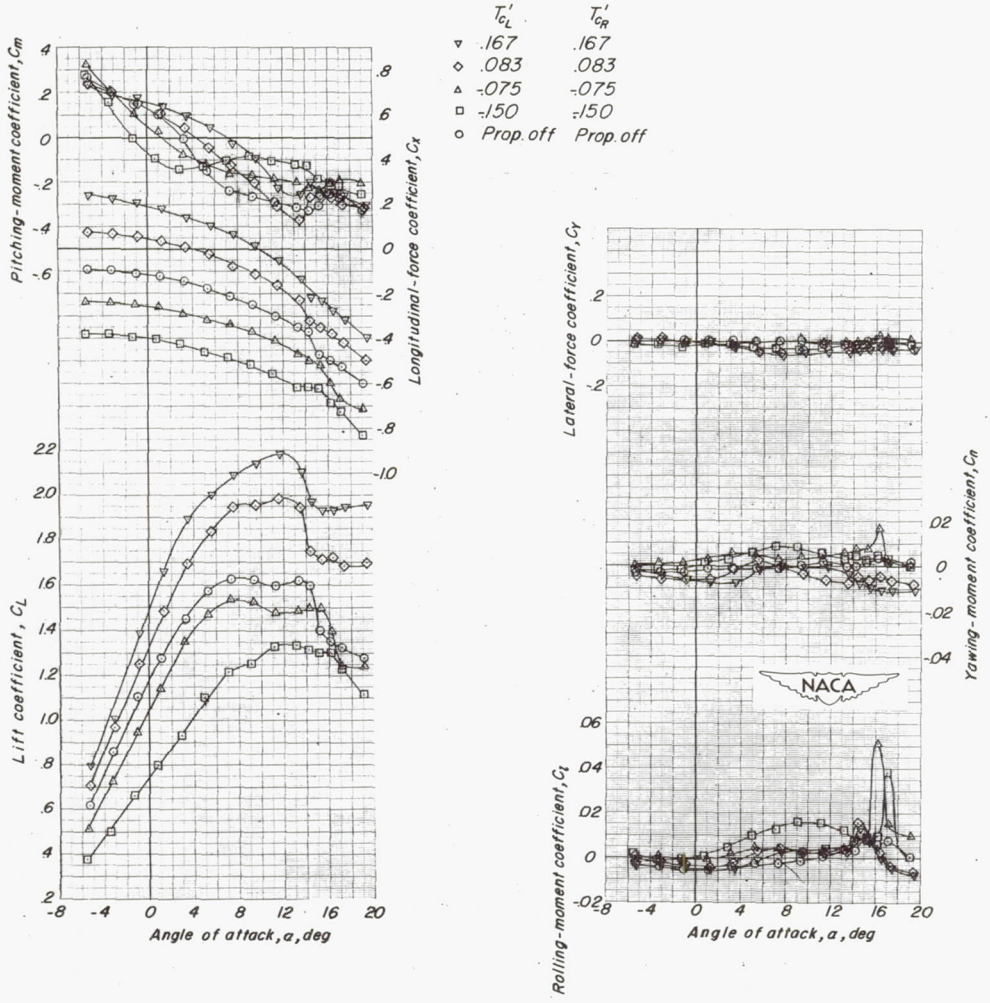

(a) Symmetric thrust.

Figure 10.- Effects of symmetric and asymmetric thrust on the aerodynamic characteristics. $\delta_f = 25^\circ$; $i_t = 0^\circ$.

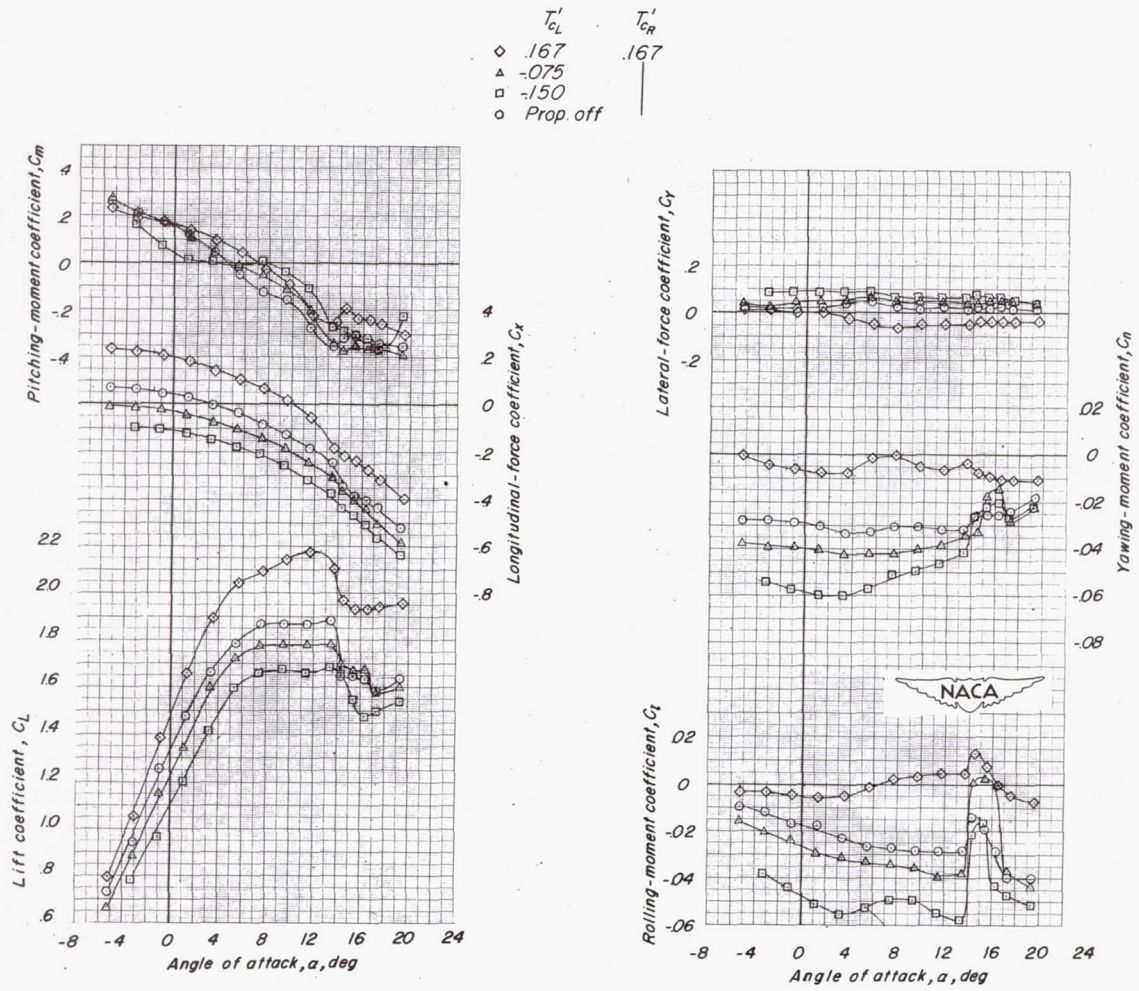

(b) Asymmetric thrust.

Figure 10.- Continued.

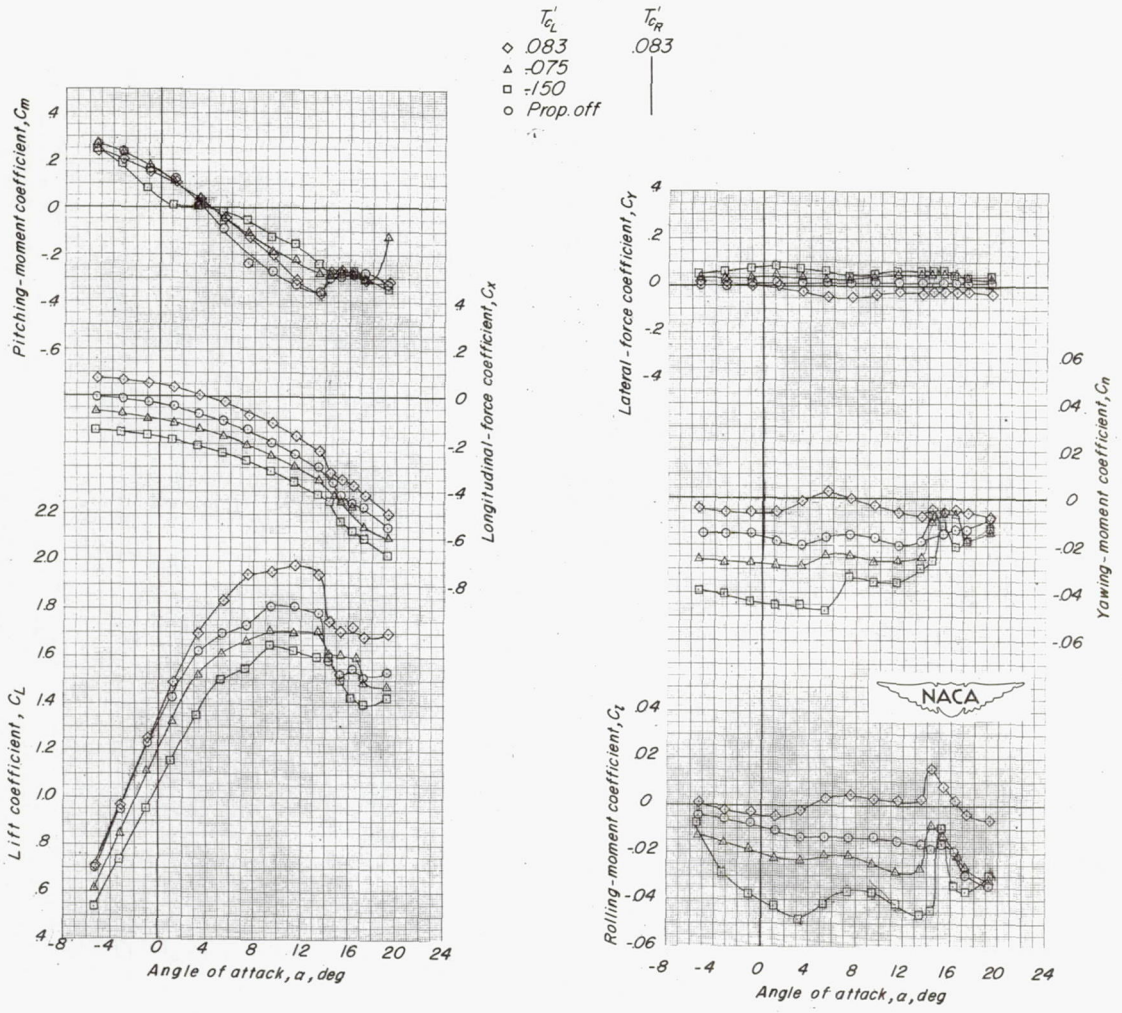

(b) Concluded.

Figure 10.- Concluded.

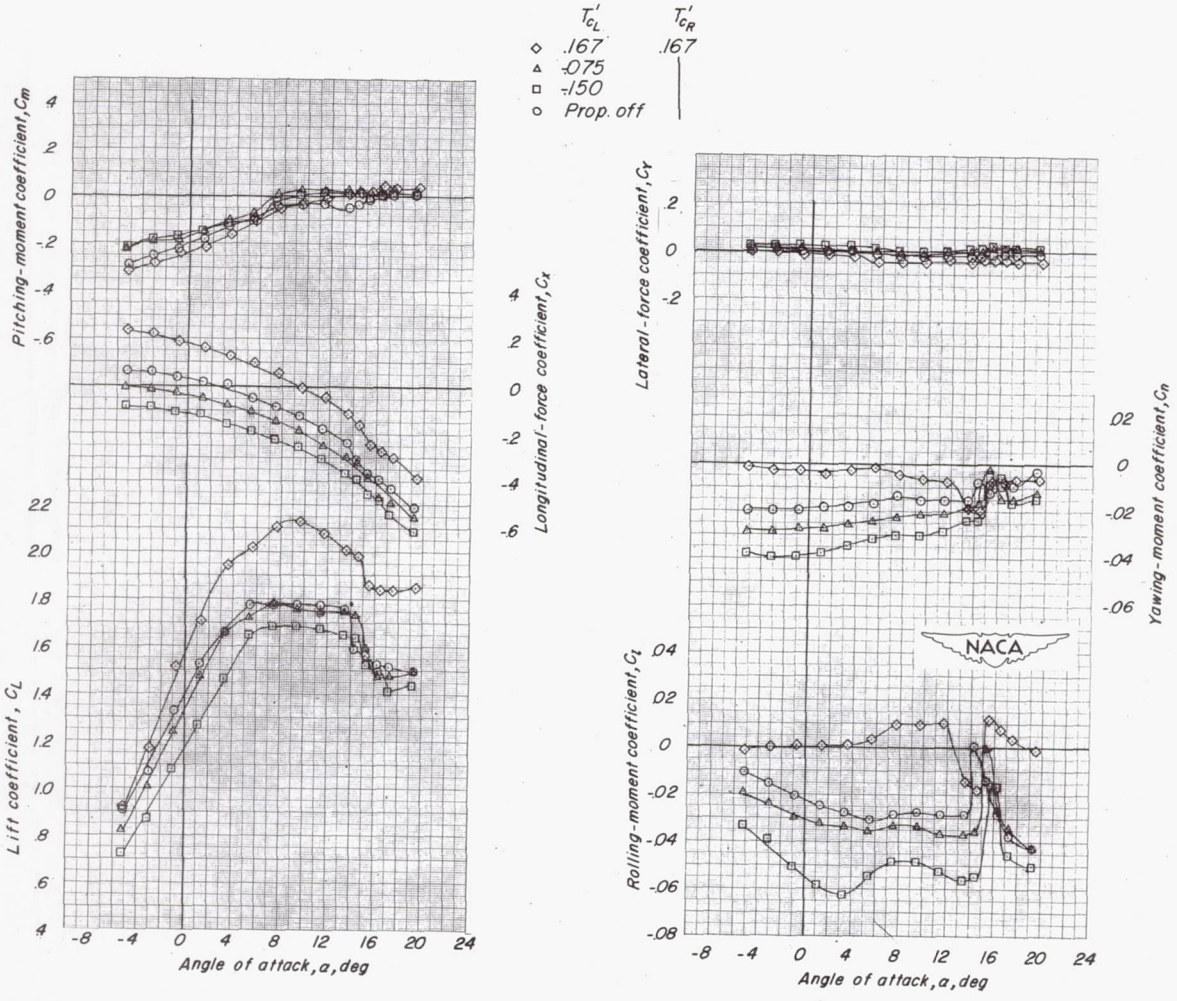

Figure 11.- Effects of asymmetric thrust on the aerodynamic characteristics. Tail off; $\delta_f = 25^\circ$.

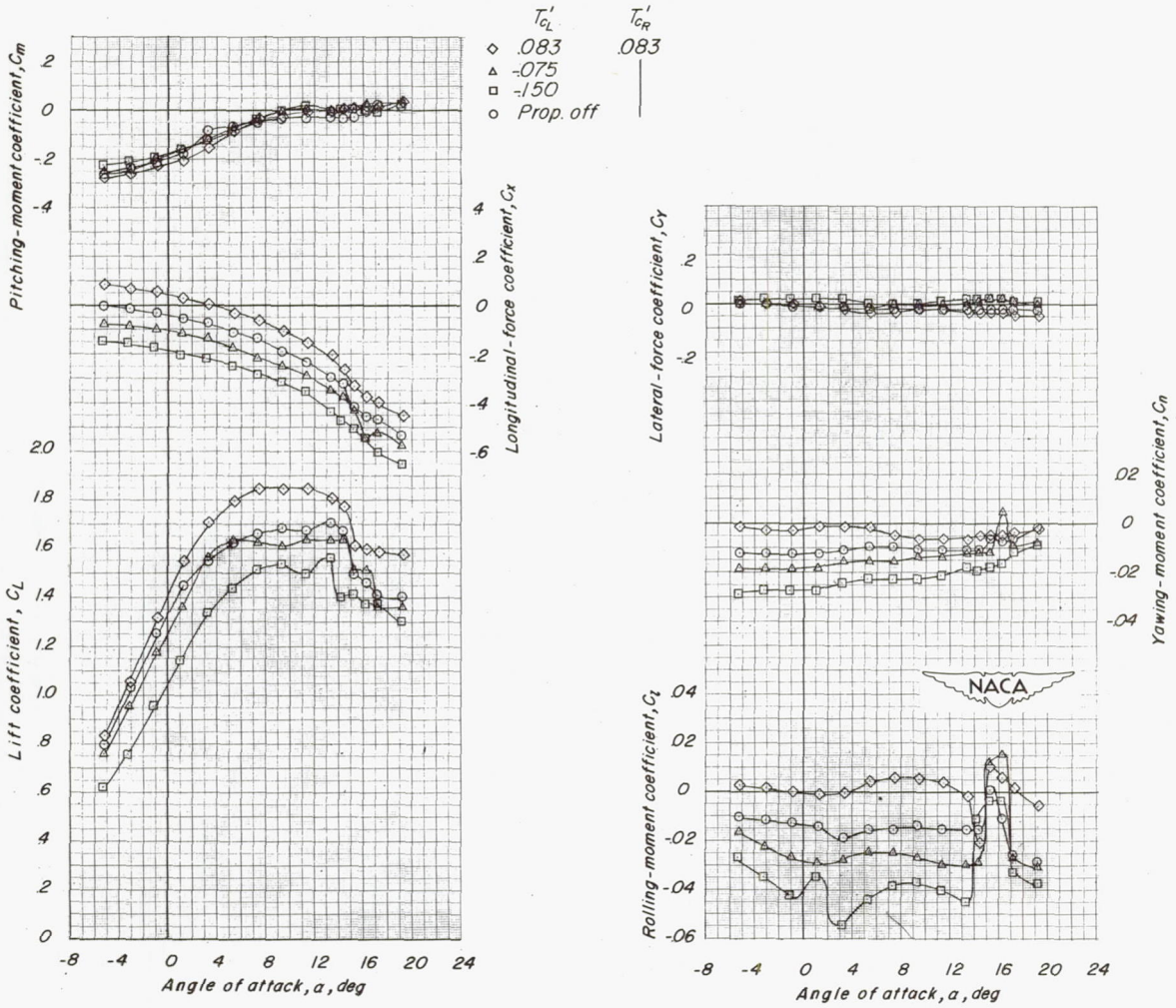

Figure 11.- Concluded.

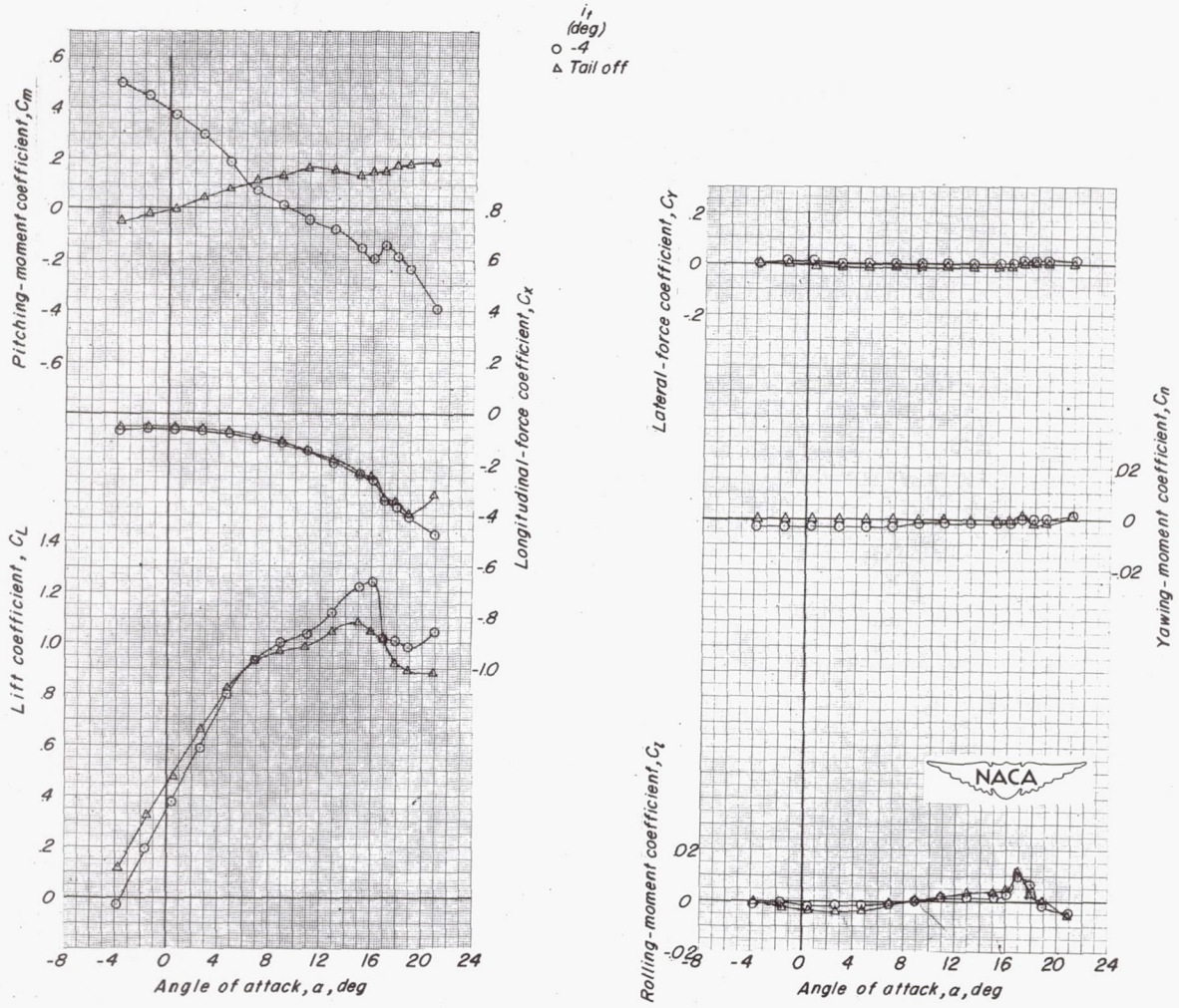

(a) $\delta_f = 0^\circ$.

Figure 12.- Comparison of tail-on and tail-off data. Propellers removed.

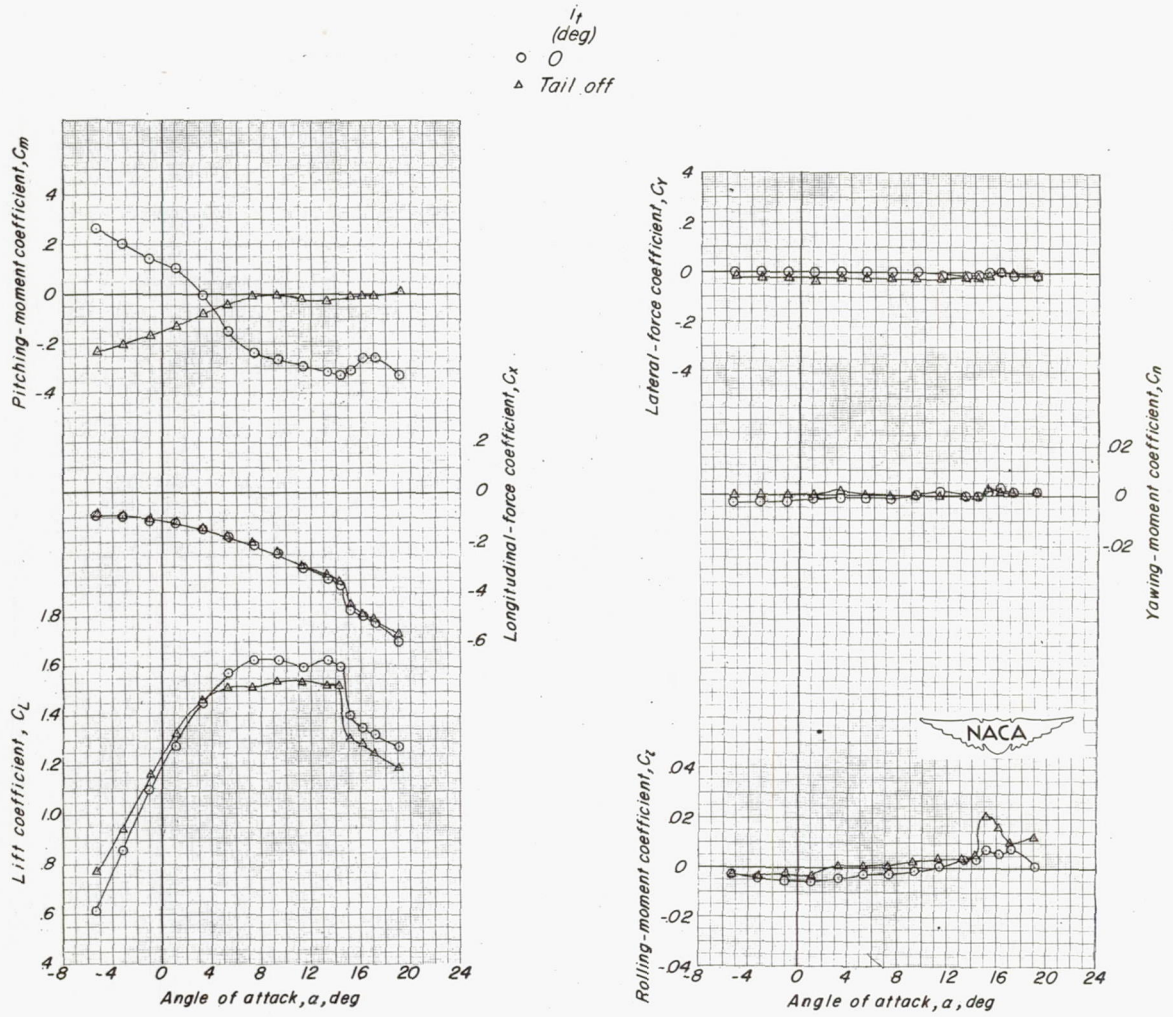

(b) $\delta_f = 25^\circ$.

Figure 12.- Concluded.

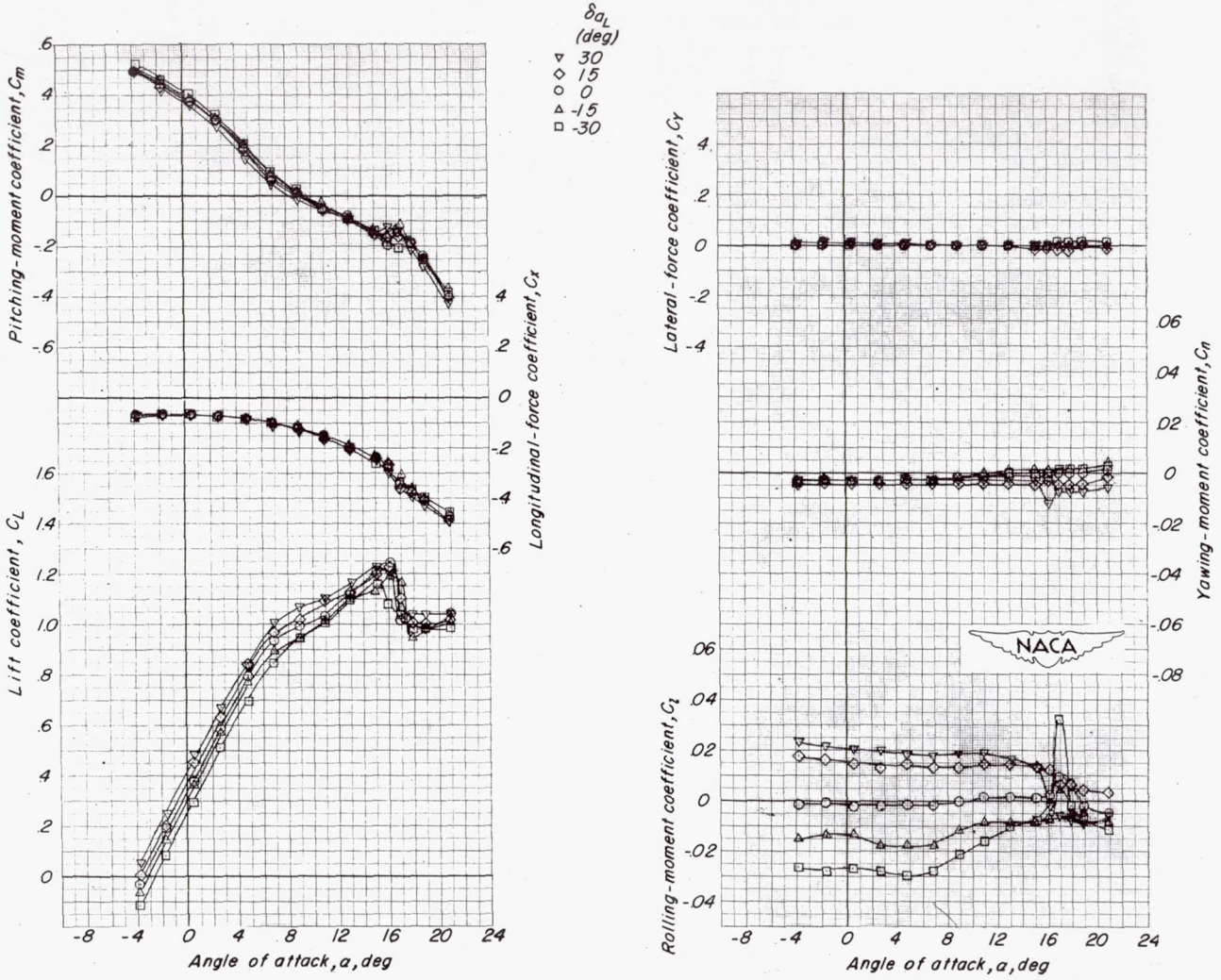

Figure 13.- Effect of aileron deflection on the aerodynamic characteristics. Propellers removed; $\delta_f = 0^\circ$; $i_t = -4^\circ$.

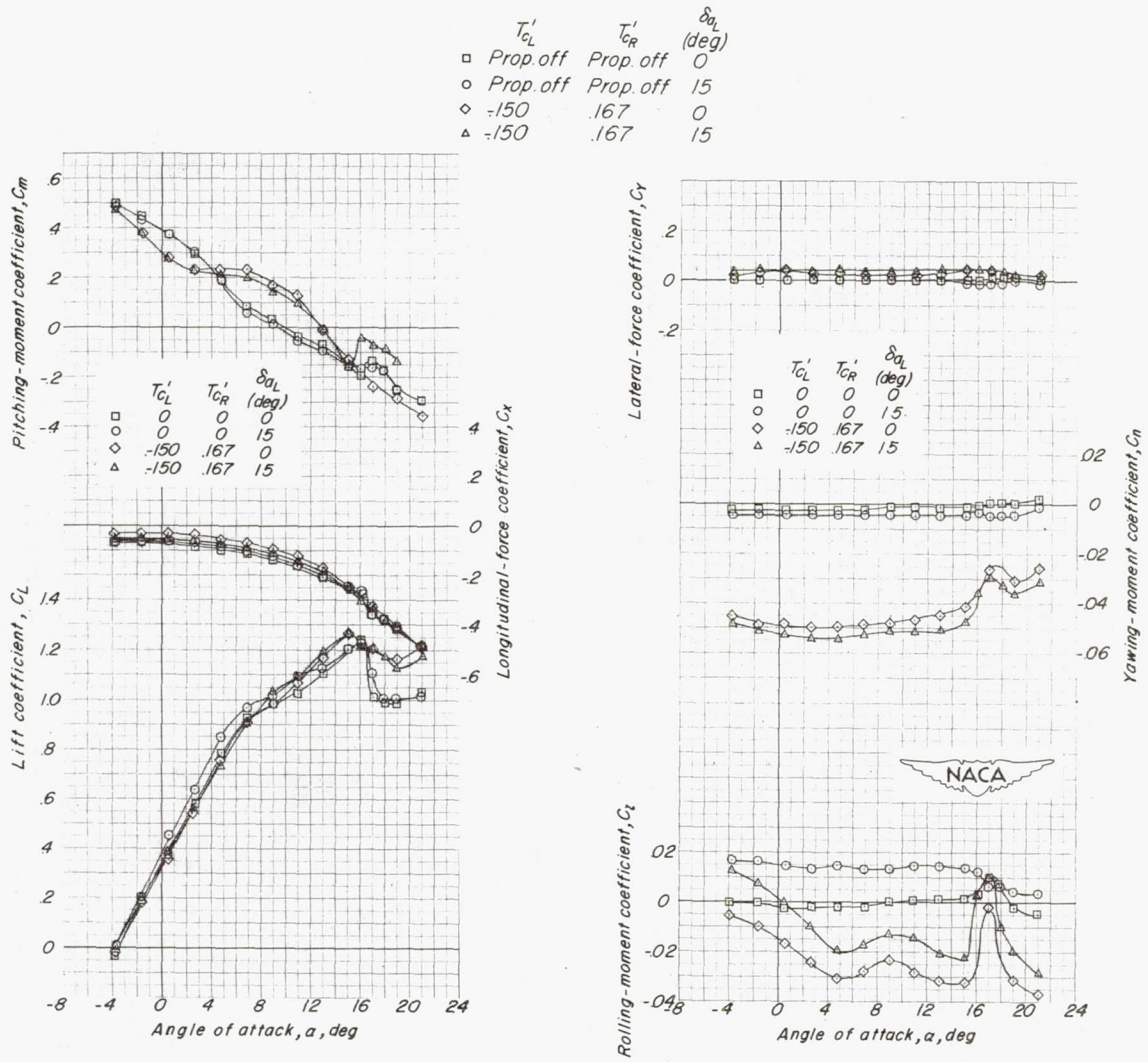

Figure 14.- Effect of thrust on the aerodynamic characteristics with ailerons deflected. $\delta_f = 0^\circ$; $i_t = -4^\circ$.

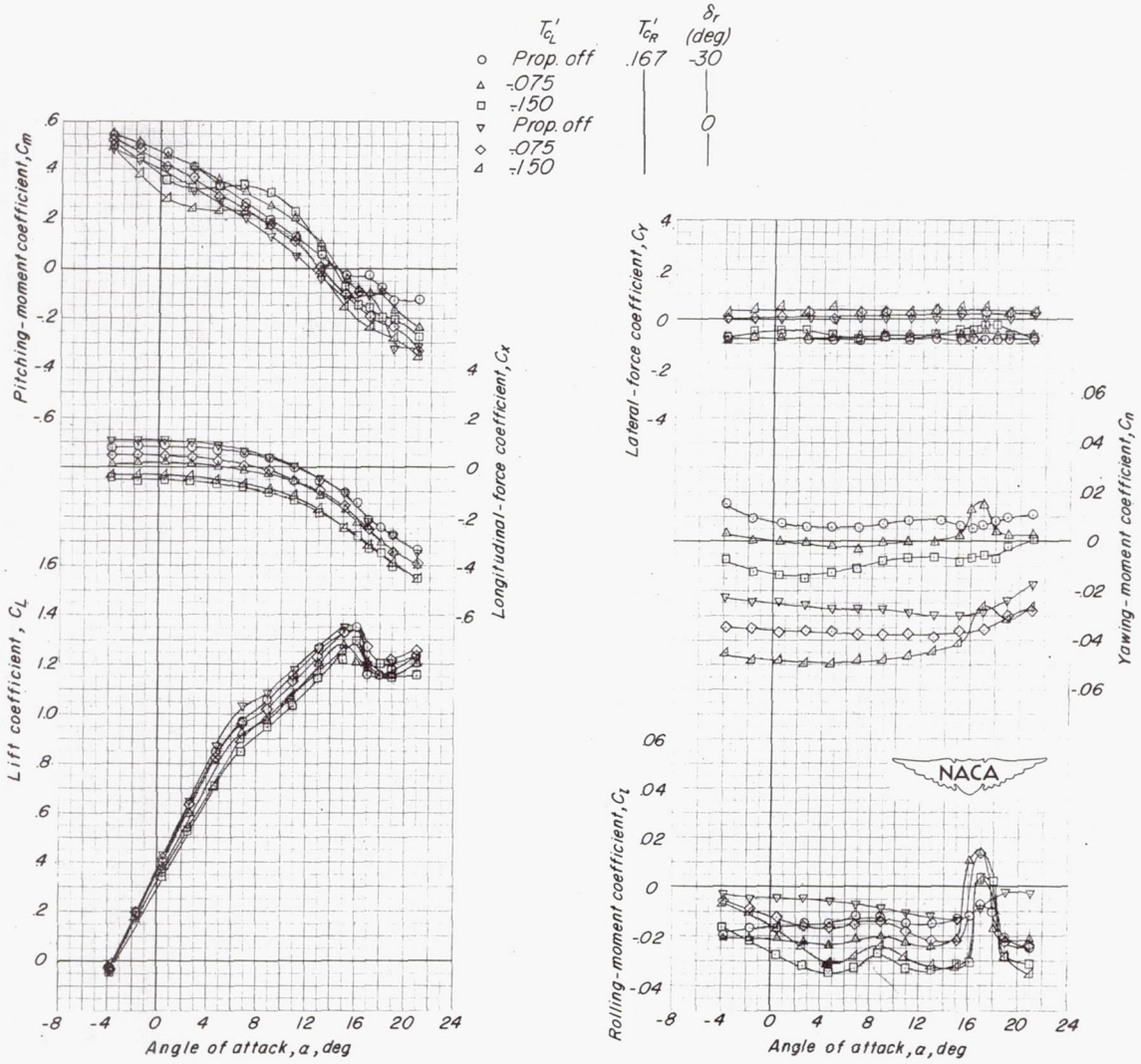

Figure 15.- Effect of asymmetric thrust on the aerodynamic characteristics with the rudder deflected. $\delta_f = 0°$; $i_t = -4°$.

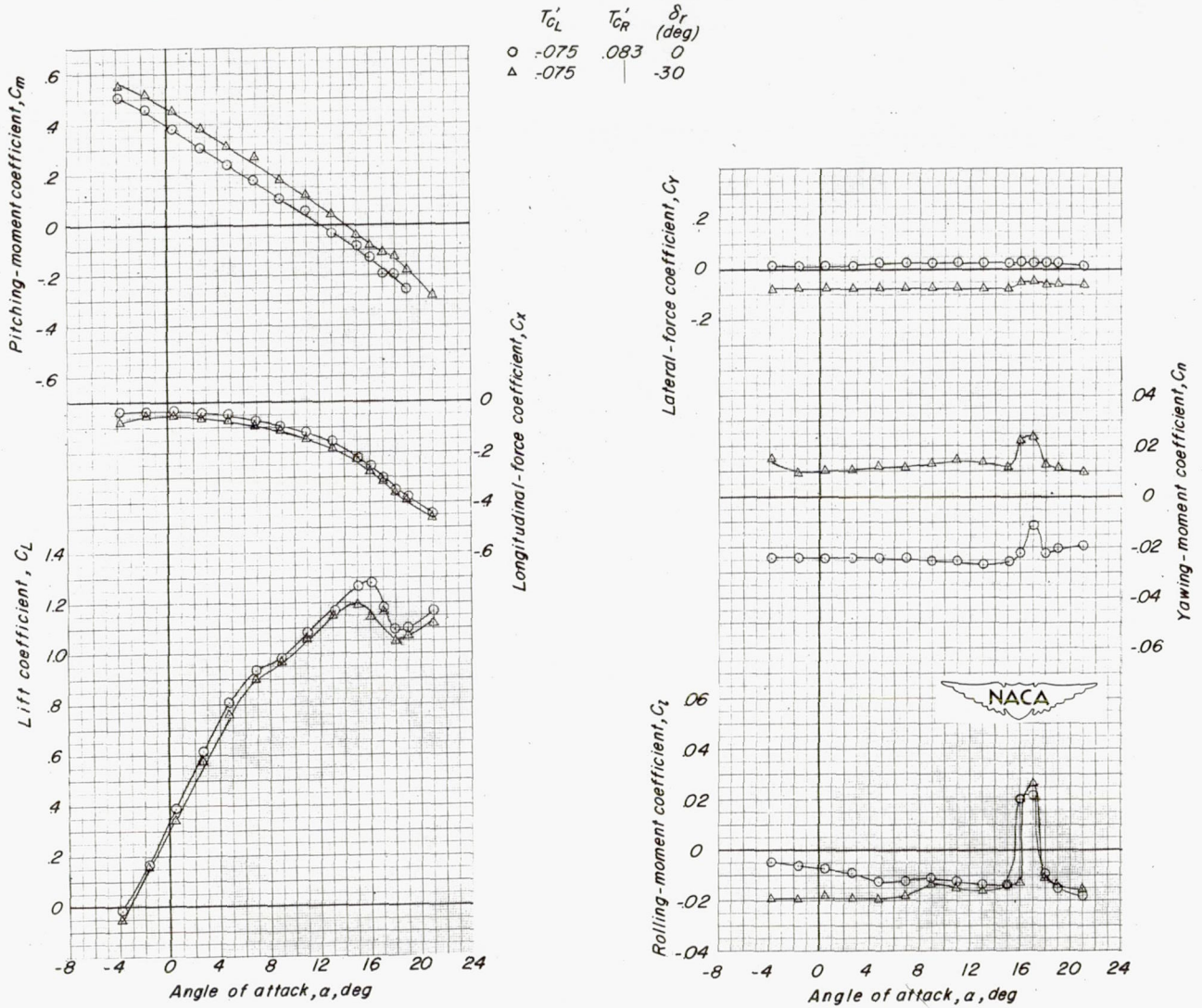

Figure 15.- Concluded.

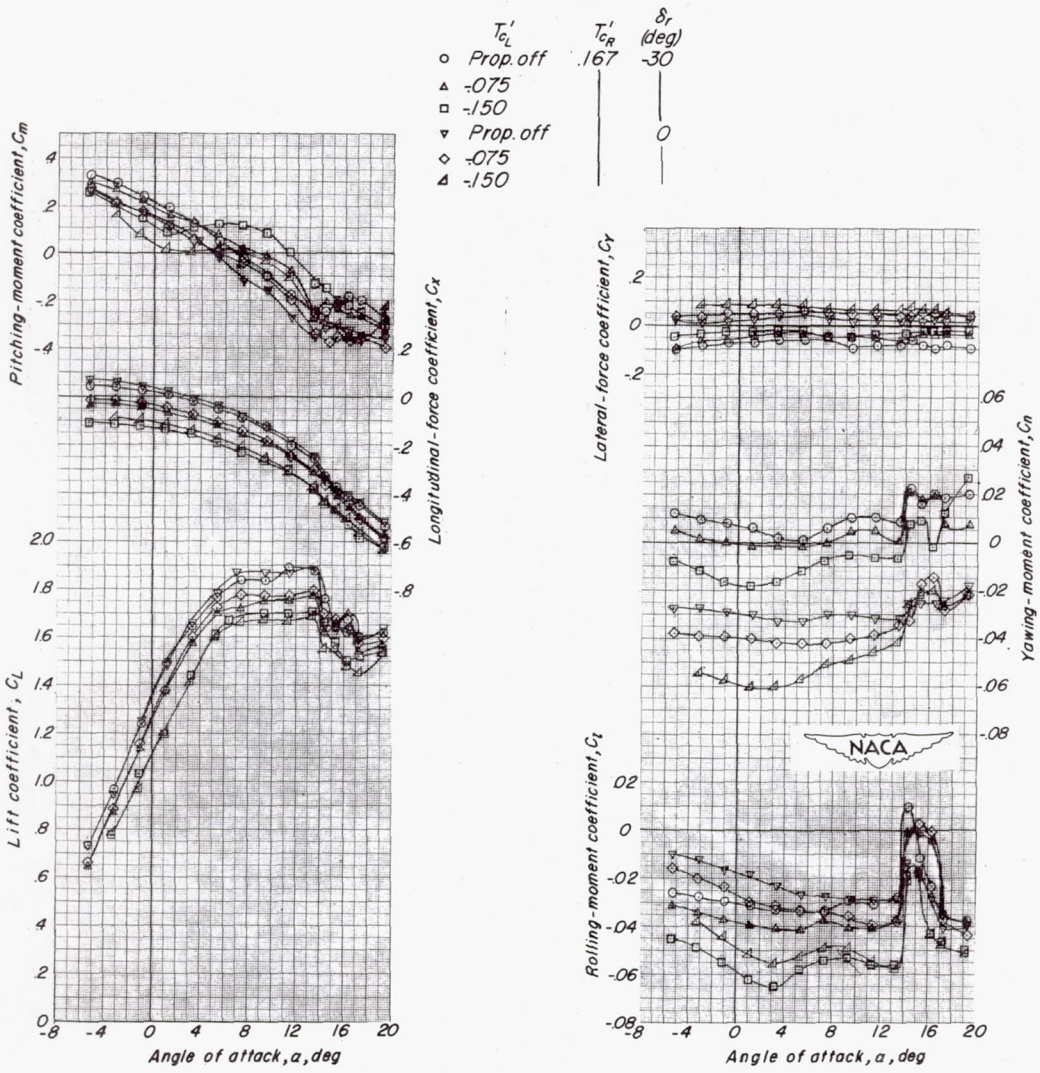

Figure 16.- Effect of asymmetric thrust on the aerodynamic characteristics with the rudder deflected. $\delta_f = 25^\circ$; $i_t = 0^\circ$.

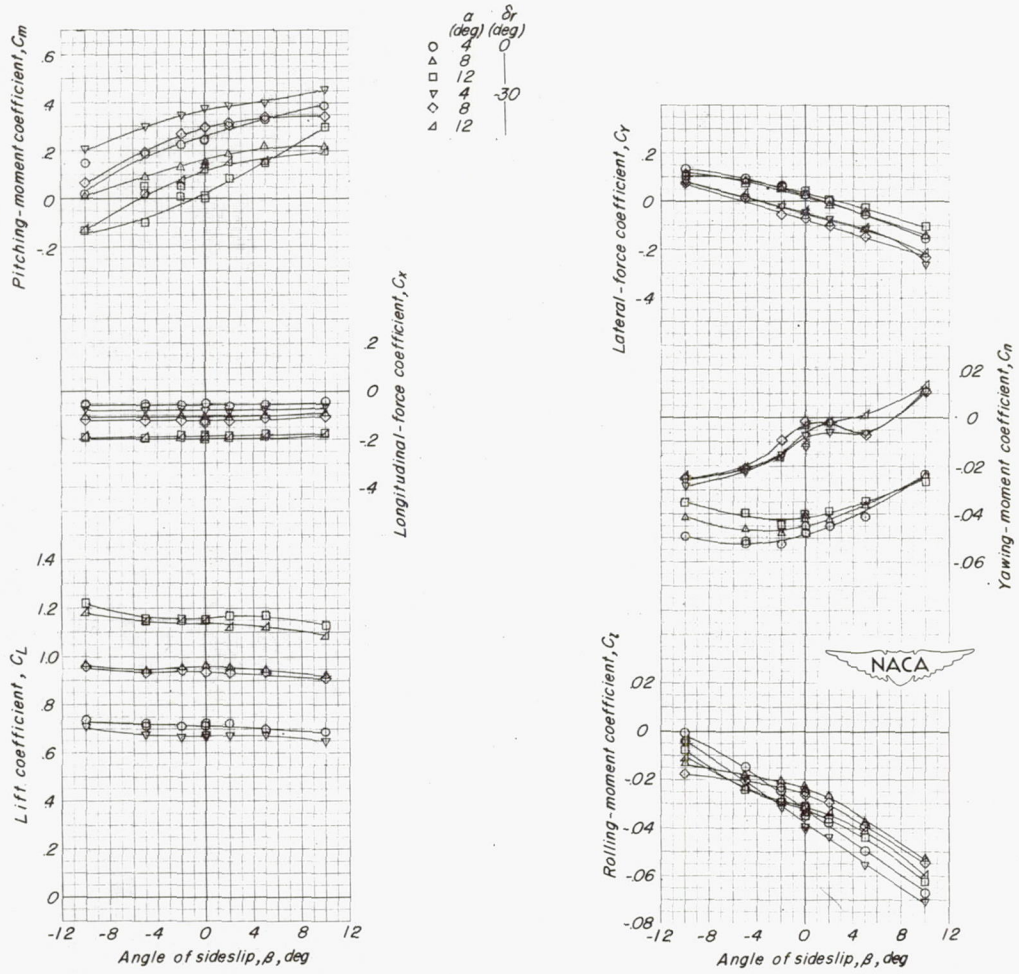

(a) $\delta_f = 0^\circ$; $i_t = -4^\circ$.

Figure 17.- Effect of asymmetric thrust in sideslip at several angles of attack with and without rudder deflection. $T_c{}'_L = -0.150$; $T_c{}'_R = 0.167$.

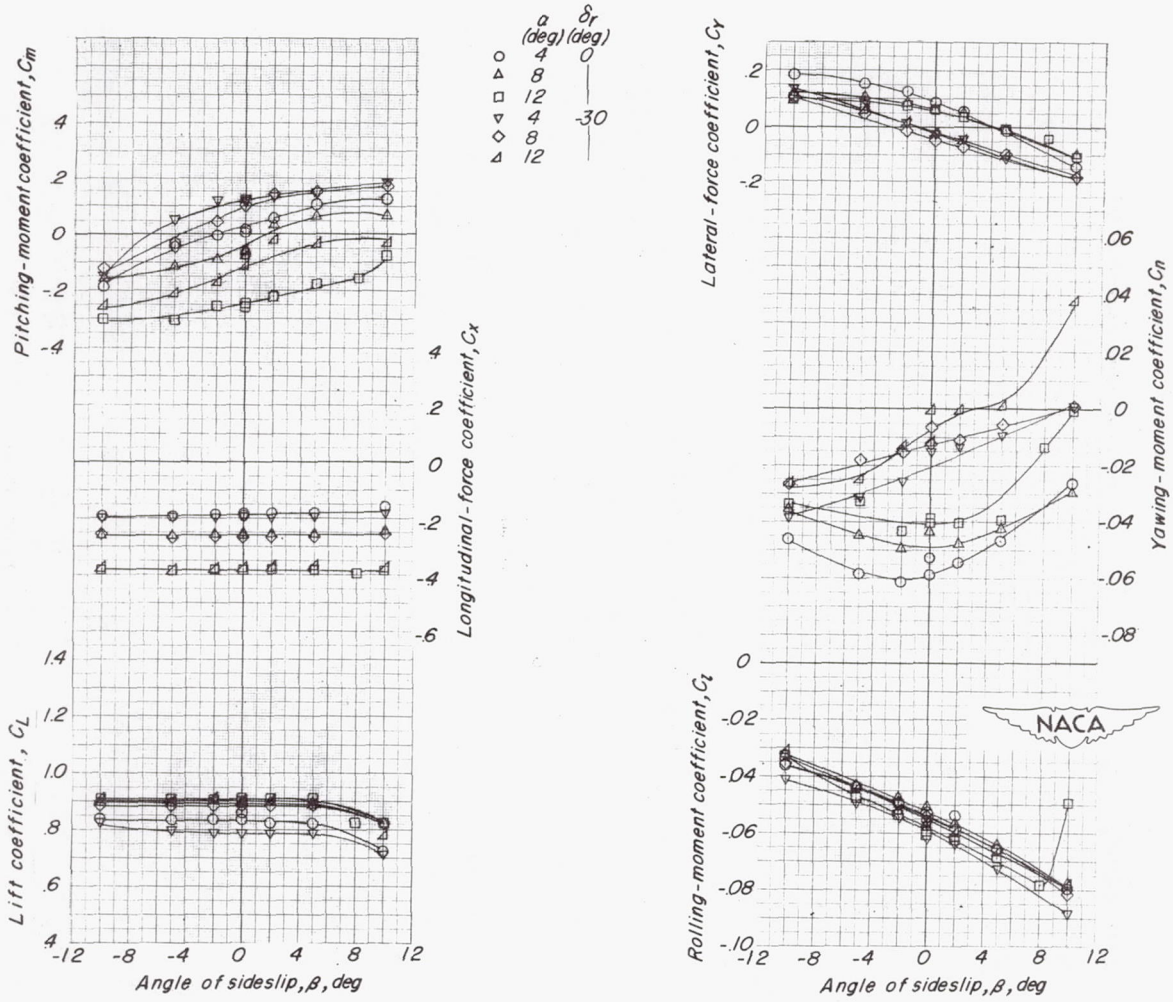

(b) $\delta_f = 25^\circ$; $i_t = 0^\circ$.

Figure 17.- Concluded.

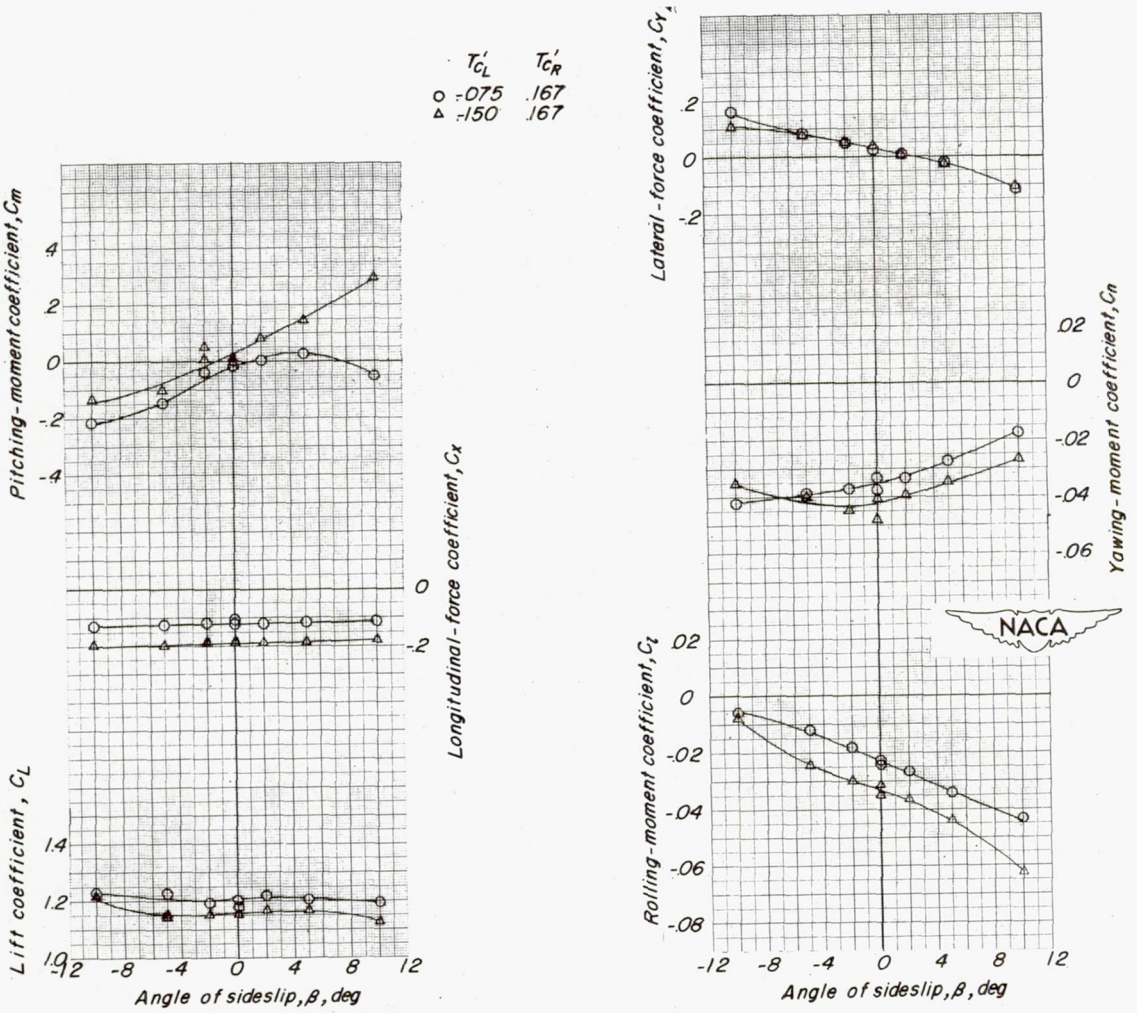

(a) $\delta_f = 0^\circ$; $i_t = -4^\circ$.

Figure 18.- Effect of asymmetric thrust in sideslip. $\alpha = 12^\circ$; $\delta_r = 0^\circ$.

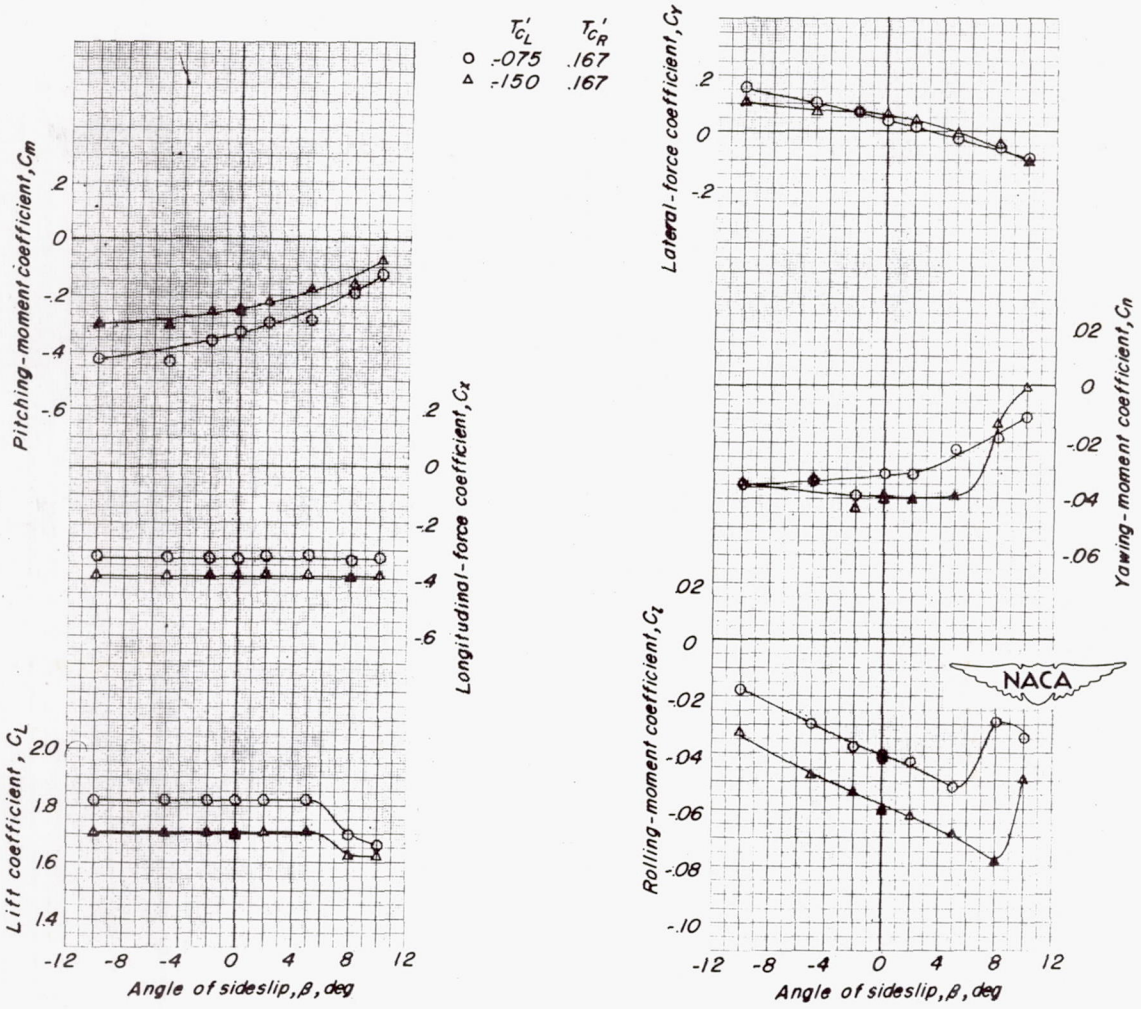

(b) $\delta_f = 25°$; $i_t = 0°$.

Figure 18.- Concluded.

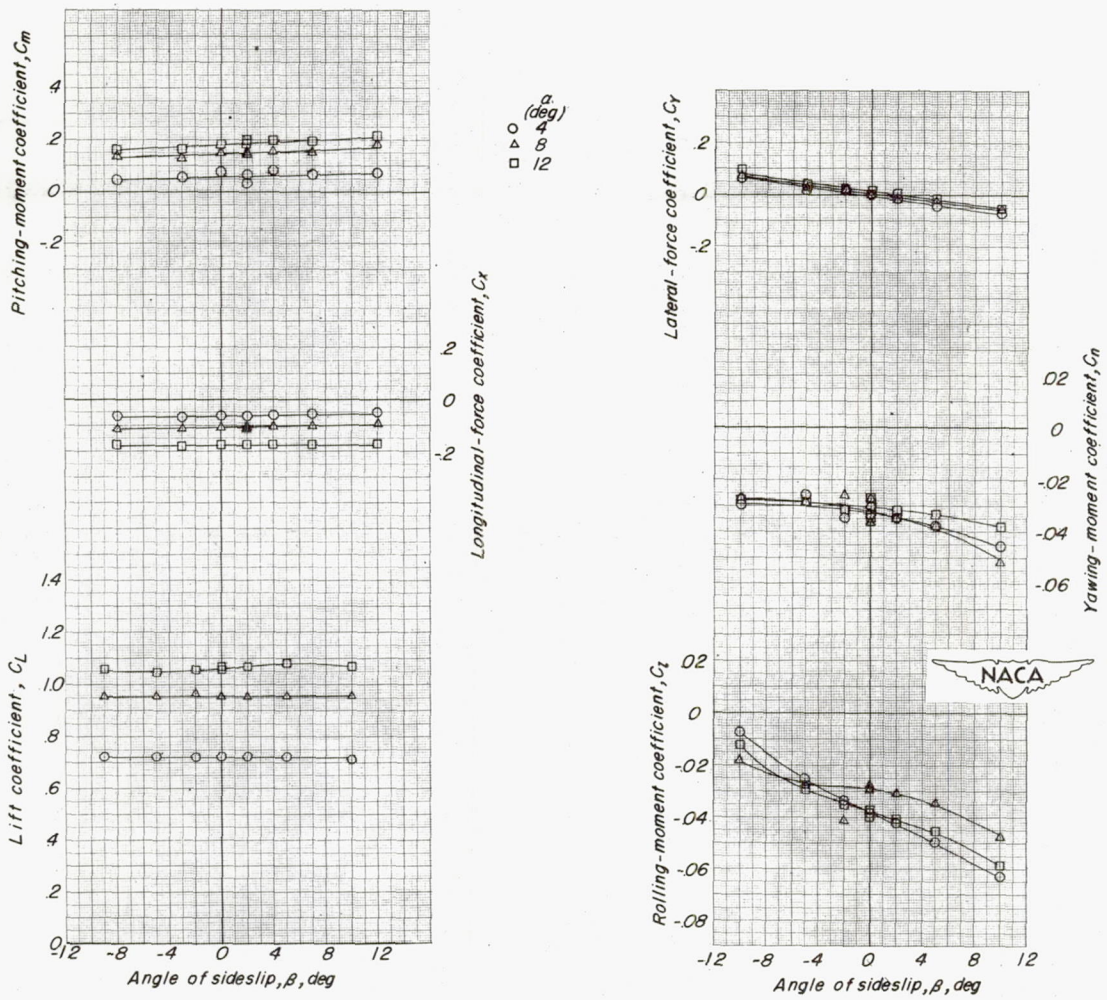

(a) $\delta_f = 0^\circ$.

Figure 19.- Effect of asymmetric thrust in sideslip for several angles of attack. Tail off; $T_c'_L = -0.150$; $T_c'_R = 0.167$.

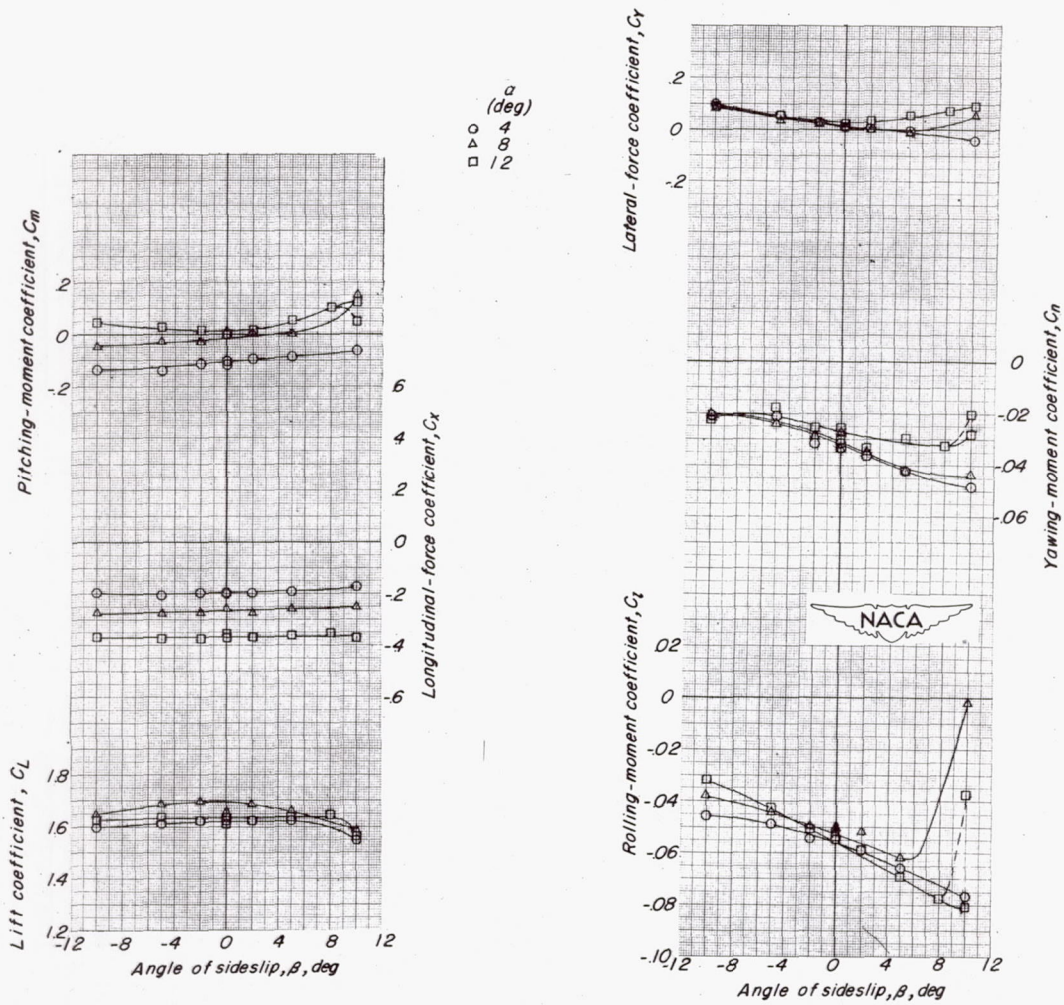

(b) $\delta_f = 25^\circ$.

Figure 19.- Concluded.

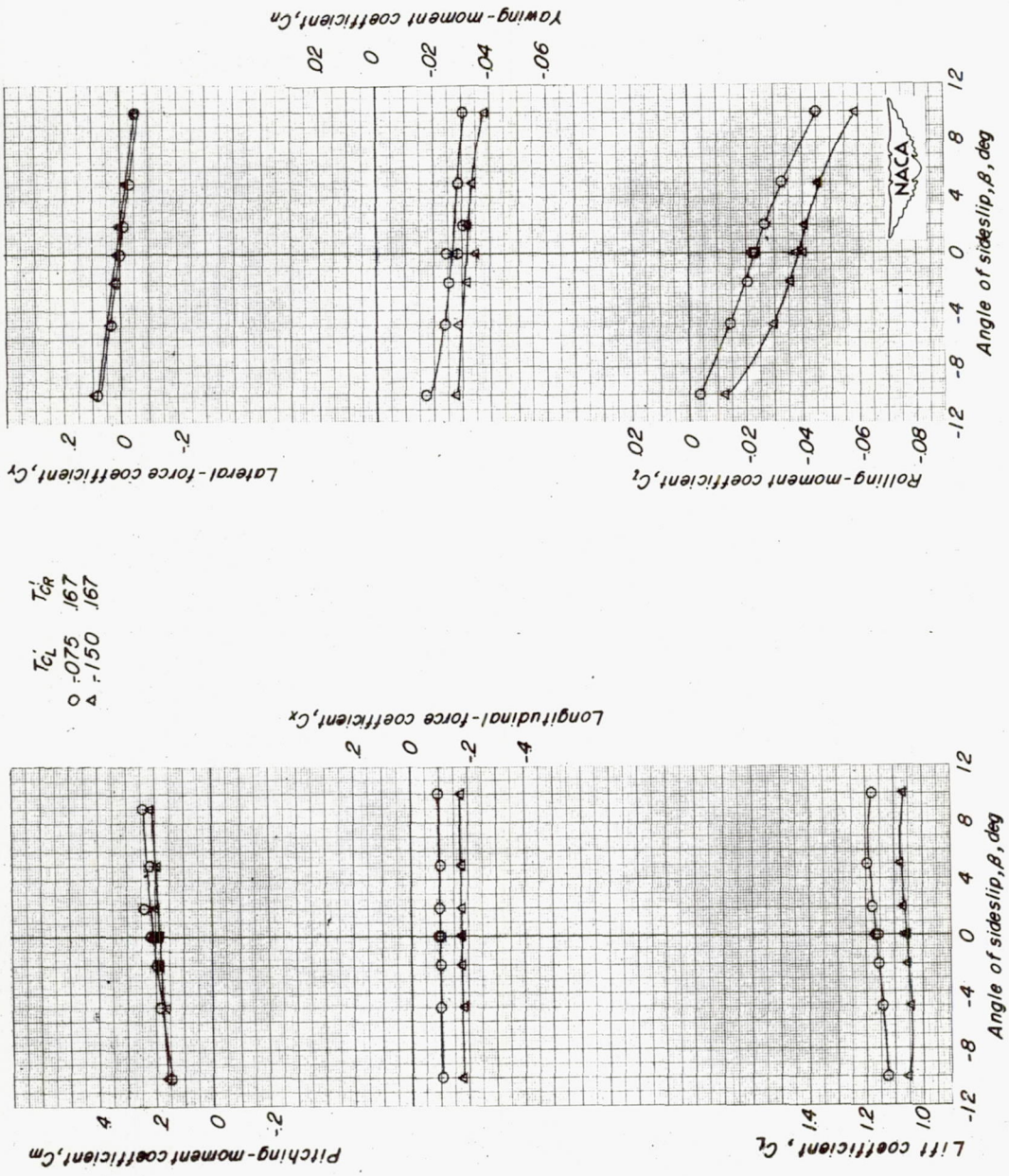

(a) $\delta_f = 0^\circ$.

Figure 20.- Effect of asymmetric thrust in sideslip. Tail off; $\alpha = 12^\circ$.

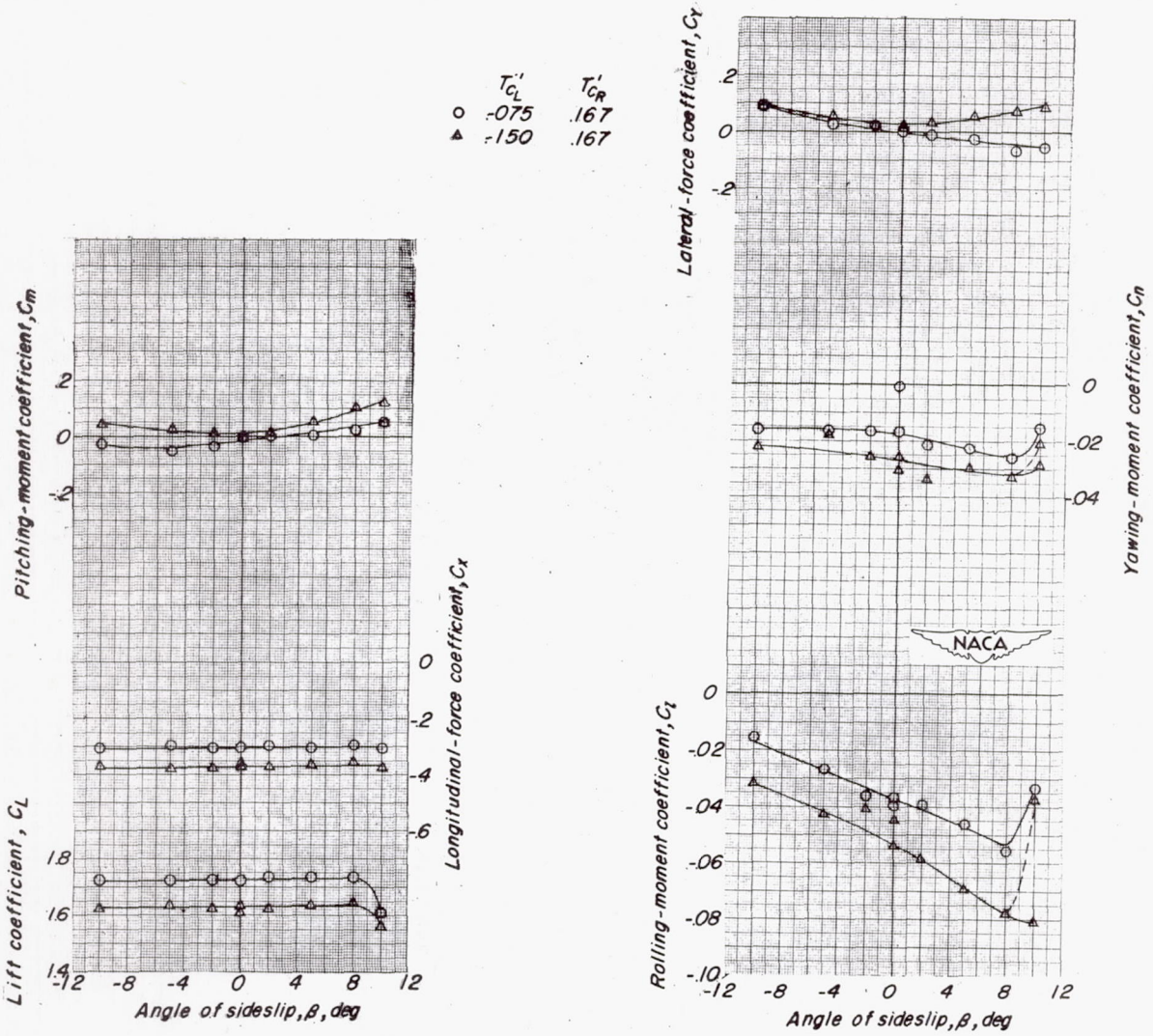

(b) $\delta_f = 25^\circ$.

Figure 20.- Concluded.

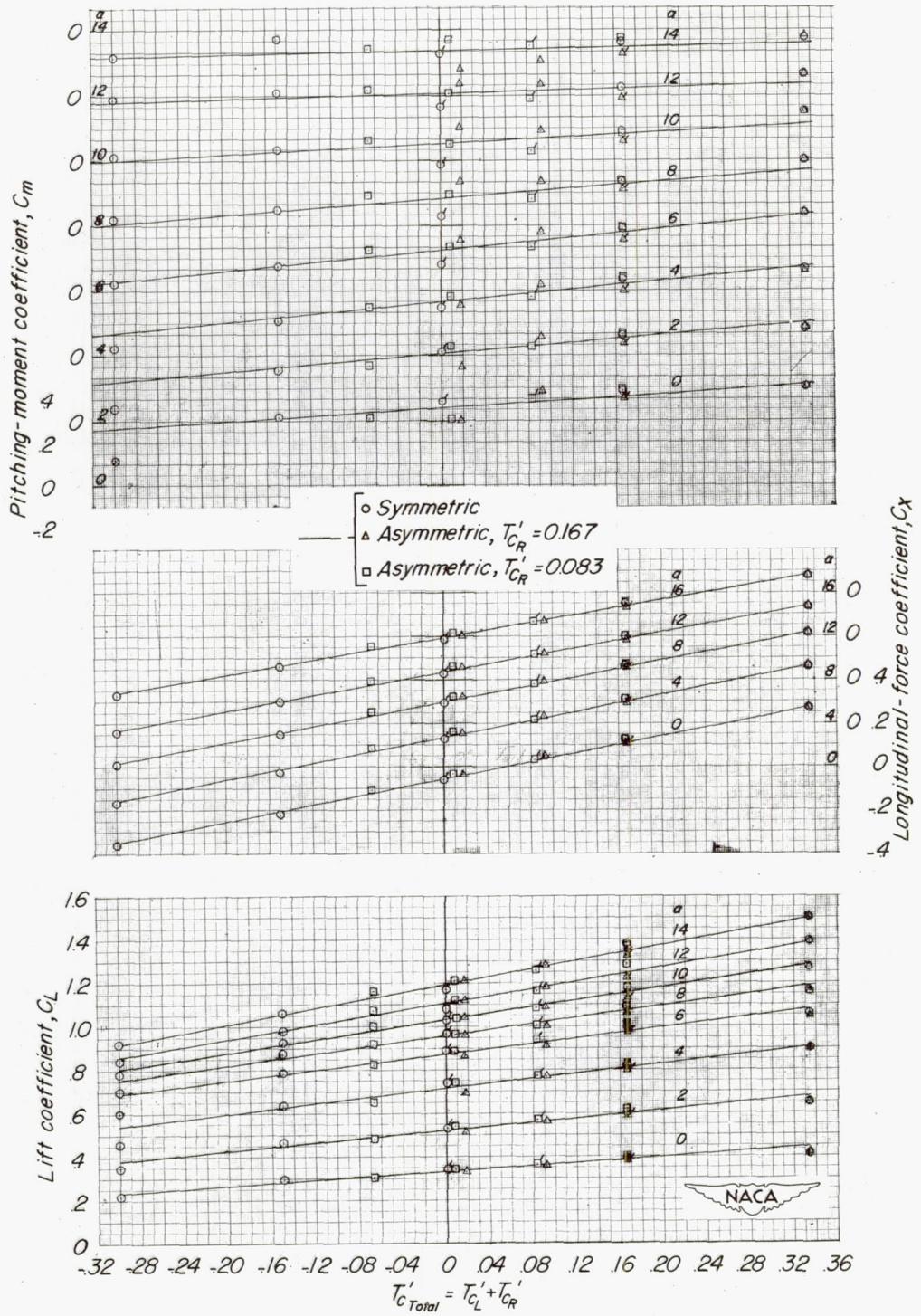

(a) Effect of total thrust coefficient on aerodynamic characteristics.

Figure 21.- A cross plot of basic aerodynamic data against thrust coefficient. $\delta_f = 0^\circ$; $i_t = -4^\circ$.

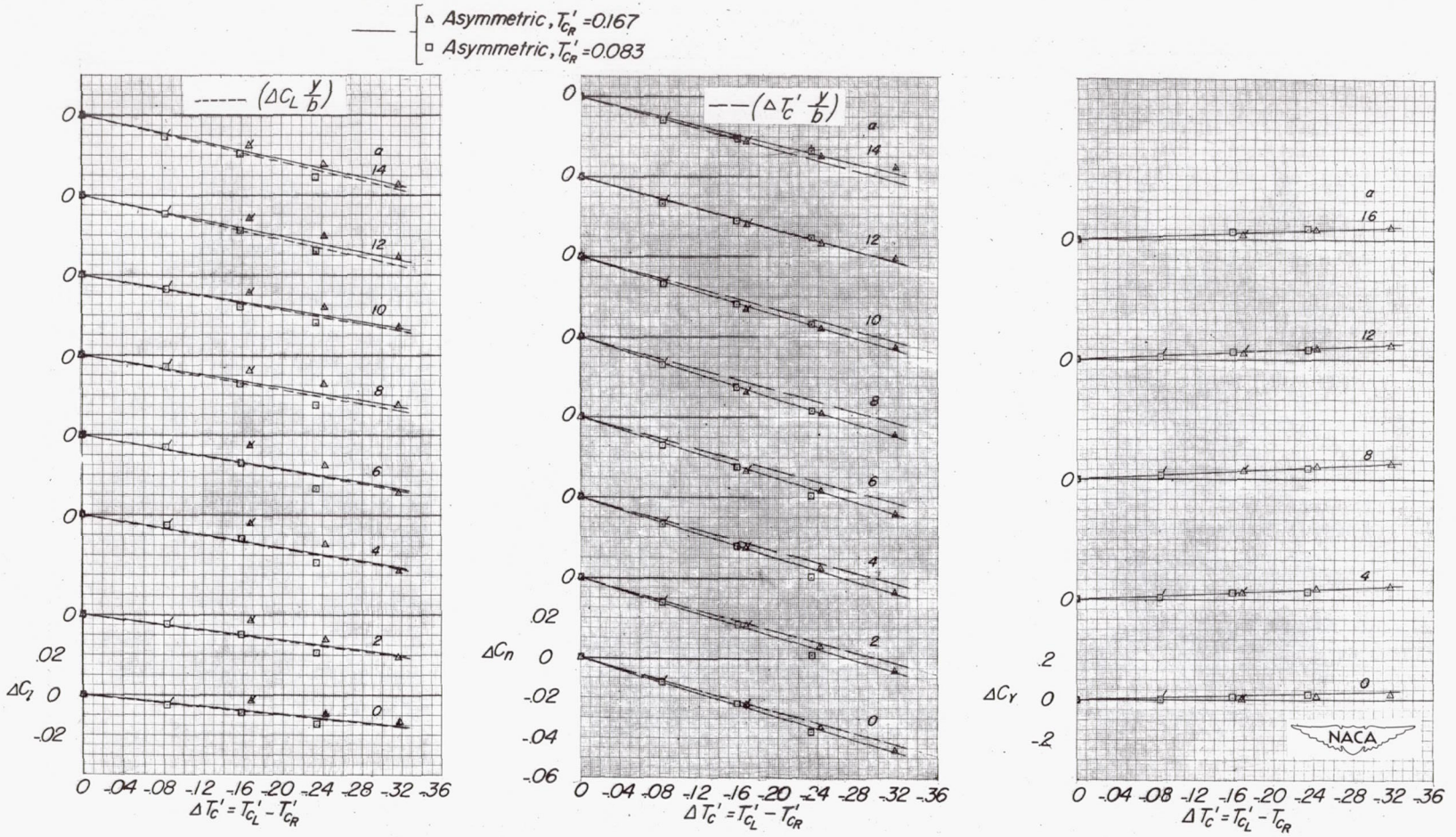

(b) Effect of asymmetric thrust coefficient on aerodynamic characteristics.

Figure 21.- Concluded.

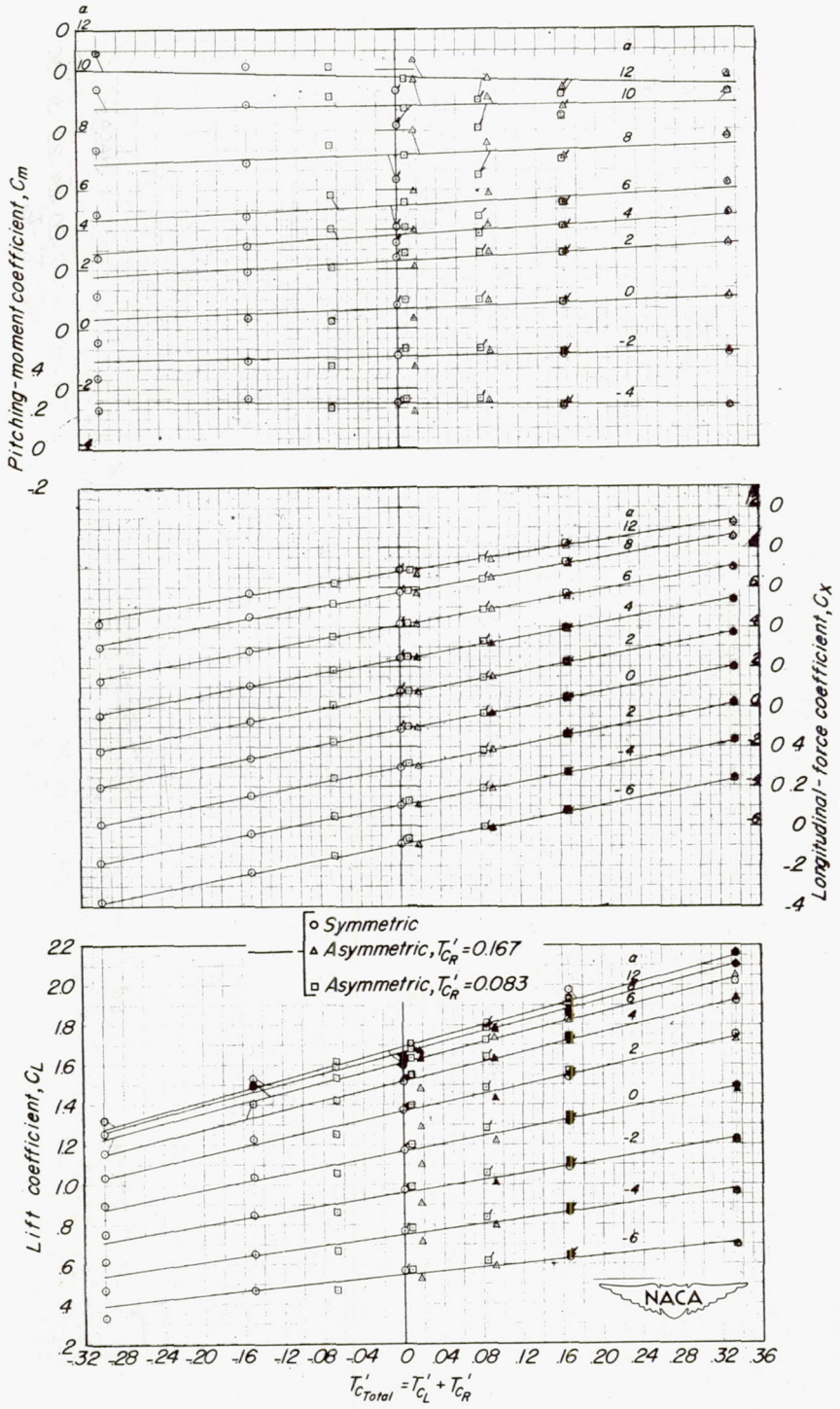

(a) Effect of total thrust coefficient on aerodynamic characteristics.

Figure 22.- A cross plot of basic aerodynamic data against thrust coefficient. $\delta_f = 25^\circ$; $i_t = 0^\circ$.

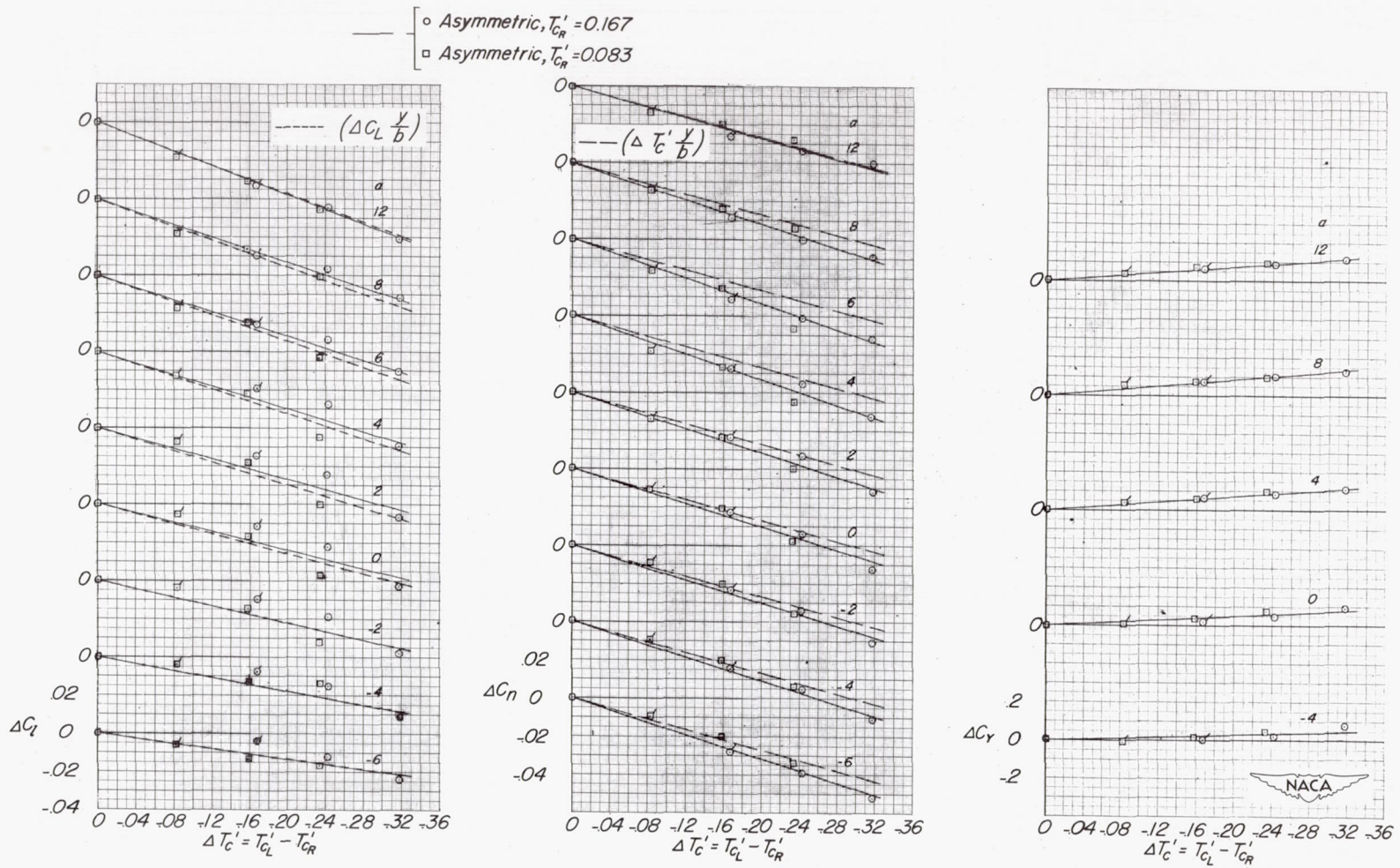

(b) Effect of asymmetric thrust coefficient on aerodynamic characteristics.

Figure 22.- Concluded.

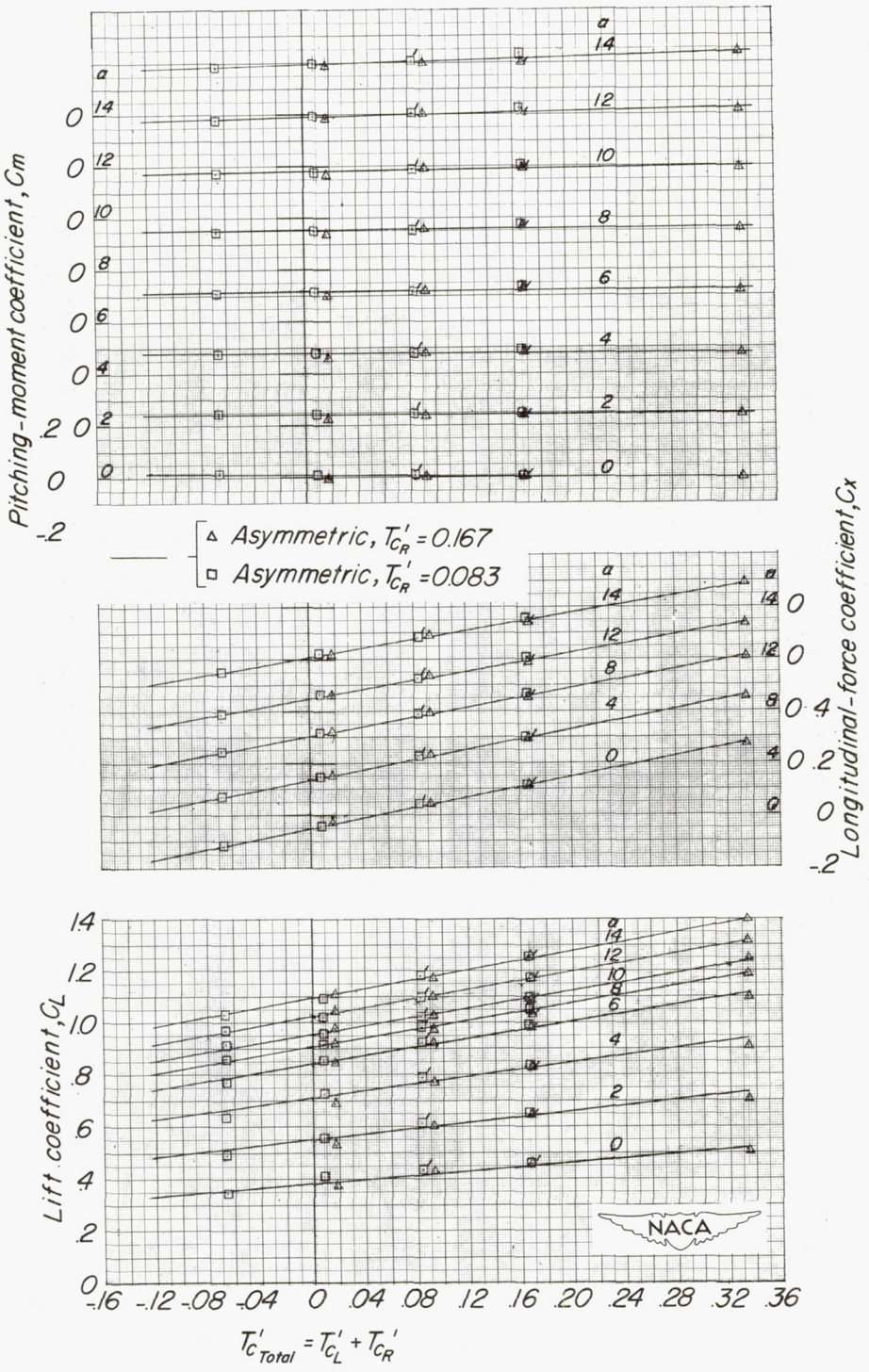

(a) Effect of total thrust coefficients on aerodynamic characteristics.

Figure 23.- A cross plot of basic aerodynamic data against thrust coefficient. Tail off; $\delta_f = 0^o$.

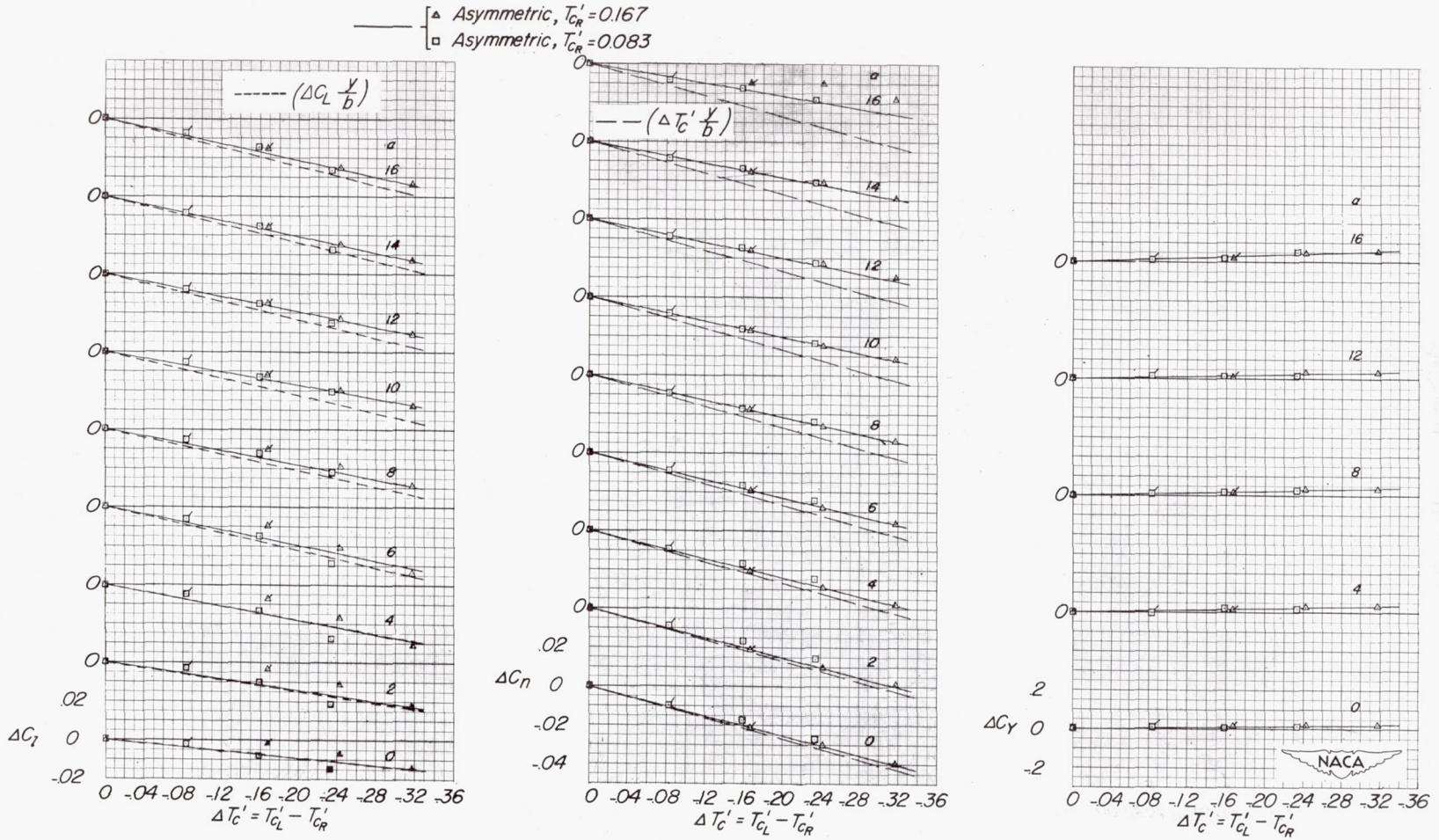

(b) Effect of asymmetric thrust coefficient on aerodynamic characteristics.

Figure 23.- Concluded.

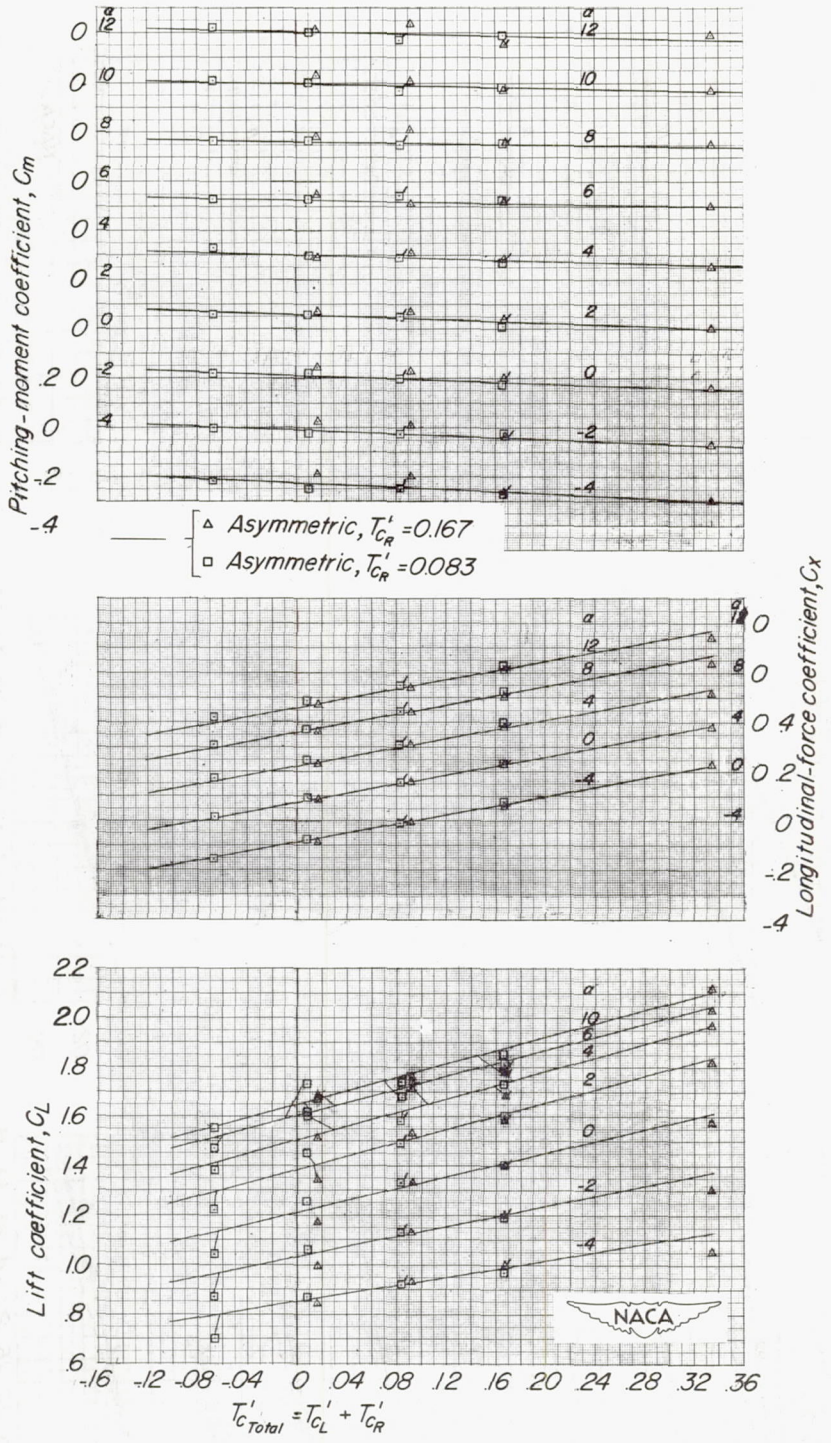

(a) Effect of total thrust coefficient on aerodynamic characteristics.

Figure 24.- A cross plot of basic aerodynamic data against thrust coefficient. Tail off; $\delta_f = 25^\circ$.

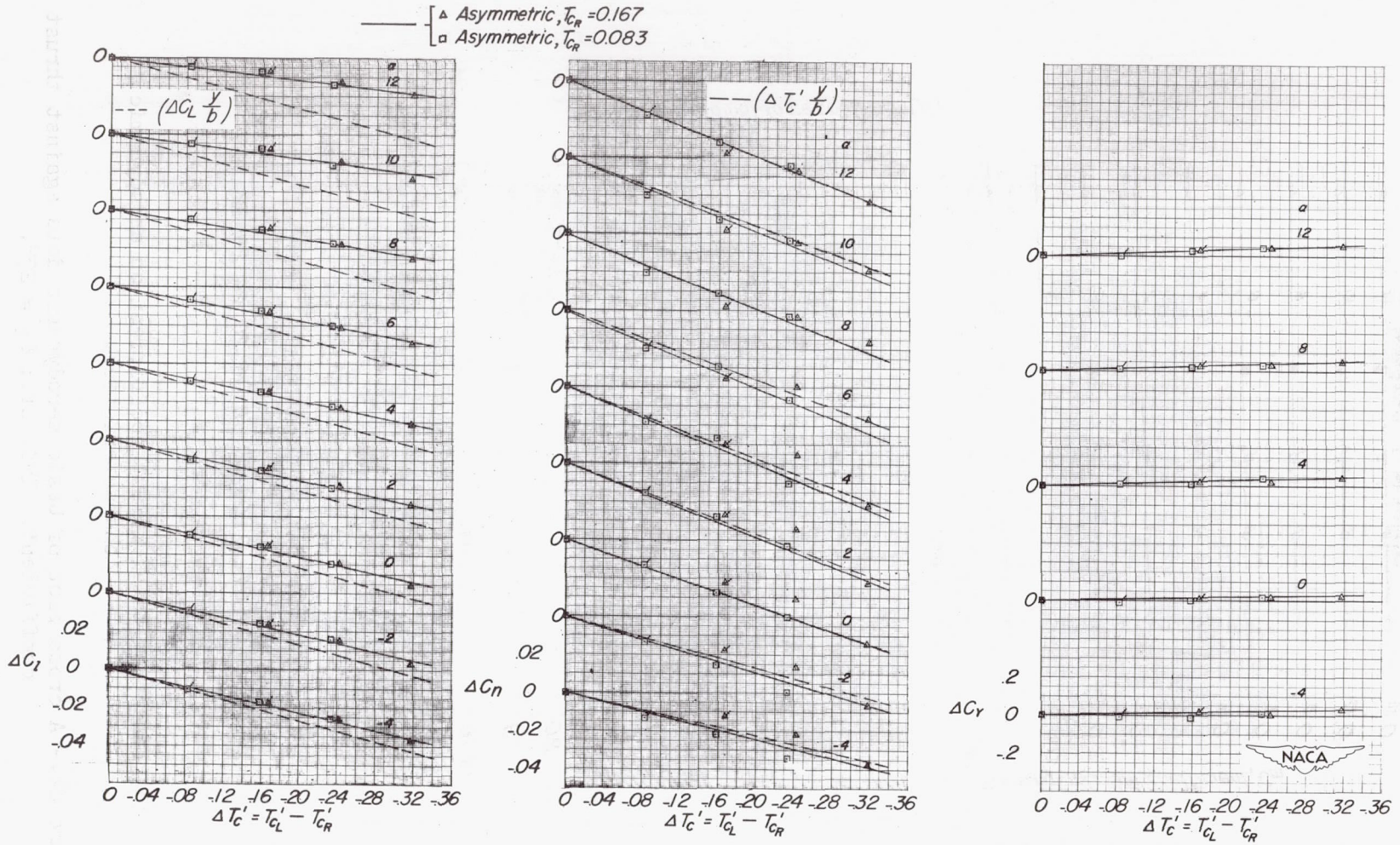

(b) Effect of asymmetric thrust coefficient on aerodynamic characteristics.

Figure 24.- Concluded.

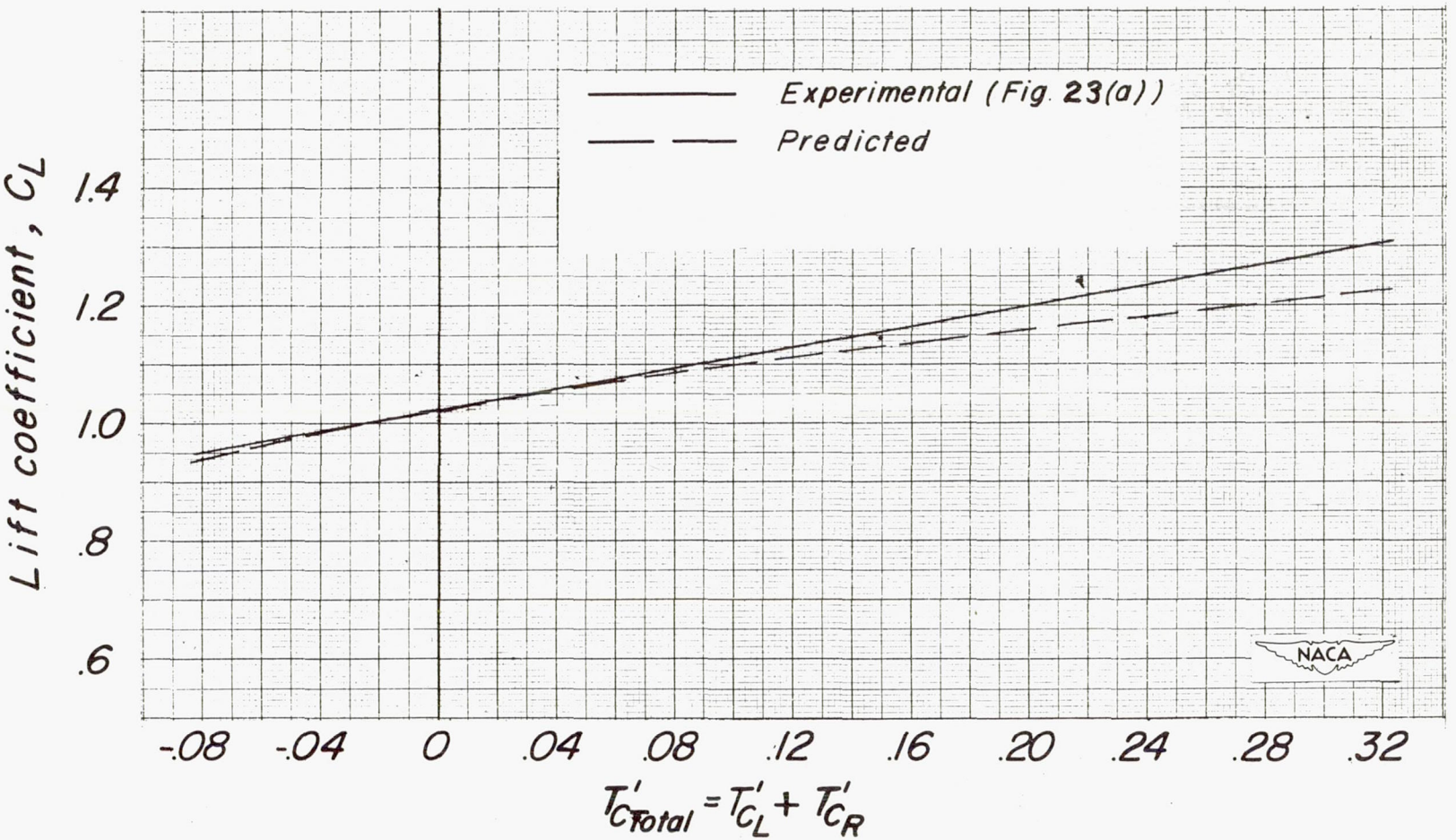

Figure 25.- Comparison of experimental and empirical lift variations with total thrust coefficient. Tail off; $\alpha = 12^{\circ}$.

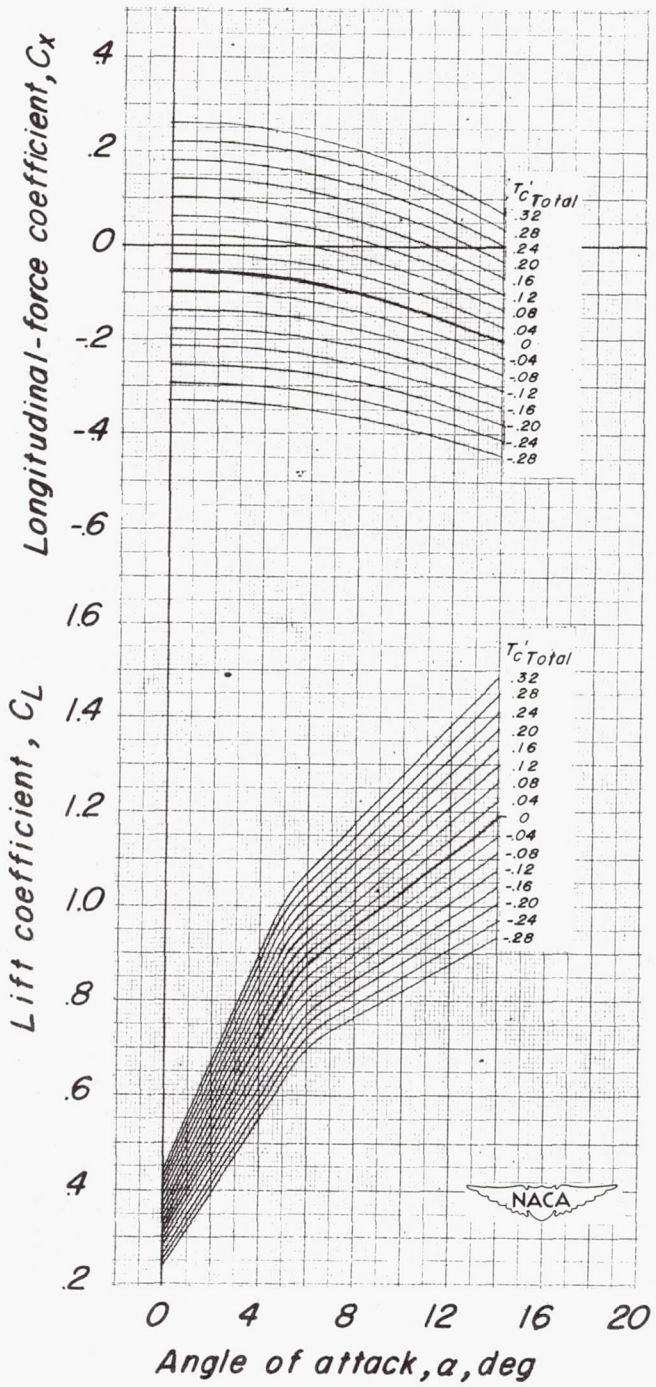

(a) Effect of total thrust coefficient on aerodynamic characteristics.

Figure 26.- Typical plots for various thrust conditions obtained from plots of linearized aerodynamic characteristics against thrust coefficient. Tail on; $\delta_f = 0^\circ$; $i_t = -4^\circ$.

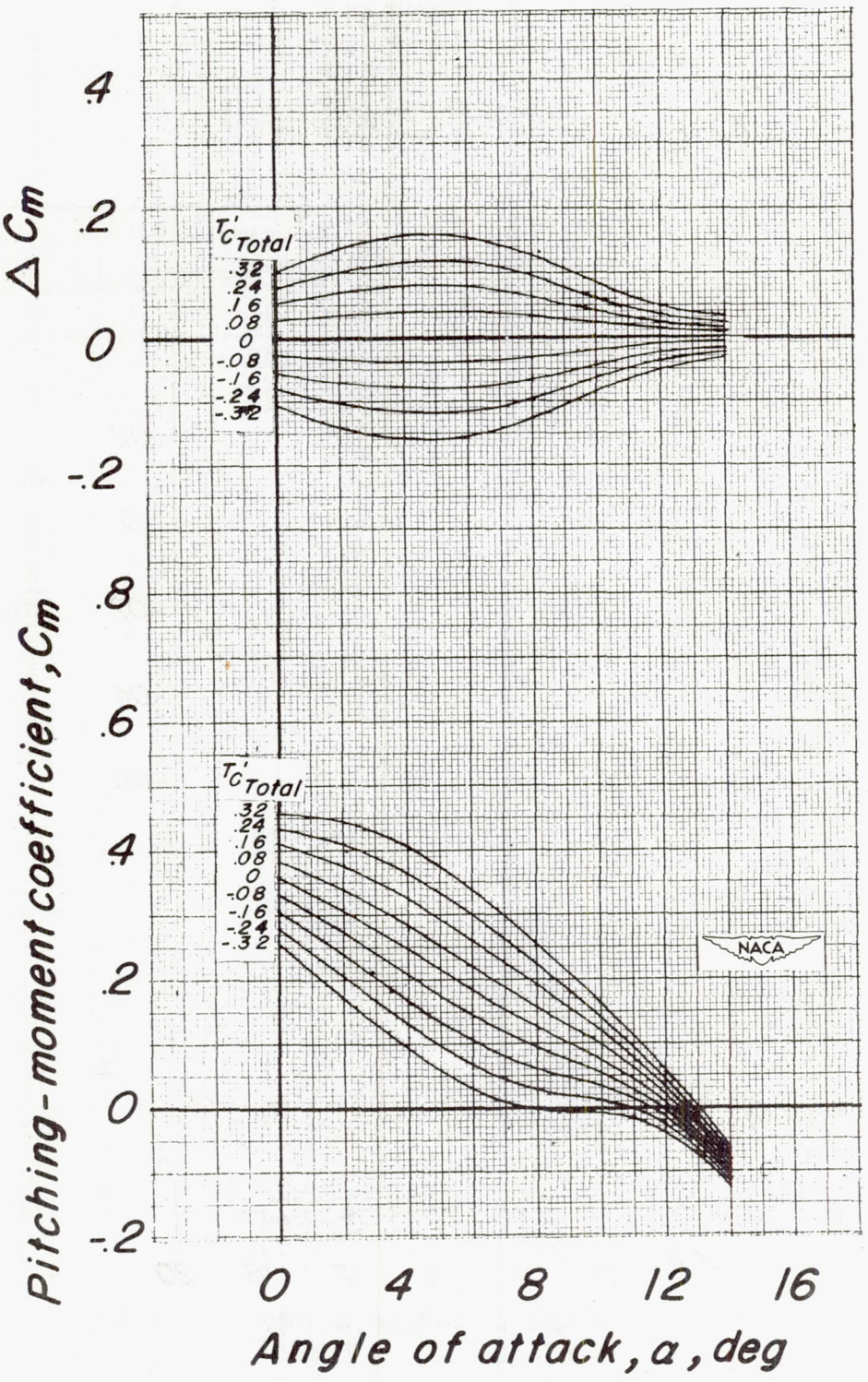

(a) Concluded.

Figure 26.- Continued.

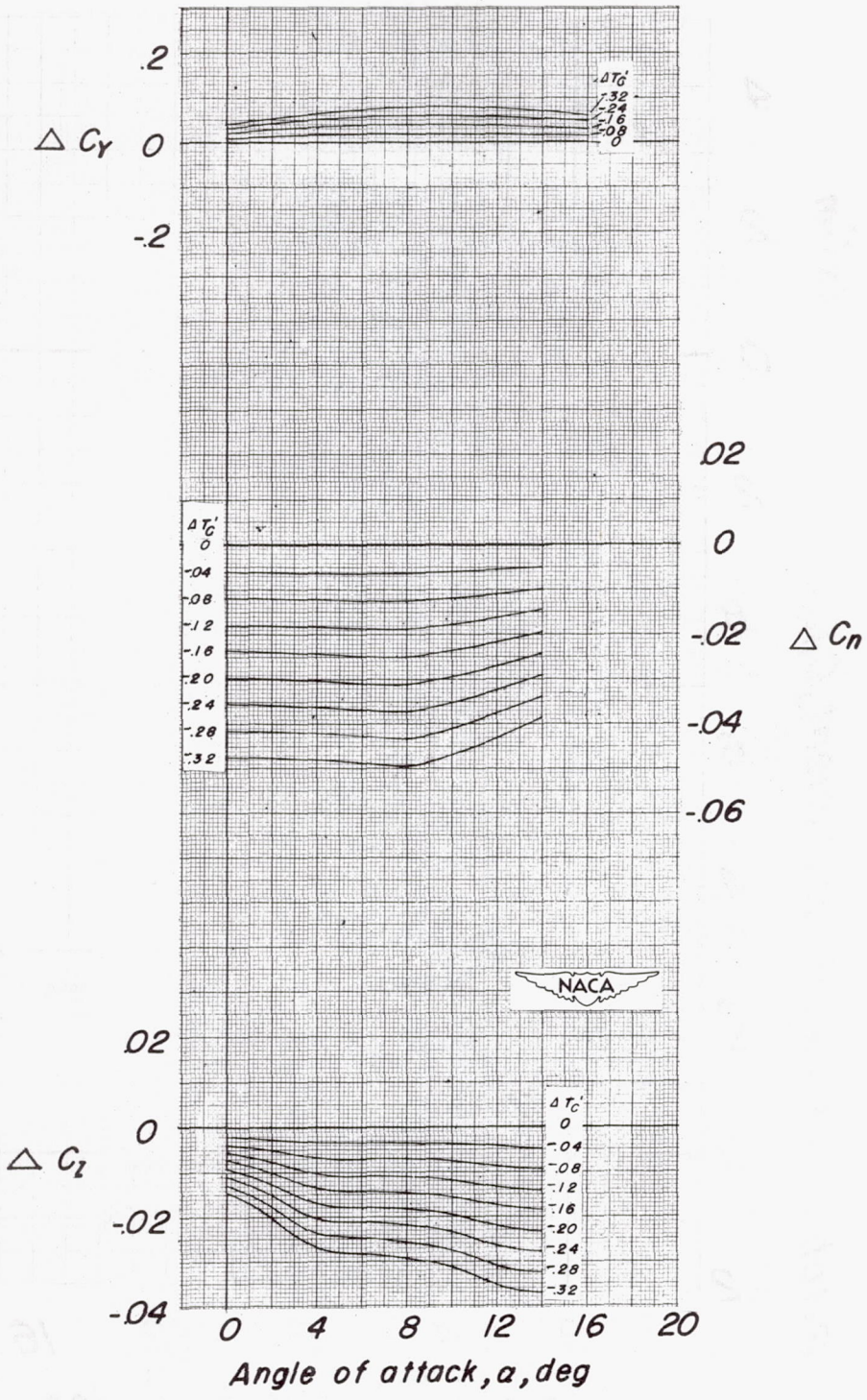

(b) Effects of asymmetric thrust coefficient on aerodynamic characteristics.

Figure 26.- Concluded.

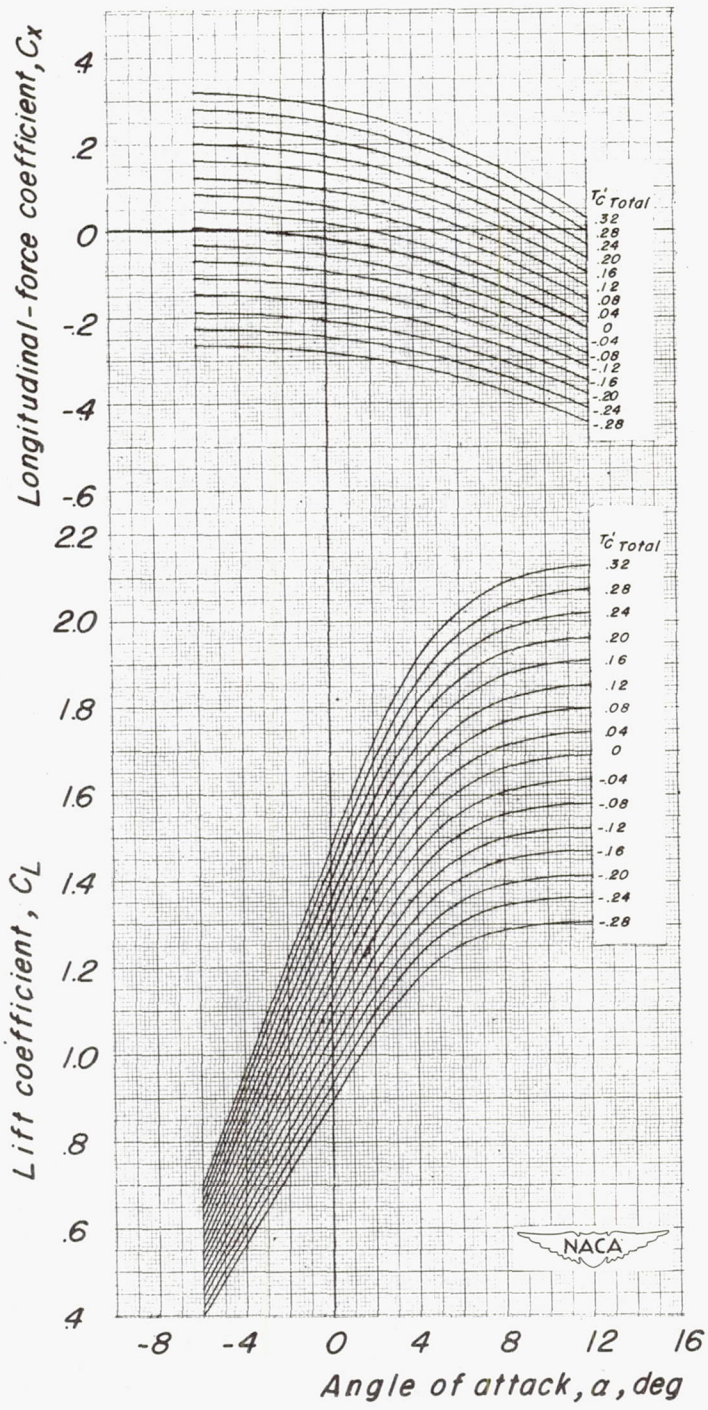

(a) Effect of total thrust coefficient on aerodynamic characteristics.

Figure 27.- Typical plots for various thrust conditions obtained from plots of linearized aerodynamic characteristics against thrust coefficient. Tail on; $\delta_f = 25^\circ$; $i_t = 0^\circ$.

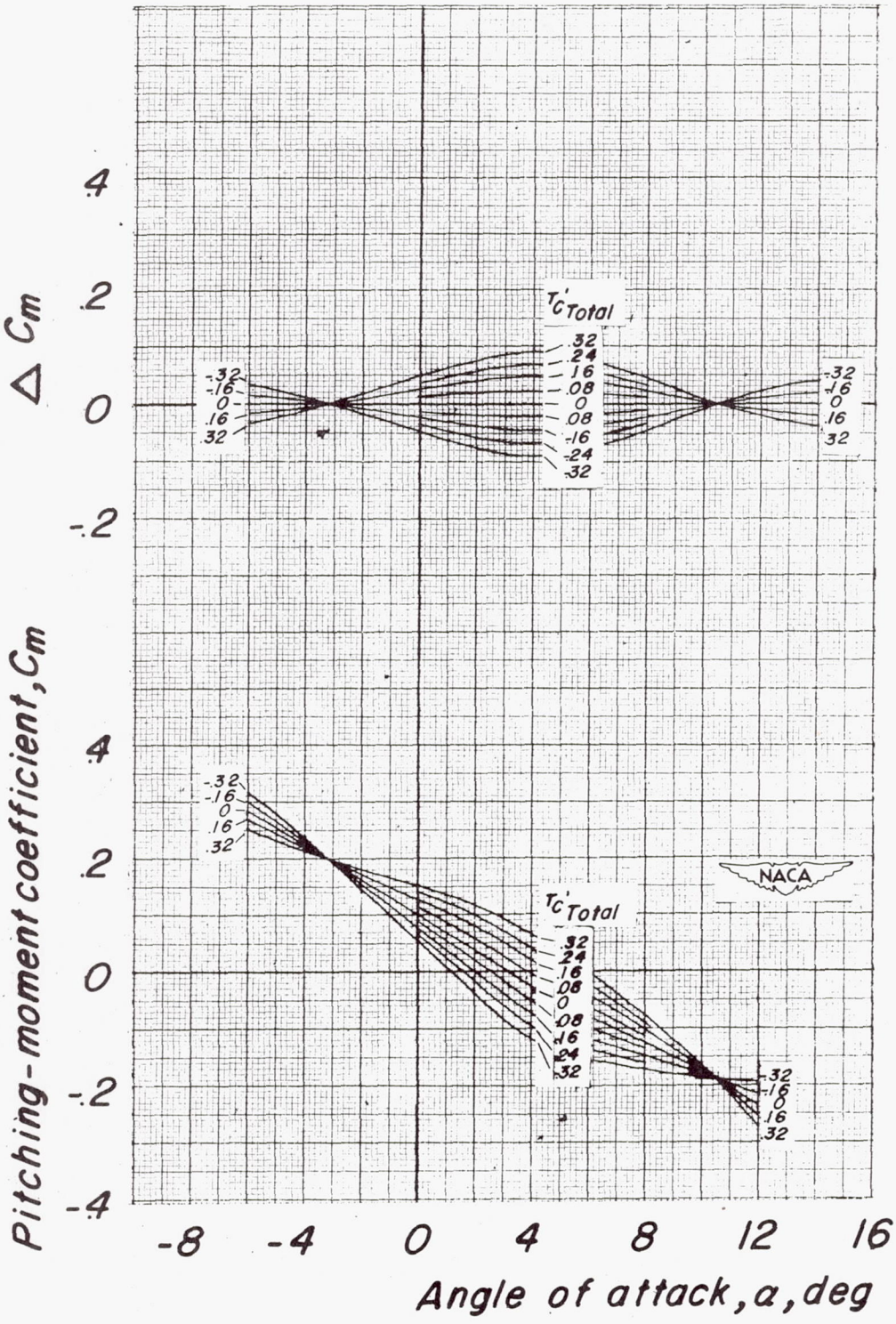

(a) Concluded.

Figure 27.- Continued.

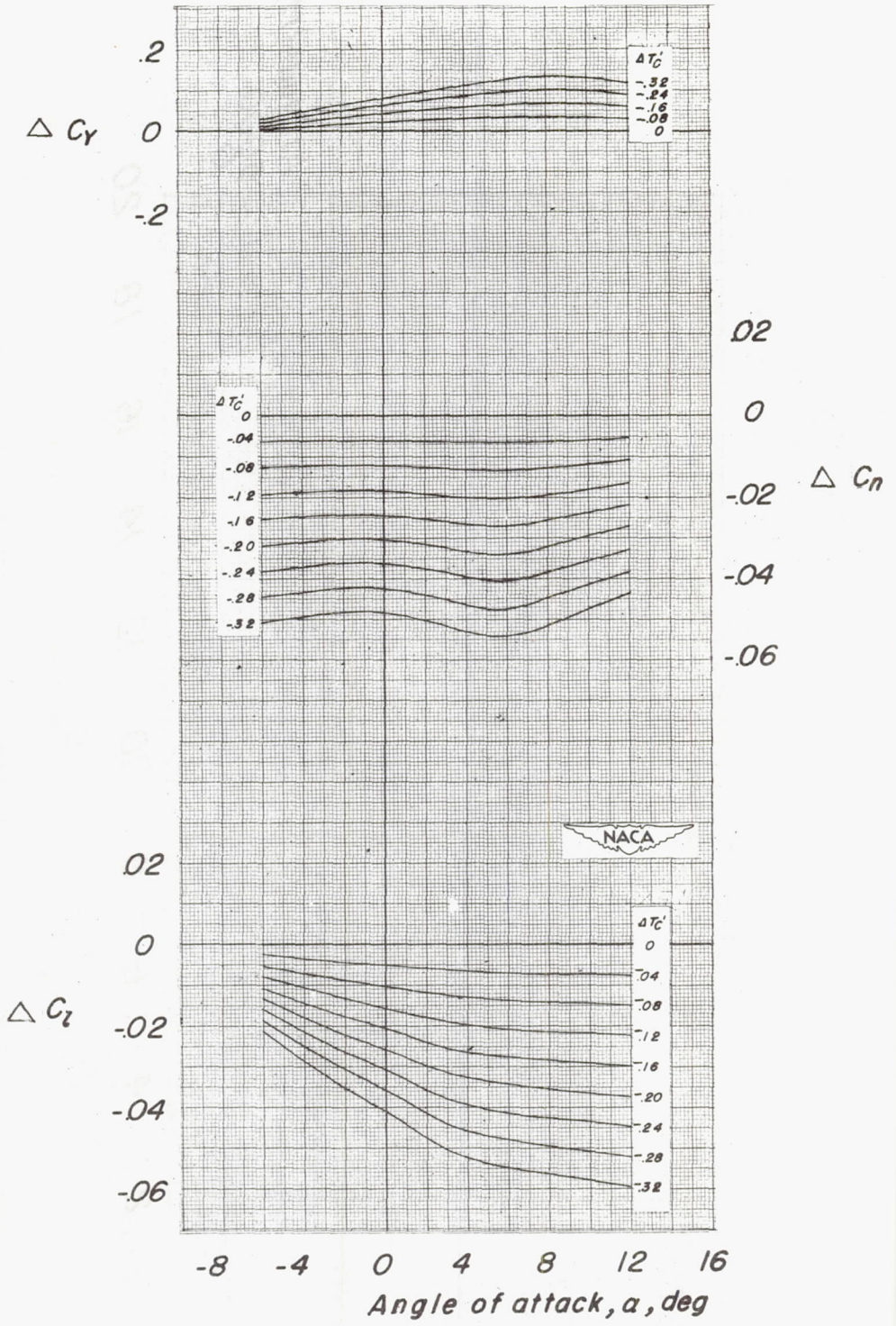

(b) Effect of asymmetric thrust coefficient on aerodynamic characteristics.

Figure 27.- Concluded.

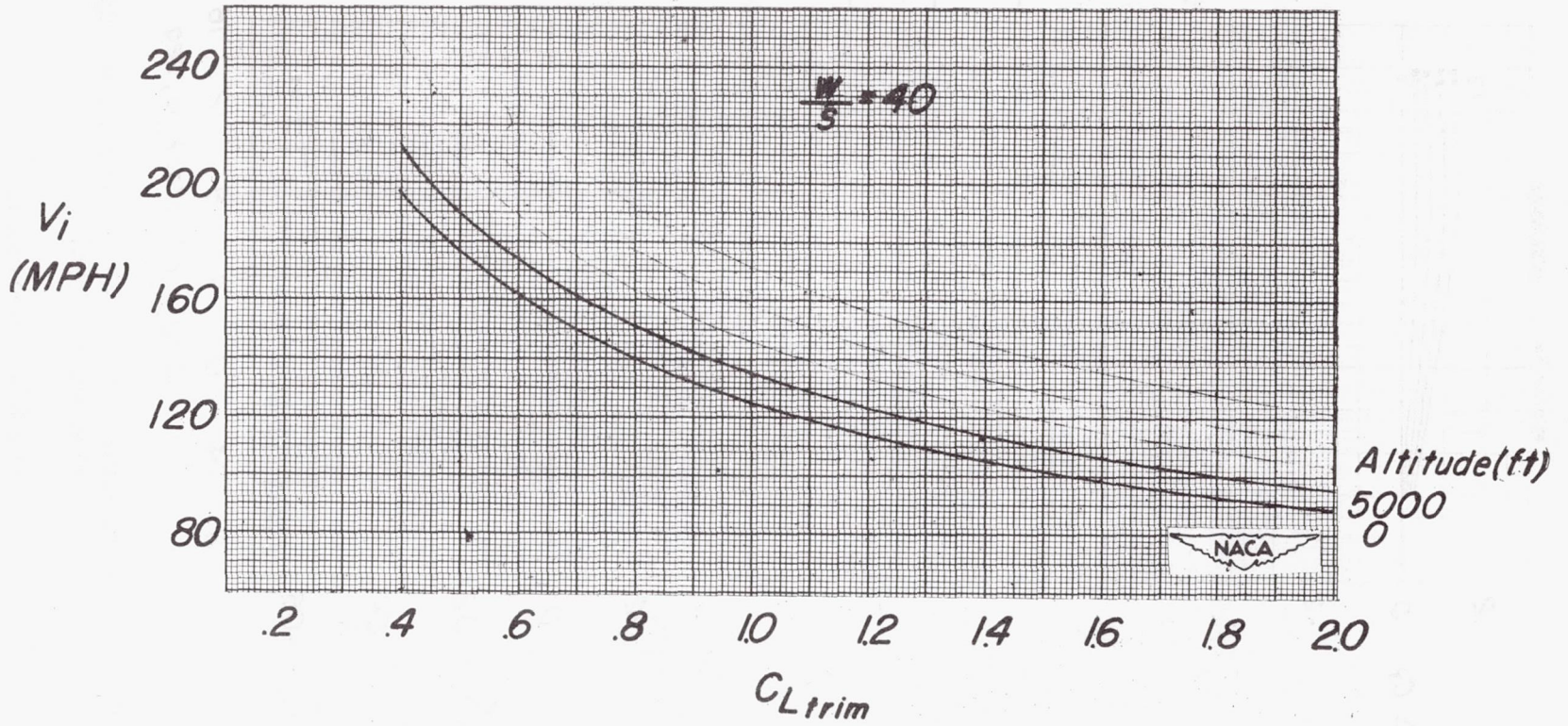

Figure 28.- Variation of indicated velocity with trim lift coefficient for a typical twin-engine airplane.

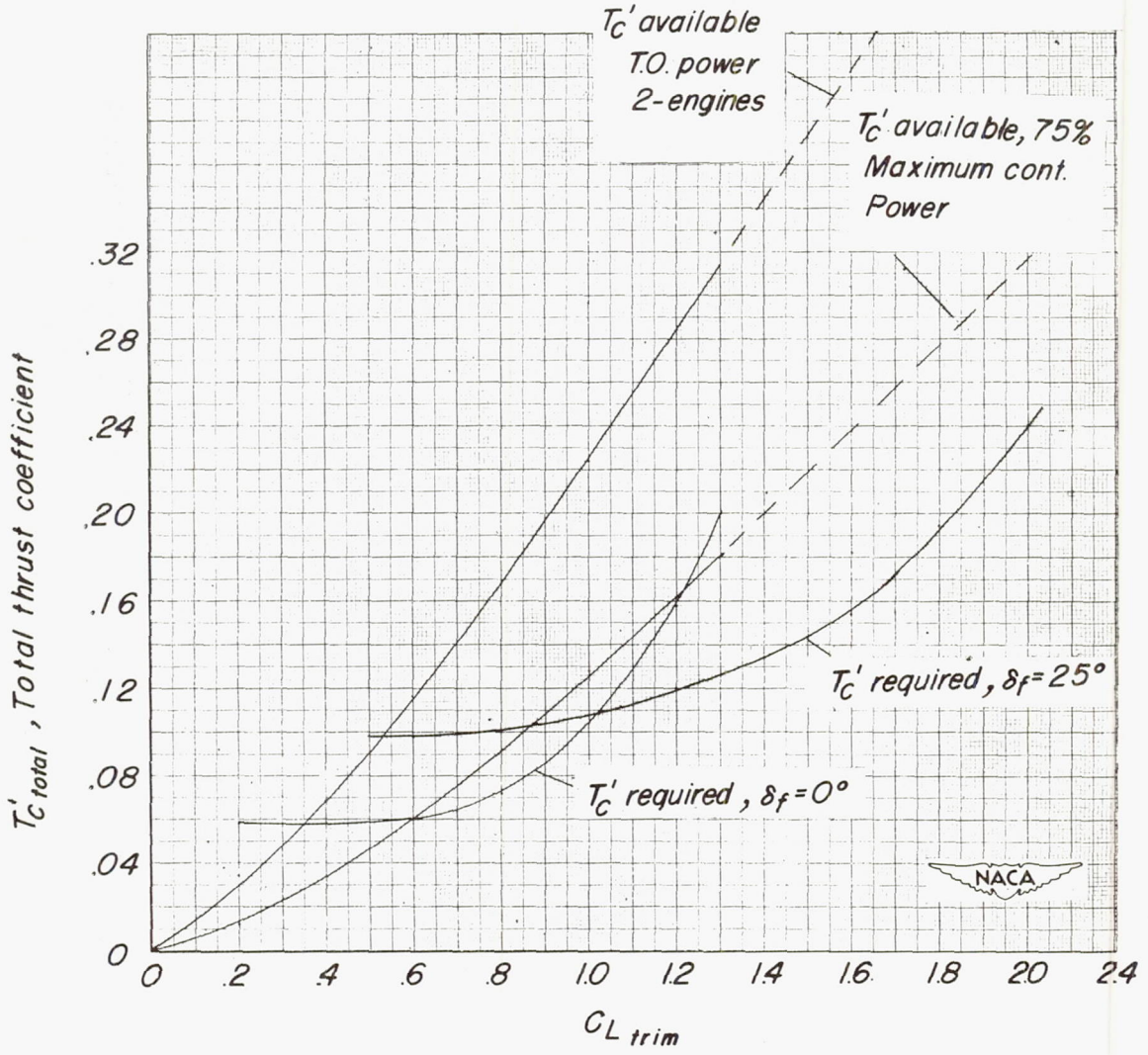

Figure 29.- Illustrative variation of total thrust coefficient with trim lift coefficient for a typical twin-engine airplane. Model drag data not corrected for strut tares.

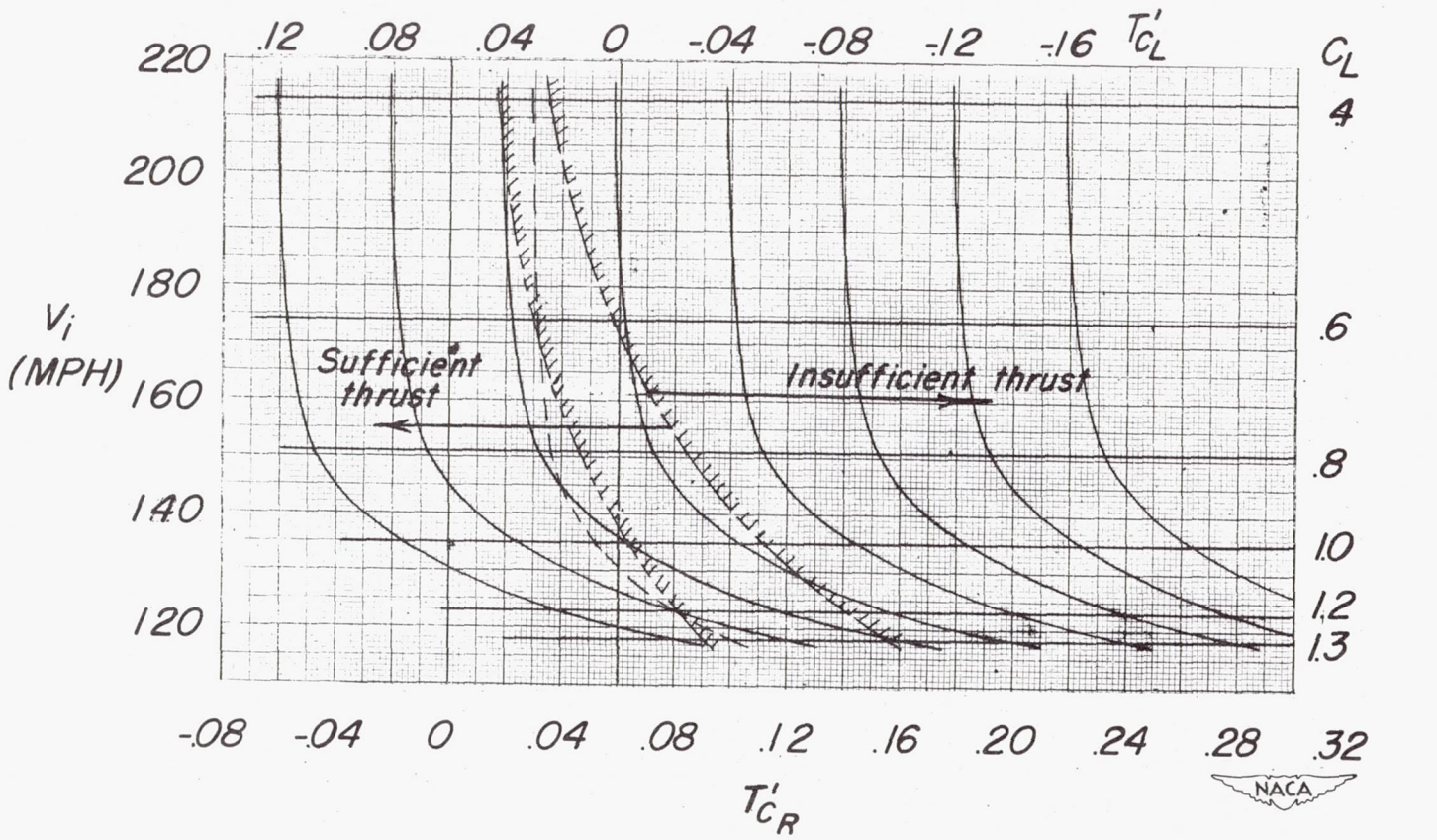

Figure 30.- Illustrative variation of indicated velocity with thrust coefficient of the right propeller of a twin-engine airplane for various increments of thrust coefficient on the left engine. Model drag data not corrected for strut tares. $\delta_f = 0^\circ$; altitude, 5,000 feet; $\frac{W}{S} = 40$ pounds per square foot.

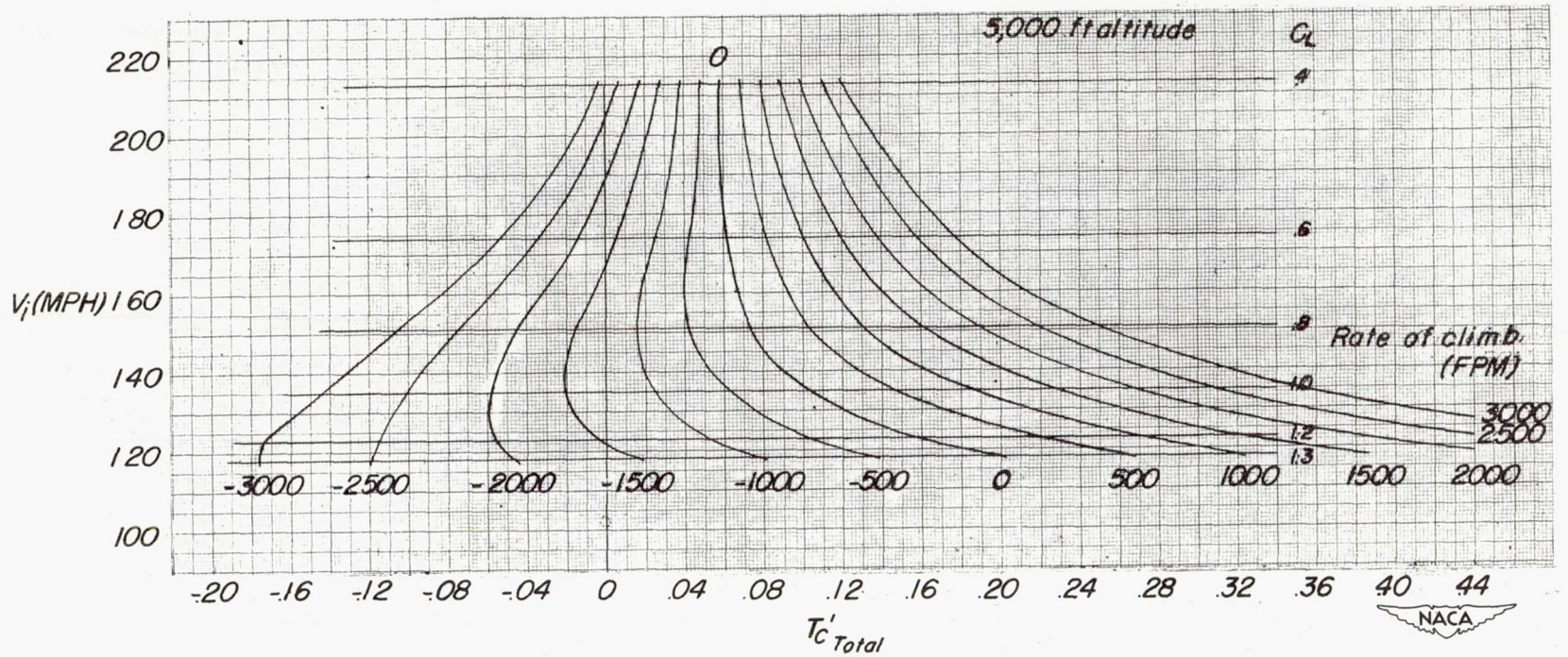

Figure 31.- Illustrative variation of indicated velocity with total thrust coefficient for various rates of climb for a typical twin-engine airplane. Model drag data not corrected for strut tares. $\delta_f = 0^\circ$; $\frac{W}{S} = 40$ pounds per square foot.

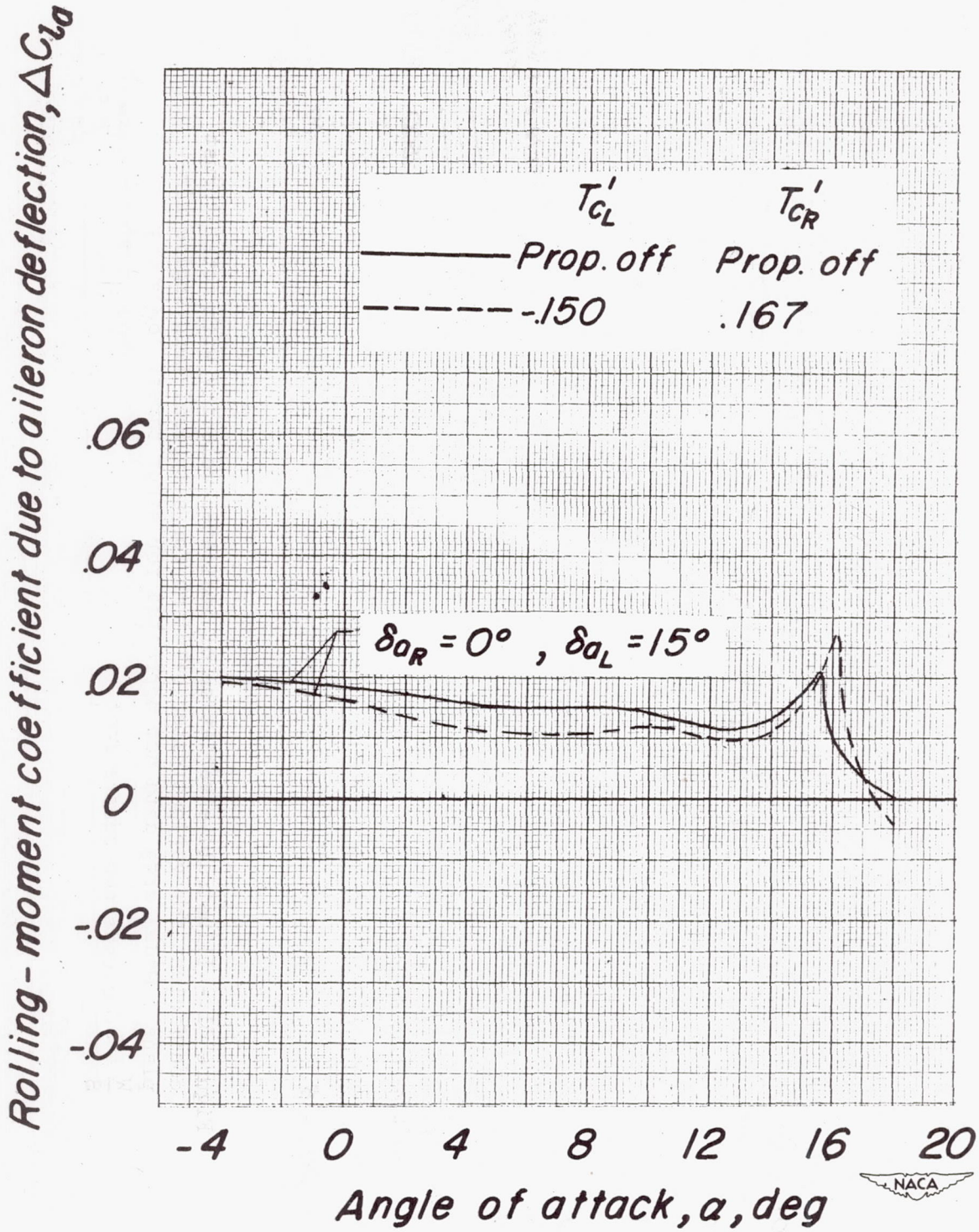

Figure 32.- Effect of thrust coefficient on aileron characteristics. $\delta_f = 0°$.

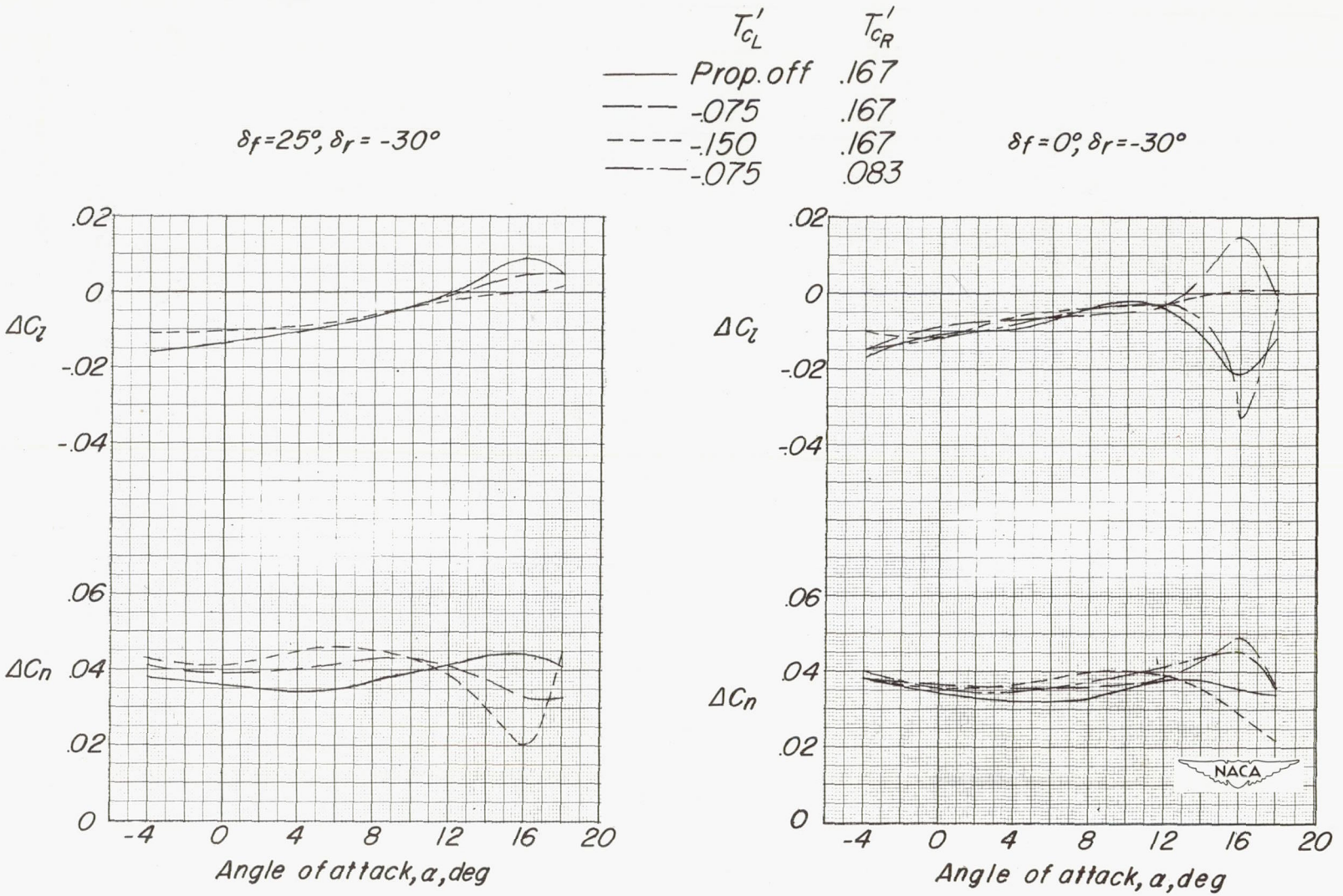

Figure 33.- Rudder characteristics of the model for various asymmetric-thrust conditions.

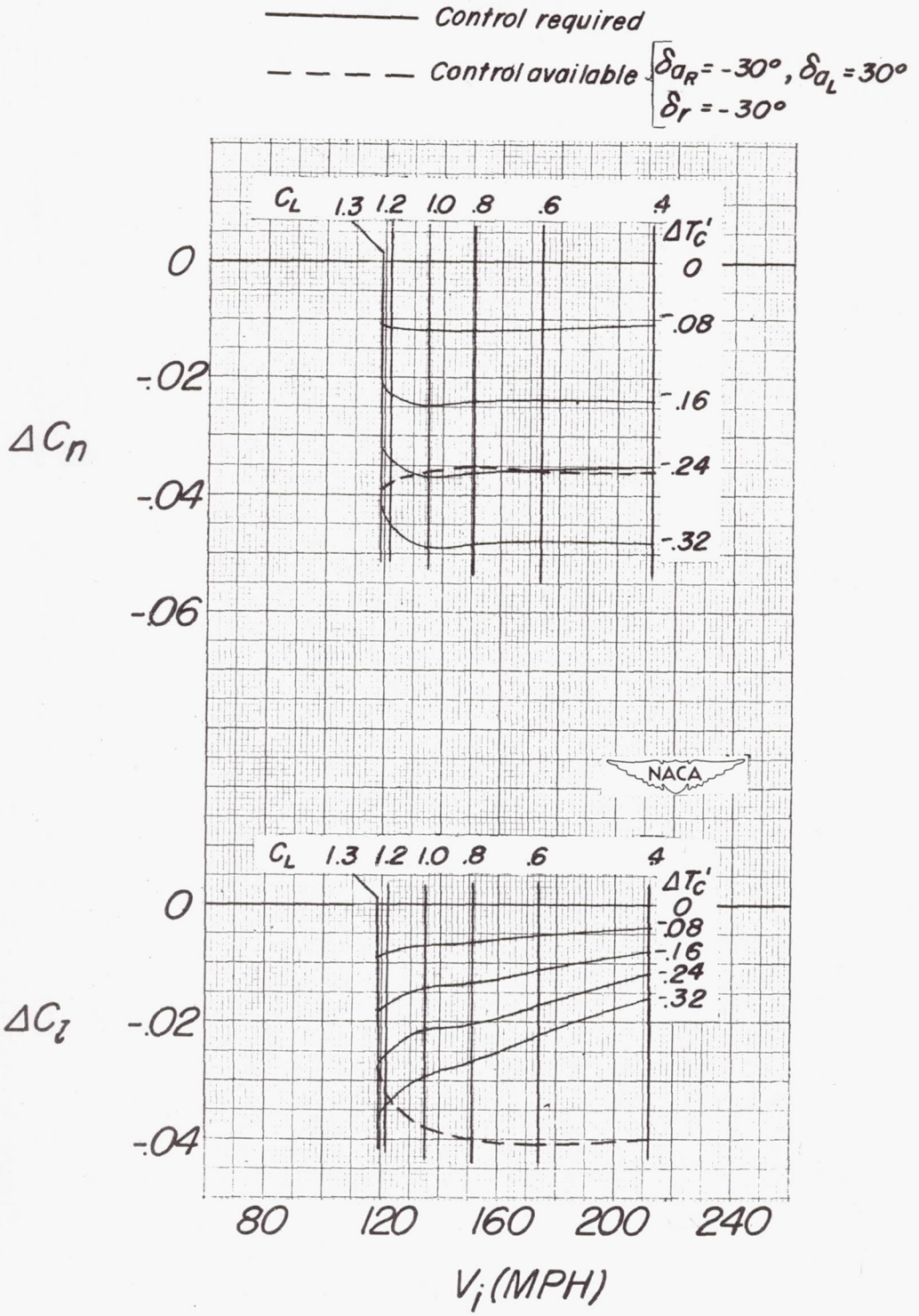

Figure 34.- Effect of asymmetric thrust coefficient on the level-flight lateral control characteristics of a typical twin-engine airplane. $\delta_f = 0°$; $\frac{W}{S} = 40$ pounds per square foot.

NACA-Langley - 9-21-53 - 1000